



Oceanic anoxic events, photic-zone euxinia, and controversy of sea-level fluctuations during the Middle-Late Devonian

Pavel Kabanov^{a,b,*}, Tyler E. Hauck^c, Sofie A. Gouwy^a, Stephen E. Grasby^{a,b},
Annick van der Boon^{d,e}

^a Geological Survey of Canada, Calgary, Alberta, Canada

^b Department of Geoscience, University of Calgary, Alberta, Canada

^c Alberta Geological Survey, Edmonton, Alberta, Canada

^d Geomagnetism Laboratory, University of Liverpool, UK

^e Centre for Earth Evolution and Dynamics, University of Oslo, Norway

ARTICLE INFO

Keywords:

Devonian

Oceanic anoxic events

Greenhouse Earth

Biomarkers

$\delta^{13}\text{C}$

Trace metals

Geochemistry

Eustasy

Review

ABSTRACT

This paper reviews global records of anoxic events of the Middle Devonian – earliest Mississippian, as well as the possible triggers and controls of these events. These “anoxic events” are complex multistage paleoenvironmental disturbances manifested in multiple proxies, which we showcase with the Horn River Group (HRG) – a succession of basinal organic-rich shales and cherts deposited during the latest Eifelian – earliest Late Frasnian (~386–373 My ago) on the western continental margin of Laurentia near the paleo-equator. Four major events imprinted in the HRG are the Kačák, Frasnian, basal *punctata*, and late *punctata* events, but positive $\delta^{13}\text{C}$ excursions (measured on organic matter) are more numerous and can potentially be matched to other global events. The Kačák event in the base of the HRG manifests as a regional switch from carbonate-platform to anoxic sedimentation. Three major events of the latest Givetian – Middle Frasnian display repeating sequences characterized by: (1) an early shift to heavier $\delta^{13}\text{C}$ values coupled with siliciclastic enrichment and mercury enrichment spikes of up to 0.48 ppm; (2) late-stage $\delta^{13}\text{C}$ reversal to background values coincident with the onset of severe anoxia (buildup of authigenic U, Mo, V) and attenuation of siliciclastic supply. Devonian anoxic sediments, including HRG, display widespread presence of chlorobi biomarkers, which indicates episodes of photic-zone euxinia in the water column. Most of these sediments were deposited under open ocean conditions, precluding a Black Sea water-column stratification scenario. These observations indicate Devonian anoxic events are similar to classical Mesozoic oceanic anoxic events (OAEs), consistently with growing evidence for a volcanic trigger for these events (e.g. spikes in Hg and negative $^{187}\text{Os}/^{188}\text{Os}$ anomalies). Oxygen minimum zones in a greenhouse ocean, such as the one recorded in basinal HRG, were prone to expansion under volcanic CO_2 reinforcement. This volcanic press-pulse also intensified the hydrological cycle, which resulted in a boost of weathering and eutrophication of shelfal seas. These factors, amplified by deoxygenation and acidification of the habitable upper ocean, drove extinctions of various magnitude. As a proxy for the input of land-plant detritus, the oxygen index from pyrolysis data shows zero response to anoxic events in the HRG, which aligns with broader evidence that counters expanding vascular vegetation to be the driver of the marine biotic crises. Finally, our review highlights how controversial the evidence of high-frequency (3rd to 5th orders) sea-level fluctuations is in the Devonian. In particular, none of the geochemical proxies usually employed to interpret sea-level changes translates unequivocally into transgressions and regressions in the greenhouse world. This sea-level puzzle clearly calls for new scrutiny and justifies scepticism in the validity of the classical “eustatic sea-level curve of the Devonian”, as well as estimates of eustatic amplitudes in excess of ~25 m for 3rd and 4th order cycles.

1. Introduction

The Devonian Period (419.0–359.3 Myr; [Gradstein and Ogg, 2020](#)) represents a profound change of Earth's land surface, from mostly

plantless by the end of the Silurian to thickly vegetated wetlands inhabited by amphibian-grade tetrapods by the conclusion of the Devonian Period ([Algeo and Scheckler, 1998](#); [Dahl and Arens, 2020](#); [Becker et al., 2020](#); [Capel et al., 2022](#)). The Devonian also experienced

* Corresponding author at: Geological Survey of Canada, Calgary, Alberta, Canada.

E-mail address: Pavel.Kabanov@nrcan-rncan.gc.ca (P. Kabanov).

<https://doi.org/10.1016/j.earscirev.2023.104415>

Received 29 September 2022; Received in revised form 1 April 2023; Accepted 4 April 2023

Available online 10 April 2023

0012-8252/© 2023 Published by Elsevier B.V.

several mass extinctions and radiations in the marine realm (Fig. 1), four of which are consistently rated within the 10 worst mass extinctions of the post-Cambrian Phanerozoic at genus-level taxonomic loss (Sepkoski, 1996; Bambach et al., 2004; McGhee et al., 2013). Vigorous deposition of Devonian planktogenic organic carbon within shelfal seafloors created major oil and gas resources on different continents (Fig. 1B; North, 1988; Klemme and Ulmishek, 1991; Dyni, 2006), making this time period also one of significant economic interest. Stratified conditions with a chemocline at least intermittently above the seafloor were required for such high organic burial. In addition, recent research reveals oxygenation of the atmosphere from 10 to 12% O₂ (0.5–0.6 of present-day level) at the Silurian/Devonian boundary to about the present-day level of 21% by the early Mississippian, accompanied by a mirroring trend of CO₂ drawdown (Krause et al., 2018; Mills et al., 2019; Dahl and Arens, 2020). Consistent with atmospheric oxygenation, a major shift to mostly oxygenated oceanic watermass is revealed with the uranium isotope ($\delta^{238}\text{U}$) proxy across the Emsian/Eifelian boundary (Elrick et al., 2022). Whether these remarkable features of the Devonian Period are related, and what were the overall controlling factors, has long been a matter of debate (Algeo et al., 1995; Bond et al., 2004; Racki, 2020a; Piszczowska and Racki, 2020; Kabanov, 2021; McGhee and Racki, 2021).

Warm epochs with little or no ice on Earth, including the Devonian Period, represent collectively ~70–80% of the Phanerozoic. Thus, greenhouse conditions have been the “default state” of the planetary ocean-atmosphere circulation systems (Kidder and Worsley, 2010) since Late Ordovician – Early Silurian drawdown of atmospheric CO₂ reduced temperature fluctuations to the range experienced by the Earth surface during the last ~100 My (Mills et al., 2019; Scotese et al., 2021). Understanding this default state is critical as we try to understand the impacts of warmer atmosphere-ocean systems unexperienced by *Homo sapiens* Linnaeus, but considered a near future condition if greenhouse gas drawdown fails to follow optimistic projections (Kidder and Worsley, 2012; Ganopolski et al., 2016; Oschlies, 2021; Wallmann et al., 2022; <https://www.ipcc.ch/srocc/home/>).

The discourse around Devonian anoxic events and biotic crises mostly revolves around prominent mass extinctions at the Frasnian-Famennian boundary (e.g., Averbuch et al., 2005; Bond and Wignall, 2008; Racki, 2005; Racki, 2020a, 2020b; Carmichael et al., 2019; Da Silva et al., 2020; Lu et al., 2021) and the Devonian-Carboniferous boundary (e.g., Carmichael et al., 2016; Kaiser et al., 2016; Percival et al., 2022). In this paper we broaden this narrow focus by enquiring into environmental factors that kept the marine realm at the tipping point of multiple crises for over 30 Myr, starting from the Eifelian-Givetian boundary (385.3 Myr) into the early Mississippian (Fig. 1). We point out how the sedimentary and geochemical signatures of Devonian marine strata, such as the time-specific facies architecture and widespread occurrence of photic-zone euxinia (PZE) biomarkers, attest for the non-uniformitarian character of Devonian seawater circulation. We review the main anoxic events recognized to date, then critically discuss factors called upon to explain these events: sea-level fluctuations, redox state of the marine realm, ocean circulation specifics for greenhouse planetary condition, state of the Earth’s magnetic field, evolution of land plants, and large-scale volcanism. Fig. 1 summarizes some of these records and interpretations. To examine these events in more detail, we also present a new detailed archive of an open ocean record of the Devonian system, the latest Eifelian – Frasnian Horn River Group (HRG) of NW Canada, which provides important insights.

2. Events in the Devonian marine realm

2.1. Rise of Devonian event stratigraphy

As pointed out by House (1996, 2002), it is the recognition of oceanic anoxic events (OAEs) in the Cretaceous that triggered the discourse on similar events in the Devonian marine realm. In their pioneering work,

Schlanger and Jenkyns (1976) interpreted their two Cretaceous OAEs as expansions of oxygen minimum zones (OMZs) during sea-level rise. At that time, the extent of coastal onlaps and facies successions were seen in favor of high-amplitude sea level fluctuations during the Cretaceous, and international synchronization of sea-level curves prompted to call these fluctuations eustatic (Hancock and Kauffman, 1979). Appointing sea level fluctuations as the main and invariable driving force creating sedimentary cyclicity was greatly promoted by development of the classical sequence stratigraphy (Vail et al., 1977 and successive works).

Shortly after the discovery of OAEs, Scholle and Arthur (1980) published compelling evidence that the two OAEs of Schlanger and Jenkyns (1976) coincided with positive $\delta^{13}\text{C}$ excursions as measured on pelagic limestones. The number of recognized OAEs has increased since then. Jenkyns (2010) lists 9 main events in the Jurassic-Eocene interval. Gale et al. (2020) depicts 11 OAEs in the Cretaceous only, while pointing out that global carbon isotopic excursions are more numerous than known synchronous spreads of anoxic sediments (see also Cramer and Jarvis, 2020). Some OAEs are associated with selective extinctions of marine organisms and declines in reef building, whereas others are not (Föllmi et al., 1994; Leckie et al., 2002; Freymueller et al., 2019).

Events in the Devonian marine realm were defined based on prominent faunal turnovers, either extinctions of select genera and families or combined extinctions-radiations (Walliser, 1984, 1985, 1996; House, 1985, 2002; Becker, 1993b). Coincident facies shifts, interpreted as marine transgressions, were also entered in event definitions (*ibid.*). This inborn biotic-depositional duality resulted in mixed naming for some events, e.g. the latest Eifelian *Nowakia otomari* – *Cabrieroceras rouvillei* faunal event (Walliser, 1984, 1985) and its *alter ego* Kačák event, named after the Kačák Member of the Srbsko Formation in Prague Synclinorium (House, 1996). This dual definition of Devonian events is currently mainstream (Becker et al., 2020), and numerous studies of the last two decades provide a wide array of geochemical proxies extending the character of each event far beyond paleontological metrics and observed facies changes. In particular, $\delta^{13}\text{C}$ stratigraphy, first done on brachiopod calcites and micritic limestones, revealed negative and positive $\delta^{13}\text{C}$ swings of significant amplitude (~2–4‰) associated with the Upper and Lower Kellwasser levels in many sections around the world (McGhee et al., 1986; Goodfellow et al., 1989; Joachimski and Buggisch, 1993). Additional $\delta^{13}\text{C}$ data characterized the lower part of the Devonian (excluding the basal Devonian Klonk anomaly) as a general quiescence in isotope fluctuations, and the Givetian-Frasnian as an interval of abrupt, high-amplitude $\delta^{13}\text{C}$ shifts (Fig. 1F).

Inception of Devonian event stratigraphy came with development of a sea level curve for this system (Fig. 1C). The search for an eustatic signal initially focused on stratal successions of Laurussian shelves with advanced biostratigraphic age control (House, 1983; Johnson et al., 1985). While creating their Devonian sea-level curve, Johnson et al. (1985) used facies progressions in stratigraphic sections as their primary tool to decipher transgressive-regressive cycles (T-R cycles), and exerted caution in using coastal onlap estimates. Johnson et al. (1985) interpreted distinct tongues of black shales in the foreland clastic wedge of the Appalachian Basin (a.k.a. the Catskill Delta succession) as transgressive and deepest-water deposits. These spectacular cycles with black-shale tongues as sea level highstands were correlated with sedimentary cycles of Belgium and Germany, demonstrating the coeval spread of black shales at certain intervals coincident with biotic events (*ibid.*). Other regions in the western U.S. and western Canada were also involved in this correlation. The resultant “eustatic sea level curve”, with its subsequent modifications (Fig. 1C; Sandberg et al., 2002; Becker et al., 2012; Becker et al., 2020), is the most popular reference (“standard”) of today, although different interpretations of T-R cyclicity do exist (Filer, 2002; Bond and Wignall, 2008; Brett et al., 2011; Wong et al., 2017).

Thus, the definition of events in the Devonian historically diverged from their Mesozoic OAE prototypes which were unambiguously defined as synchronous spreads of anoxic sediments in disjunct world

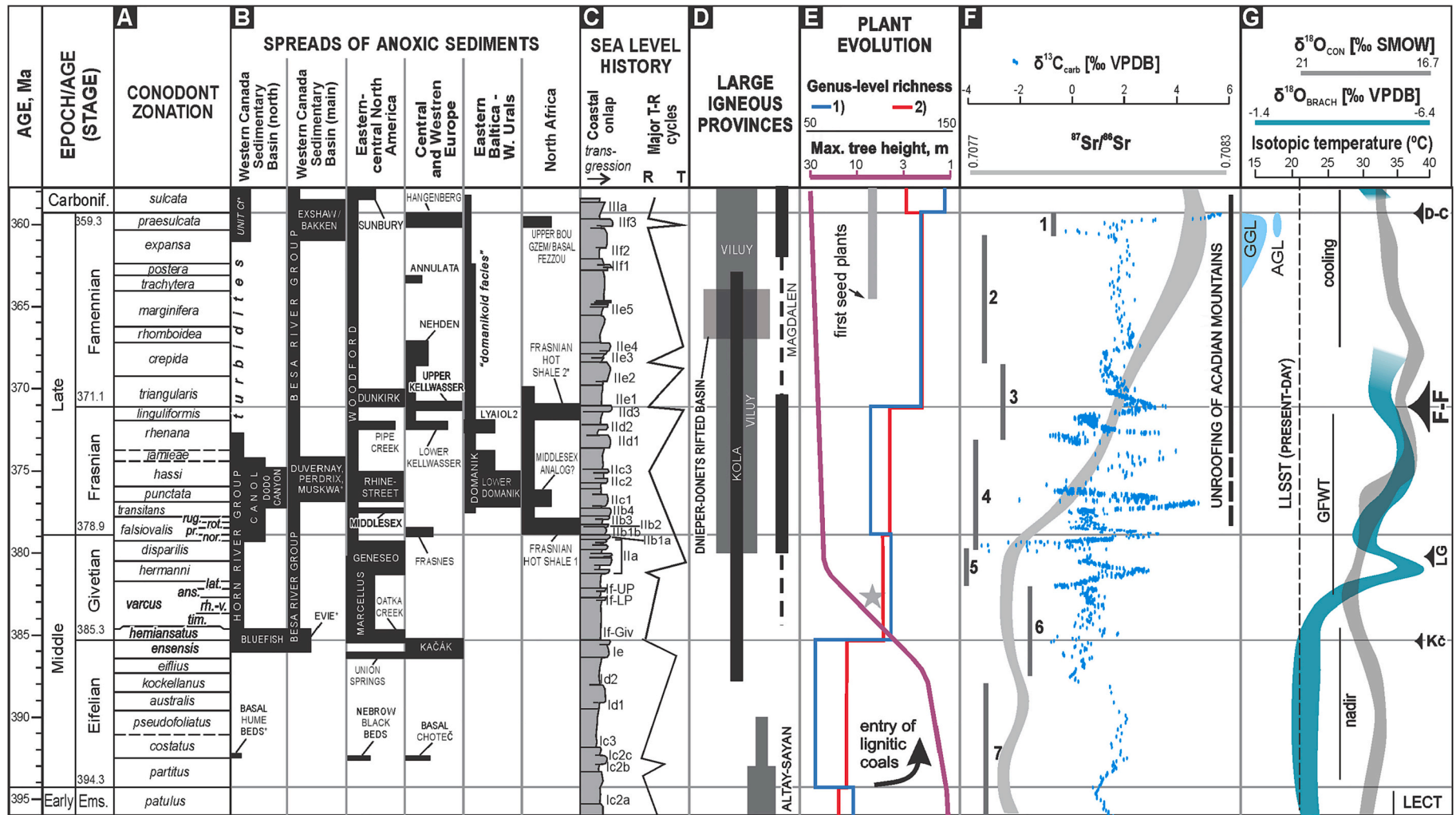


Fig. 1. Summary of records and potential controls of Middle-Late Devonian anoxic events:

A. Binomial names of conodont zones, bottom to top (from GTS 2020): *Polygnathus patulus*; *P. partitus*; *P. costatus*; *P. pseudofolius*; *Tortodus australis*; *T. kockelianus*; *Polygnathus eiflii*; *P. ensensis*; *P. hemiansatus*; *P. varcus*; *P. timorensis* (*tim.*); *P. rhenanus* - *P. varcus* (*rh.-v.*); *P. ansatus* (*ans.*); *Schmidtognathus latifossatus*/*Ozarkodina semialternans* (*lat.*); *Schmidtognathus hermanni*; *Klapperina disparilis*; *Mesotaxis falsiovalis*; *Skeletognathus norrisi* (*nor.*); *Ancyrodella rotundiloba pristina* (*pr.*); *A. rotundiloba rotundiloba* (*rot.*); *A. rugosa* (*rug.*); *Palmatolepis transitans*; *P. punctata*; *P. hassi*; *P. jamieae*; *P. rhenana*; *P. linguliformis*; *P. triangularis*; *P. crepida*; *P. rhomboidea*; *P. marginifera*; *P. rugosa trachytera*; *P. perlobata postera*; *P. gracilis expansa*; *Siphonodella praesulcata*; *S. sulcata*.

B. Main spreads of anoxic sediments in six world regions, updated from Kabanov (2019). Western Canada Sedimentary Basin (north) is the Horn River Group in the Northwest Territories between 64 and 68°N (case study in this work). Western Canada Sedimentary Basin (main) refers to the subsurface of Alberta and northeastern British Columbia. Asterisk (*) denotes black shales with notably poor age control.

C. Sea level history is redrawn from Becker et al. (2020); coastal onlap curve and main transgression-regression cycles (T-R cycles) are interpretations of Haq and Shutter (2008); depophas indexing is evolved from Johnson et al. (1985).

D. Age ranges of large igneous provinces based on available absolute dating: Kravchinsky (2012), Bond and Wignall (2014), Racki (2020a), and Ernst et al. (2020). Bar width denotes relative volumes of emplaced effusives in cited sources.

E. Evolution of land plants. Maximum tree height trend: Algeo and Scheckler (1998). Total genus-level taxonomic richness of (1) plant macrofossils and (2) plant spores: Cascales-Miñana (2016). Entry of lignitic coals into sedimentary record: Kennedy et al. (2013). Entry of seed plants (grey bar) and the earliest known sporophyte precursor of seed plants (grey star): Prestianni and Gerrienne (2010).

F. Reference carbonate carbon isotope curve ($\delta^{13}\text{C}_{\text{carb}}$) from Cramer and Jarvis (2020) and $^{87}\text{Sr}/^{86}\text{Sr}$ trend from McArthur et al. (2020). Dark grey bars denote $\delta^{13}\text{C}_{\text{carb}}$ data sources: 1. Stolfus et al. (2020); 2. Buggisch and Joachimski (2006); 3. Xu et al. (2012); 4. Holmden et al. (2006); 5. Zambito et al. (2016); 6. van Hengstum and Gröke (2008); Buggisch and Mann (2004). The $^{87}\text{Sr}/^{86}\text{Sr}$ trend (pale grey ribbon) represents 95% confidence range of LOWESS data fitting (McArthur et al., 2020); ^{87}Sr enrichment trend of the Late Devonian is matched to Acadian Orogeny.

G. Low-latitude isotopic paleotemperatures, glaciation records, and extinctions of marine faunas. Isotopic paleotemperatures are from Grossman and Joachimski (2020): cyan and grey ribbons capture $\pm 95\%$ confidence range of Locfit regressions on the $\delta^{18}\text{O}$ from brachiopod calcite (cyan) and conodont phosphate (grey); gap in brachiopod calcite trend reflects lack of data in the Middle-Late Famennian; dashed line is the present-day average low-latitude sea-surface temperature (LLSST); cooling and warming trends are explained in text. Glacial records are from Isaacson et al. (2008): GGL is high-latitude glacial deposits of Gondwana; AGL is the evidence for alpine glaciers in the Appalachian region of Laurentia. Black arrows denote major extinctions in marine realm (arrow size reflect severity): latest Eifelian or Kacák (Kc), late Givetian (LG), Frasnian-Famennian (F–F), and end-Devonian (D–C).

regions. This semantic tangle can perhaps be resolved by retaining taxonomic names for biotic events only and reserving lithostratigraphic co-names for anoxic events. Separating the discussion of biotic and depositional events is also warranted by the growing awareness that exact extinction levels and anoxic episodes can mismatch when stratigraphic records are scrutinised (e.g., Hallam and Wignall, 1999; Bond and Wignall, 2008; Kaiser et al., 2016).

2.2. World record of Devonian anoxic events

Table 1 summarizes the age constraints and diagnostic features of the Middle-Late Devonian events. The events are expressed most typically as incursions of dark, laminated, organic rich sediments in more oxic and less organic rich strata, or if a section is black shale throughout, as horizons of authigenic trace metal enrichment indicating pulses of severe anoxia (Kabanov, 2019). Ages of the events are referred to in conodont zones. Since the zonation is rapidly evolving and no “standard” is currently adopted for international use, double reference to conodont age is sometimes unavoidable. We consider two zonal scales published in the Geological Time Scale (GTS) volumes of 2012 and 2020 to be sufficient for the purpose (Becker et al., 2012, Becker et al., 2020). Many anoxic and faunal events of the Devonian are step-wise rather than expressed in one pulse (Becker et al., 2020). Since interregional correlation of every pulse within one event is not presently possible, Table 1 lists only the main conventionally recognized events. In columns “Event name” and “Faunal event name”, originators are those who first applied a name consistently to sedimentary and coupled biotic perturbations recognized in more than one world jurisdiction. Typically, the name had already been in long use before as a local litho- or biostratigraphic unit.

Becker et al. (2020) provided the most recent comprehensive overview of Devonian events. For Late Devonian events, the $\delta^{13}\text{C}$ excursions in carbonate and organic matter records are summarized by Piszarszowska and Racki (2020). The reference $\delta^{13}\text{C}_{\text{carb}}$ curve for the entire Devonian is provided in GTS 2020 (Cramer and Jarvis, 2020), although this curve is constructed from a selection of published data which is not comprehensive (Fig. 1F). The column “biotic response” is based on the summaries of McGhee et al. (2013) and Becker et al. (2020). It should be noted that the ranking of biotic events, albeit based on the same Paleobiology Database, varies depending on database treatment (e.g., Stigall, 2012; Stanley, 2016). Nevertheless, four of the Devonian extinctions at the Eifelian/Givetian boundary, in the Late Givetian, at the Frasnian-Famennian and Devonian-Carboniferous boundaries (Fig. 1G) stay in the ten worst post-Cambrian mass extinctions despite variations in statistical approach (Sepkoski, 1996; Bambach et al., 2004; McGhee et al., 2013).

Certainly, the character of Devonian events extends beyond features listed in Table 1. Stable isotope records are increasingly used, notably $^{18}\text{O}/^{16}\text{O}$, $^{34}\text{S}/^{32}\text{S}$, $^{187}\text{Os}/^{188}\text{Os}$, and $^{87}\text{Sr}/^{86}\text{Sr}$ systems (see respective chapters in GTS 2020), also $^{15}\text{N}/^{14}\text{N}$ (Śliwiński et al., 2011; Uveges et al., 2019; Percival et al., 2022; Sahoo et al., 2023), molybdenum and uranium isotope systems (White et al., 2018; Kendall et al., 2020; Elrick et al., 2022). Oxygen isotope records obtained from conodont phosphate (francolite-apatite) and brachiopod calcite currently provide the highest density of data for the Devonian (Grossman and Joachimski, 2020). Being least prone to diagenetic alteration, these materials provide $\delta^{18}\text{O}$ records which can be translated into ambient seawater temperature (Fig. 1G). The $\delta^{18}\text{O}$ -based seawater temperature data are scattered broadly and are offset between sampling regions, although all sampling regions are within $0\text{--}35^\circ$ paleo-latitudes, i.e., generally warm-water settings. These regional offsets are most vivid in conodonts, and moreover, a substantial decoupling of temperature trends is observed between brachiopod and conodont data (Joachimski et al., 2004, 2009; van Geldern et al., 2006). This is not surprising in view of differences in bottom and sea-surface temperature, and moreover, different conodont genera inhabited different depth ranges (review in Grossman and Joachimski, 2020). Nevertheless, long-term trends are consistent in both

Table 1
World records of Middle-Late Devonian anoxic events.

Age	Event name (originator)	Faunal event name	Event zonal range	Anoxic event	Duration of anoxic event	Carbon isotope excursions	Biotic response
Devonian-Carboniferous boundary	Hangenberg (Walliser, 1984)		<i>praesulcata</i> , <i>cockeli</i> , lower <i>sulcata</i> in Europe ¹ ; upper <i>expansa</i> -lower <i>duplicata</i> in W. Canada ^{2,13}	black shale within <i>praesulcata</i> - <i>cockeli</i> interregnum in Central Europe ^{1,3} ; more protracted black shale deposition in W. Canada ^{1,2} ; black shales in N. Africa, elsewhere in Europe, China dated with various precision ¹ ; no definite anoxic incursions in Russian Platform -Urals ¹¹	100–300 kyr ¹ ; 50–100 kyr in Poland ³⁸	Brief negative $\delta^{13}\text{C}(\text{carb})$ swing (ca. 1.5‰) in middle <i>praesulcata</i> in USA and S. China; more protracted major (ca. 4‰); positive excursion during <i>cockeli</i> - <i>duplicata</i> in many regions ^{1,4,5} ; similar $\delta^{13}\text{C}(\text{org})$ response in Europe ⁸ ; decoupled response of $\delta^{13}\text{C}(\text{carb})$ and $\delta^{13}\text{C}(\text{org})$ in central USA ³⁹	Major extinction: rank 4 in taxonomic severity and rank 7 in ecologic severity ⁶ mostly prior to <i>cockeli</i> ¹ ; rapid diversity rebound at DC boundary ¹ .
Famennian	Dasberg (Becker, 1993a)		<i>gracilis expansa</i> - <i>aculeatus aculeatus</i> ³	thin, locally phosphatic black shales in Central Europe and Morocco; described as marine transgression elsewhere ^{3,7}	two very short anoxic pulses ^{3,8}	Low amplitude positive $\delta^{13}\text{C}(\text{carb})$ swing in Europe ⁸ ; low amplitude negative $\delta^{13}\text{C}(\text{carb})$ swing in Utah ⁹	Radiation in goniatites; no extinction ⁸
Famennian	N/A	<i>annulata</i> (etim.: <i>Platyclymenia annulata</i>) (Walliser, 1984)	upper <i>trachytera</i> ^{8,13} or <i>gracilis sigmoidalis-styriacus</i> ³	Central Europe (Germany, Czech Republic, Poland), Bulgaria, NW China ^{3,8}	two thin black shales in central Europe and NW China ^{3,8}	two covariant negative $\delta^{13}\text{C}(\text{carb})$ and $\delta^{13}\text{C}(\text{org})$ swings of low amplitude in Europe; low amplitude positive excursion just above; described as muted in many sections ⁸	nothing significant ⁸
Famennian	Nehden (House, 1985)		Entire Early Famennian (<i>triangularis-gracilis gracilis</i> Zones) ³	black shale deposition in Germany; described as long lasting eustatic rise elsewhere ³ ; last two anoxic pulses recognized as Condroz event ³	acme of black shale deposition in <i>terminipectinata</i> Zones (~1 myr) ³	not clear	Diversity recovery after F–F extinction ³ ; constriction in diversity of select goniatite groups ¹⁰
Frasnian-Famennian boundary	Upper Kellwasser (UKW) and Lower Kellwasser (LKW) (Walliser, 1984; Schindler, 1990)		UKW: <i>linguliformis</i> ¹³ or <i>linguliformis-ultima</i> ³ LKW: upper <i>rhenana</i> or <i>bogartensis</i> ³	Two incursions of anoxic sediments (LKW & UKW) amply documented in many regions of the World ^{3,8} ; not expressed in most N. American sections ¹¹ ; LKW is less widespread in the World.	~ 150 kyr for UKW (and similar for LKW) in Germany; total crisis duration ≤ 800 kyr ¹²	Well documented positive $\delta^{13}\text{C}(\text{carb})$ and $\delta^{13}\text{C}(\text{org})$ excursions at and just above LKW and UKW anoxic beds, preceded by abrupt low-amplitude negative swing in some sections ⁸	Major extinction: rank 5 in taxonomic severity and rank 4 in ecologic severity ⁶ ; gradual decline of metazoan reef diversity during Late Frasnian until reef building demise at F–F boundary ³⁷
Frasnian	N/A	<i>semichatovae</i> (Sandberg et al., 1992)	lower <i>rhenana</i> ¹³ or <i>feisti</i> ³	described as transgression; mass spread of offshore pelagic fauna on carbonate shelves ^{3,14} ; local incursions of anoxic sediments ¹⁵	no estimates (likely very short)	Positive $\delta^{13}\text{C}(\text{carb})$ excursion with amplitude peering $\delta^{13}\text{C}$ sway at UKW in China ¹⁶	Radiation in conodonts and goniatites; no extinction ^{3,14}
Frasnian	Rhinestreet (Becker et al., 1993)		lower-middle <i>hassi</i> (MN 7–9) ¹³ ; or <i>nonaginta-proversa</i> ³	Major spread of black shales in N. America and E. Russian Platform - Urals; locally separated in two black-shale tongues (New York State) and merging in one major source rock unit in W. Canada and Russia ^{11,20,35,36} ; ; expressed as several incursions of pelagic (dacryoconarid) sediments in overall non black-shale sections ³	~2.3 Myr in W. Canada and Russia (entire Middle Frasnian except upper <i>hassi</i>). NW Canada and New York State: two acmes of anoxia within Middlesex/ <i>punctata</i> and Rhinestreet/ <i>hassi</i> ¹¹	New York State: modest positive $\delta^{13}\text{C}$ (org) deflection in basal Rhinestreet shale, poorly separated from higher-amplitude Middlesex/ <i>punctata</i> excursion ¹⁷ ; very low amplitude to no $\delta^{13}\text{C}$ excursion elsewhere ¹⁷	faunal migrations, spread of pelagic forms; no extinctions ^{3,8}
Frasnian	Middlesex (Becker, 1993a, 1993b)	<i>punctata</i> (Yans et al., 2007)	<i>nodosa</i> (upper <i>transitans</i>) to <i>punctata</i> ^{3,8,16}	expressed as several incursions of pelagic (dacryoconarid) sediments in overall non black-shale sections ³	Middlesex/ <i>punctata</i> and Rhinestreet/ <i>hassi</i> ¹¹	High-amplitude $\delta^{13}\text{C}(\text{carb})$ and $\delta^{13}\text{C}(\text{org})$ excursions: brief, low-amplitude negative deflection in <i>nodosa</i> succeeded by major and abrupt positive excursion in terminal <i>nodosa</i> -early <i>punctata</i> (usually ~3‰, maximum 6–8‰) ^{6,8,16,40}	faunal migrations, spread of pelagic forms; no extinctions ^{3,8}
Frasnian	Timan (Becker and House, 1997)	<i>Timanites</i> (Becker and House, 1997: after entry of genus <i>Timanites</i>)	<i>transitans</i> ³	event defined as global transgression based on spread of pelagic faunas ^{3,19} ; co-spread of black shales not detected or not enough documented ^{3,19,20}	N/A	Short positive low-amplitude $\delta^{13}\text{C}$ swing just below pre-Middlesex negative deflection in some sections; not expressed in other sections ^{3,8}	global spread of goniatites of the genus <i>Timanites</i> ; no extinction ^{3,8,19}
Givetian-Frasnian boundary to Frasnian	Frasnes (House, 1985)	<i>Manticoceras</i> (Walliser, 1985, 1996)	<i>norrisi</i> - lower <i>soluta</i> ³ ; or <i>falsiovalis</i> ¹³	described as transgression; mass spread of offshore pelagic fauna on carbonate shelves ^{3,14} ; local incursions of anoxic sediments ¹⁵	pulses of anoxia within Frasnian event interval are likely short but not sufficiently studied ³	Rather poorly known. Short, high amplitude (~2 to ~4‰) negative sways of $\delta^{13}\text{C}(\text{carb})$ just below and at lower (<i>norrisi</i>) pulse ⁴ ; more protracted	Givetian biotic crisis s.l. ⁶ : protracted (~2.5 Myr), multiphase extinction and reef declines in <i>semialternans-norrisi</i> Zones or Taghanic-lower Frasnian

(continued on next page)

Table 1 (continued)

Age	Event name (originator)	Faunal event name	Event zonal range	Anoxic event	Duration of anoxic event	Carbon isotope excursions	Biotic response
Givetian	Geneseo (House, 2002?)		lower <i>hermanni</i> ³	black shale in New York State ²² ; described as transgression; ³ no transgressive successions or black shale incursions in Morocco ²³	not clear	positive (~3‰) excursion in earliest Frasnian ^{4,40} Distinct, short positive excursion in Germany but not in Morocco ²⁴	event interval ³ . Ranked 6 in taxonomic loss and 8 in ecologic severity ⁶ ; taxonomic loss largely compensated by radiations and extensive species migration ⁶
	Givetian	Taghanic (House, 1985)	<i>Pharciceras</i> (House, 1985)	late <i>ansatus-semialternans</i> ³	no prominent spreads of anoxic sediments ¹⁰	N/A	
	Positive $\delta^{13}\text{C}(\text{carb})$ excursion of ~2–3‰ in upper <i>ansatus-semialternans</i> Zones; in New York State (not in other sections) preceded by a low-amplitude negative swing ^{4,22}						
Givetian	Pumilio (Lottmann, 1990)		<i>rhenanus-varcus</i> ³	no truly anoxic facies known; two horizons of specific brachiopod and dactryoconarid faunas in Europe and N. Africa ^{3,10} ; interpreted as transgression pulses or tsunami events ^{3,10}	N/A	Positive $\delta^{13}\text{C}(\text{carb})$ excursions of 1.5–2.0‰ at both <i>pumilio</i> horizons known in Germany and France ³¹	none
Eifelian-Givetian boundary	Kačák (House, 1985)	<i>otomari</i> (Walliser, 1984, 1985)	<i>ensensis-hemiansatus</i> ³	Incursion of black shales and pelagic dactryoconarid sediments in Europe, N. Africa, China, Canada ^{3,10,11,28,29,30} . Abrupt demise of carbonate shelf and its drowning under anoxic sediments in NW Canada ^{11,40}	Entire event is ~370 kyr in Morocco ³⁴ . Main anoxic pulse likely very short (≤ 100 kyr?), at Eifelian-Givetian boundary	A succession of abrupt, low to moderate amplitude (<i>ca.</i> 1‰ to 1.5‰), negative and positive swings in $\delta^{13}\text{C}(\text{carb})$ and $\delta^{13}\text{C}(\text{org})$ in many regions ^{3,4,28,29,30,31} ; negative can be more pronounced (up to 2‰) in $\delta^{13}\text{C}(\text{org})$ ²⁹	Second-order multiphase extinction ranked 9 in ecological severity and 8 in taxonomic loss ⁶ . Conodont and trilobite extinctions at the base, ammonoid extinction near the top of event interval ^{3,6}
Eifelian	Bakoven (DeSantis and Brett, 2011)		<i>australis</i> ^{3,32}	onset of oxygen-deficient (not truly anoxic) sedimentation in E. North America ³² ; referred to as might-be eustatic sea level rise ³	not clear	positive $\delta^{13}\text{C}(\text{carb})$ excursion of modest amplitude (similar or slightly less than Kačák excursion) ^{31,33}	minor (4th order) faunal turnover ³²
Eifelian	Basal Choteč (Chlupáč and Kukal, 1988)	<i>Pinacites jugleri</i> (Walliser, 1985)	uppermost <i>partitus</i> to <i>costatus</i> ³	thin anoxic horizon intervening in oxic facies successions in Czech Rep., Morocco, S. Siberia and S. China ^{3,10}	not clear; likely very short	Very low-amplitude (<1‰) positive $\delta^{13}\text{C}(\text{carb})$ shift preceded by weak negative deflection in Czech Rep. ²⁶	Minor extinction affecting several groups ³

References in Table 1: ¹Kaiser et al., 2016; ²Johnston et al., 2010; ³Becker et al., 2020; ⁴Cramer and Jarvis, 2020; ⁵Stupakova et al., 2017; ⁶McGhee et al., 2013; ⁷Hartenfels and Becker, 2009; ⁸Pisarzowska and Racki, 2020; ⁹Stock and Sandberg, 2019; ¹⁰House, 2002; ¹¹Kabanov, 2019; ¹²Percival et al., 2018; ¹³Becker et al., 2012; ¹⁴Sandberg et al., 2002; ¹⁵Bond and Wignall, 2005; ¹⁶Pisarzowska et al., 2020a; ¹⁷Lash, 2019; ¹⁸Lüning et al., 2004; ¹⁹Becker and House, 1997; ²⁰House et al., 2000; ²¹Wendte and Uyeno, 2005; ²²Zambito et al., 2016; ²³Aboussalam and Becker, 2011; ²⁴Aboussalam, 2003; ²⁵Lottmann, 1990; ²⁶Vodrážková et al., 2013; ²⁷House, 1996; ²⁸Kabanov and Jiang, 2020; ²⁹van Hengstum and Gröke, 2008; ³⁰Qie et al., 2018; ³¹Buggisch and Joachimski, 2006; ³²DeSantis and Brett, 2011; ³³van Geldern et al., 2006; ³⁴Ellwood et al., 2011; ³⁵Pană et al., 2018; ³⁶Liang et al., 2020; ³⁷Copper, 2002; ³⁸Myrow et al., 2014; ³⁹Heath et al., 2021; this work⁴⁰.

records (Fig. 1G): the Lochkovian to Emsian cooling trend is followed by the Middle Devonian nadir (19–25 °C in brachiopods, 30–35 °C in conodonts), and then by the Givetian-Frasnian warming trend (GFWT). The GFWT started with the Taghanic overheating anomaly, particularly abrupt in brachiopod records (Joachimski et al., 2004). Average seawater temperatures reached a maximum during the Middle to Late Frasnian (~30–45 °C in both records), followed by a Famennian cooling trend as measured on conodont phosphate (Grossman and Joachimski, 2020). Most recent data indicate that sea-surface waters during the mid-Devonian Kačák event were warmer than previously thought (Suttner et al., 2021).

3. Devonian sea level changes – a critical outlook

The debate on Devonian sea-level fluctuations continues over decades with no sign of resolution (e.g., Johnson, 1971; Filer, 2002; Bond and Wignall, 2008; Elrick et al., 2009; Brett et al., 2011; Becker et al., 2020). This is not surprising. Extraction of the eustatic signal from regional stratigraphic records is challenging, and even if some consensus is achieved on the number and hierarchy of cycles, the absolute amplitudes of sea level change usually remain unscaled (Simmons et al., 2020). Noteworthy, sea level fluctuations of 3rd–5th orders are also highly debatable in the better preserved and better understood greenhouse stratigraphic archive of the Cretaceous – early Cenozoic (Immenhauser, 2005; Sames et al., 2016, 2020; Ray et al., 2019; Davies et al., 2020).

3.1. To what extent does sedimentary cyclicity reflect sea level fluctuations?

Although facies repetitions manifesting 4th and 5th order cyclicity (< 0.5 My) are not uncommon in Devonian shallow-marine strata (e.g., Elrick, 1995; Brett and Baird, 1996; Da Silva and Boulvain, 2006; Tucker and Garland, 2010; Vierek, 2014; Brady and Bowie, 2017), the evidence for base-level changes is rather short. This is equally true for the 3rd order cycles (0.5–3.0 My *sensu* Haq and Shutter, 2008) which describe the recurrence of anoxic events. Moreover, the eustatic interpretation of the 3rd order cycles in the Catskill Delta succession, the heartbeat of Johnson et al. (1985) sea level curve, is challenged by rather strong arguments for tectonic control (Ettensohn, 1994; Smith et al., 2019).

Amongst the most rigorous indications of sea- and base-level fluctuations are subaerial unconformities. In the Middle-Upper Devonian, subaerial exposure surfaces separating 4th order cycles are documented only in very shallow water settings referred to as upper ramps (Elrick, 1995), peritidal successions (Tucker and Garland, 2010; Kabanov, 2014; Kabanov, 2021), epicontinental sea strata (Witzke and Bunker, 1996; Brady and Bowie, 2017), tops of carbonate buildups (Wong et al., 2017), or marine-fluvial cyclic packages (McClung et al., 2013). The depth of pedogenic penetrations and paleokarsts in the tops of these cycles is often described in centimetres (Elrick, 1995; Brady and Bowie, 2017; Wong et al., 2017), whereas deeper penetrating (> 1 m) subaerial exposure profiles are notably rare comparing to icehouse stratigraphic successions (Chen and Tucker, 2004; Wong et al., 2017; Kabanov, 2021) and do not appear to align at one stratigraphic level in examples of tightest age control such as the Frasnian-Famennian boundary (Hallam and Wignall, 1999; Bond and Wignall, 2008). “Erosional unconformities” of submarine origin associated with anoxic events are not correlated worldwide and are interpreted as being controlled by local tectonics (e.g., Baird and Brett, 1991; Ettensohn, 1994; Johnston et al., 2010; Kaiser et al., 2016). Moreover, some paleokarsts formerly taken as an evidence of major eustatic lowstands separating 3rd order cycles of Johnson et al. (1985) actually formed in settings of syndepositional blocky tectonics (e.g., Chow et al., 2004).

Another approximation to base level falls is fluvial incisions. Deep (> 10 m) fluvial downcutting is rarely reported in the Middle-Upper Devonian (Witzke and Bunker, 1996; McClung et al., 2016; Evans

et al., 2019). Of three cited examples, the deepest (≥ 25 m) incisions occur in settings of active syndepositional tectonics (McClung et al., 2016; Evans et al., 2019). Conspicuous changes occurring in stacking patterns of riverine sequences deposited during the later Famennian indicate the increase of fluvial downcutting during the transition to the first phase of the Late Paleozoic Ice Age (LPIA; Eriksson et al., 2019). Evidence for sea level fluctuations in the main, pre mid-Famennian part of the Devonian, is particularly meager in comparison with icehouse sedimentary archives with high resolution records of deep, frequent (4th to 5th order) base level falls, fluvial incisions, and high-amplitude marine transgressions in cyclothemic strata (LPIA examples: Soreghan and Giles, 1999; Heckel, 2008; Kabanov et al., 2010; Eriksson et al., 2019; Le Cottonnec et al., 2020; Isbell et al., 2021).

A great number of case studies interpret sea level fluctuations in the Devonian shelfal strata where tidal flat facies, shoreface units, or sub-aerial breaks do not intervene. The sequence stratigraphic models and/or sea level reconstructions in such successions heavily rely on instrumental proxies: wirelogs and its outcrop counterparts (notably gamma ray spectrometry), bulk magnetic susceptibility (MS), and diverse organic, isotopic, and elemental chemostratigraphy proxies. Literature interpreting Devonian sea level fluctuations from such proxies is immense. Examples from Western Canada are provided by Whalen and Day (2010), Dong et al. (2018), and Harris et al. (2021). Recent reviews provide more case studies (Da Silva et al., 2013; Pas et al., 2019; Becker et al., 2020; Racki, 2020a). Cyclostratigraphic calibrations of instrumental proxy records are now advanced enough to drastically narrow dating of geochronologic boundaries (e.g., Ellwood et al., 2011; De Vleeschouwer et al., 2017; Percival et al., 2018) and calibrate stage durations in the Devonian System (review in Becker et al., 2020).

High-fidelity correlation between MS, $\delta^{18}\text{O}$, and glacial-interglacials in the Quaternary initially inspired application of MS to the Paleozoic, particularly to the Devonian strata (Ellwood et al., 1999; Da Silva et al., 2013). Nevertheless, the last two decades of research have not provided an answer to the underlying question of how to deconvolve sea level fluctuations from the rhythms/cycles recorded in MS and chemostratigraphic proxies.

In pelagic sediments, bulk MS is mainly carried by single-domain magnetite or greigite produced by magnetotactic bacteria thriving at the redox boundary (magnetofossils; Kopp and Kirschvink, 2008; Roberts et al., 2013). In the Pleistocene-Holocene, a strong correlation exists between the abundance of magnetofossils and MS signals from pelagic, aeolian, and marine siliciclastic sequences on one hand, and glacial-interglacial cycles on another. However, there is still no rigorous evidence for strong temperature or sea level control over high-frequency cycles revealed by MS and other proxies in Devonian successions. As such, the initial assumption that oscillations in bulk MS reflect sea level changes in the Devonian just like in the Quaternary (e.g., Ellwood et al., 1999) is no longer embraced with enthusiasm. The same caution applies to oscillating contents of siliciclastics-associated elements such as Ti, Al, Fe, K, Cr and Zr. In Devonian marine sequences these oscillations can be at best interpreted as pulses of detrital input in response to fluctuating runoff and/or dust supply (e.g., Bábek et al., 2018; Pas et al., 2021). On the other hand, buildup of authigenic enrichment in redox sensitive metals (such as Mo, U, V) reflects pulses of oxygen deficiency (progression from oxygenated to euxinic condition). None of these elemental oscillations in stratigraphic sequences can on their own translate into sea level changes.

3.2. Oxygen isotope records of high-frequency cycles

The $\delta^{18}\text{O}$ of diagenetically stable biogenic calcites and phosphates is known to imprint two dominant signals: the temperature and isotopic balance of ambient seawater (review in Simmons et al., 2020). The isotopic balance of seawater changes by sequestering ^{16}O into ice (thus shifting seawater $^{18}\text{O}/^{16}\text{O}$ balance towards heavier values), and it also changes with fluctuating salinity (dilution by freshwater shifts $^{18}\text{O}/^{16}\text{O}$

towards lighter values). As summarized by Simmons et al. (2020), challenges in extracting ice signal are significant, but a range of techniques (e.g., Ca:Mg corrections for foraminiferal tests) seem to be working at least for the Cenozoic. In the Miocene-Quaternary, fluctuations of $\delta^{18}\text{O}$ in a variety of carrier minerals are linked to glacial-interglacials with high fidelity (Grossman and Joachimski, 2020), and the presence of similar high-frequency $\delta^{18}\text{O}$ cycles as measured on conodonts was indicated in the cyclothemic successions of LPIA (Elrick and Scott, 2010).

High-frequency $\delta^{18}\text{O}$ fluctuations also characterize the Late Cretaceous – Eocene, a time of a strongly dominant greenhouse regime, and this was interpreted as a glacio-eustatic response to ephemeral ice caps prior to establishment of the permanent ice sheet in Antarctica (e.g., Pekar et al., 2005; Miller et al., 2005). In a similar manner, an enquiry was made into how far such $\delta^{18}\text{O}$ fluctuations extend back in time from the LPIA. Using conodont phosphate, Elrick et al. (2009) revealed a few My-scale (3rd order) isotopic cycles of $\sim 1.5\%$ amplitude in the Late Emsian-Eifelian. Subsequently Elrick and Witzke (2016) revealed high-frequency (5th order, 0.5–3.0 m) $\delta^{18}\text{O}$ cycles of $\sim 0.6\text{--}1.0\%$ amplitude in the Givetian epicontinental strata. Elrick and co-authors argue that these $\delta^{18}\text{O}$ fluctuations indicate glacio-eustatic forcing during the Middle Devonian, although glacial deposits are unknown in pre-Middle Famennian Devonian and world records of isotopic paleotemperatures indicate much warmer sea-surface temperatures than today or during the LPIA (Fig. 1G). However, what if only seawater temperature variations and freshwater inflow/withdrawal were driving high-frequency $\delta^{18}\text{O}$ fluctuations during the Devonian greenhouse?

3.3. Controls on high-frequency sea level fluctuations during the greenhouse

In a model ice-free world, two hypothetical mechanisms are called upon to explain high-frequency sea level fluctuations. *Thermal eustasy* (a.k.a. *steric sea-level change*) stands for the cyclic expansion-contraction of the oceanic watermass in response to its heating and cooling (Piecuch and Ponte, 2014; Sames et al., 2016). *Aquifer eustasy* refers to the fluctuating proportion of water retained in groundwater reservoirs with minor addition from open waters in lakes and rivers (Hay and Leslie, 1990; Föllmi, 2012; Wagreich et al., 2014; Sames et al., 2016, 2020; Ray et al., 2019). In the absence of ice, the total aquifer water potentially available to cyclically discharge into the ocean and recharge back, is estimated as 8 to 50 m equivalent of the sea level change (Ray et al., 2019). The thermal or steric component of the non-glacial eustasy is considered overall minor to the aquifer potential, as not exceeding 10 m on the kyr-scale range, although capable of fast (year-scale) response, which is unavailable for the aquifer eustatic cycles (Sames et al., 2016).

Summarizing extensive knowledge on the Cretaceous, Föllmi (2012) rolls out a dynamic greenhouse scenario where the effect of CO_2 forcing into hotter climate results in the increase of vapor retention in the atmosphere, reduction of evapotranspiration through higher cloudiness, and intensification of the hydrological cycle, by which aquifers and inland lakes retain more water than during the normal (unforced) greenhouse condition. The net effect of this CO_2 forcing is seen in a sea level drop of a few meters, and moreover, surface oceanic waters will likely cool as the expanded overcast will shield the Earth surface from insolation (*ibid.*). It follows that sedimentary cycles created through such greenhouse pulses will record lowstands at the globally hottest phase, which is inverse to icehouse cycles. Furthermore, sea-surface cooling, combined with atmosphere-aquifer retention of freshwater, will shift the $\delta^{18}\text{O}$ balance in marine biogenic minerals to heavier values, thus mimicking a response of expanding ice caps in an icehouse world. This scenario, however, may not withstand an advanced simulation of global Earth-surface processes. Davies et al. (2020) simulate difference in aquifer capacity under lowest and highest possible CO_2 forcings for the Valanginian, Turonian, and Maastrichtian time slices. Their results show that arid areas moderately expand under high- CO_2 regime and

locally become much drier, whereas hydrological cycle intensifies in humid belts only, which keeps the eustatic effect of the aquifer recharge invariably below 1 m. As such, glacio-eustasy would still be required to explain Cretaceous sea-level changes (*ibid.*). Regardless of presence or absence of some form of ice and glacioeustasy, the scarcity of empirical evidence of sea-level changes in both the Cretaceous and the Devonian casts doubt on sea-level amplitude estimates (such as those by Haq and Shutter, 2008 and Haq, 2014) as routinely exceeding ~ 25 m for 4th and 3rd order cycles.

Limited isotopic data from the Devonian events fit into an ice-free greenhouse scenario better than into a glacioeustasy-driven one. From their study of Nd isotope records in conodonts, Dopieralska et al. (2016) infer that the Lower and Upper Kellwasser anoxic events coincided with sea level drops in the Variscan domain (in sections of W. Europe and Morocco). It should be noted that the $\epsilon_{\text{Nd}(t)}$ proxy measured on conodonts (or other marine minerals formed in equilibrium with ambient seawater) does not translate directly into sea level changes, but it is a tracer of degree of ocean openness. Dopieralska et al. (2016) demonstrate that the LKW and UKW events are marked by lows in radiogenic ^{143}Nd , and consequently, the inflow of oceanic waters into Variscan sea should have been more restricted during these anoxic episodes. Essential for this discussion is that the interpretation of Dopieralska et al. (2016) appears consistent with the conodont $\delta^{18}\text{O}$ record suggesting cooling of surface waters in the Tethyan realm during Kellwasser anoxia (Huang et al., 2018). Based on the compilation of Grossman and Joachimski (2020), such cooling at the Frasnian-Famennian boundary is also manifested in brachiopod records from Siberia, whereas in other regions brachiopod and conodont $\delta^{18}\text{O}$ indicate overheating. The $\delta^{18}\text{O}$ shifts to heavier values are also recorded in conodonts and carbonate materials at the Early-Middle Frasnian transition and throughout the Middle Frasnian of southern Poland (Pisarzowska and Racki, 2012).

4. Biomarker evidence for widespread photic-zone euxinia

The deep-water interpretation of black shales as a core element of the Devonian sea-level curve of Johnson et al. (1985) is further challenged by biomarker evidence. Green sulfur bacteria (GSB) and purple sulfur bacteria (PSB) are obligatory anaerobic phototrophs synthesizing precursor macromolecules to the fossil aromatic C_{40} carotenoids and specific aryl isoprenoids (e.g., Koopmans et al., 1996). Since the 1980s, these biomarkers are increasingly used as indicators of the photic-zone euxinic condition (PZE) in the stratigraphic record (Summons and Powell, 1986, 1987), providing that thermal maturation did not progress to the destruction of aromatic compounds (e.g., Kabanov and Jiang, 2020). Rapidly increasing awareness of GSB biomarkers (Table 2) suggests that PZE was a normal and geographically widespread condition of Middle-Upper Devonian shelf seas, just like it was through the Mesozoic and the Early Cenozoic (Pancost et al., 2004; Van Bentum et al., 2009; French et al., 2015). The most disastrous and protracted hothouse perturbation across the Permian/Triassic boundary has the same PZE signature (Grice et al., 2005 and following works).

The GSB (family Chlorobiaceae) include green and brown clades which vary in biosynthesis of chlorophyll and carotenoids (Imhoff and Thiel, 2010; Ma and Cui, 2022). The green-colored GSB synthesize bacteriochlorophyll *c* and *d* and chlorobactene. The brown-colored GSB synthesize bacteriochlorophyll *e* and isorenieratene. Chlorobactene adsorbs light at the wavelength of 435, 461, and 491 nm, which restricts their habitat to the highest light intensity (Britton et al., 2004), and the presence of chlorobactene (derivative of chlorobactene) conventionally indicates paleo water depth of about 15 m or less (reviews by French et al., 2015; Ma and Cui, 2022). The ability of isorenieratene to absorb light at slightly longer frequency (425 and 450 nm) makes diagenetic products of this pigment (isorenieratane and aryl isoprenoids) an indication of sulfidic environment at water depths down to ~ 100 m (*ibid.*). Another fossil C_{40} carotenoid is paleorenieratane. Its precursor pigment is unknown amongst living bacteria, and its current fossil record ends at

the Permian-Triassic boundary (French et al., 2015). Paleorenieratane usually co-occurs with isorenieratane in Paleozoic strata, and these two carotenoids exhibit a very similar carbon isotope composition, suggesting derivation of paleorenieratane from an extinct group of GSB which was phylogenetically close to extant brown GSB (*ibid.*). Isorenieratane, paleorenieratane, and aryl isoprenoids are increasingly reported from Middle Paleozoic marine sediments (Table 2). Presence of chlorobactane in the Devonian, and hence the depth of sulfidic environment within the upper ~15 m of the water column, is currently

established only in the oceanographically restricted shallow-water carbonate setting of Canning Basin in Australia (Spaak et al., 2018).

Purple sulfur bacteria (family Chromatiaceae) synthesize bacteriochlorophyll *a* or *b* and various carotenoids, of which okenone has an intermittent fossil record throughout the Phanerozoic in the form of okenane. PSB flourish in stagnant stratified water bodies, such as lakes, in planktonic layer and in bacterial mats at depths not exceeding 24 m (French et al., 2015; Ma and Cui, 2022). Unlike isorenieratane, paleorenieratane, and aryl isoprenoids, okenane rarely occurs in marine

Table 2
Reports of PZE biomarkers in Middle Devonian – Early Mississippian marine sediments.

Case study	Age range of samples	Lithostratigraphy	Basin	Major biotic extinction	PZE biomarkers	Oceanographic regime of the basin
Kabanov and Jiang, 2020	Latest Eifelian - M. Frasnian ¹	Horn River Group (Canol Fm., Bluefish Mb.)	Peel Shelf, Canada	None	trimethyl aryl isoprenoids; isorenieratane	open ¹
Jiang et al., 2001; Aderoju and Bend, 2018	L. Famennian - E. Tournaisian ²	Bakken Fm.	Williston Basin, Canada	D/C	aryl isoprenoids; isorenieratane, paleorenieratane	open to semi-restricted ³
Spaak et al., 2018	L. Givetian - L. Frasnian ^{4,13}	Sadler/Gogo Fm.	Canning Basin, Australia	None	chlorobactane, isorenieratane, paleorenieratane, aryl isoprenoids mostly in restricted settings	variable: restricted to semi-restricted ⁵
Bushnev et al., 2016	M. Frasnian ¹⁰	Domanik Fm.	Timan-Pechora Basin, Russia	None	isorenieratane, β -isorenieratane	NED
Poludetkina et al., 2017	Late E. to M. Frasnian	Domanik Fm. (M. Frasnian); Sargaevo Fm (E. Frasnian)	Volga-Urals Basin, Russia	None	“isorenieratene derivatives”, incl. aryl isoprenoids; compound X	NED
Brown and Kenig, 2004	L. Givetian - E. Mississippian	New Albany Fm., Antrim Fm.	Michigan and Illinois basins, U.S. A.	F/F, D/C	isorenieratane; diaryl isoprenoids (compound X)	semi-restricted ³
Joachimski et al., 2001	L. Frasnian - E. Famennian ⁶	Organic rich shales and carbonates of Lower and Upper Kellwasser black shales	Holy Cross Mts., Chęciny-Zbrza Basin, Poland	F/F	Isorenieratane; diaryl isoprenoids	NED; carbonate-shelf facies interbedded with black shales ⁶
Marynowski et al., 2008	latest E. Frasnian - M. Frasnian	Organic rich shales and carbonates equivalent to Rhinestreet and Middlesex sourcerocks	Holy Cross Mts., Poland	None	Isorenieratane; diaryl isoprenoids	<i>ibid.</i>
Marynowski and Filipiak, 2007; Marynowski et al., 2012	L. Famennian - E. Tournaisian	Organic rich shales equivalent to Hangenberg black shale	Holy Cross Mts., Poland	D/C	isorenieratane; aryl isoprenoids	<i>ibid.</i>
Connock et al., 2018	E. Frasnian-E. Tournaisian	Woodford Fm.	Arkoma Basin, U.S. A.	F/F, ?D/C	paleorenieratane, isorenieratane, renierapurpurane	Open to semi-restricted ³
Requejo et al., 1992	E.-M. Frasnian ⁹	Duvernay Fm.	Western Canada Sedimentary Basin	None	Aryl isoprenoids; isorenieratane	NED
Riboulleau et al., 2018	L. Frasnian - Famennian	Aouinet Ouenine Fm., units III and IV	Ghadames Basin, Libya	NED; ?F/F	palaerenieratane; isorenieratane; aryl isoprenoids	NED; likely semi-restricted ⁸
Haddad et al., 2016	L. Frasnian-E. Famennian ¹¹	Tomachi Fm., Upper Kellwasser equiv. interval	Madre de Dios Basin, Bolivia	F/F	trace isorenieratane and palaerenieratane; no isorenieratane at F/F level	NED
Haddad et al., 2016	L. Frasnian-E. Famennian ³	Hannover Fm., Upper Kellwasser equiv. interval	Appalachian Basin, U.S.A.	F/F	low abundance of aryl isoprenoids and palaerenieratane; trace isorenieratane	semi-restricted ³
Philp and DeGarmo, 2020	Givetian-Famennian ¹²	Woodford Fm.	Oklahoma Basin, U. S.A.	NED	trimethyl aryl isoprenoids; isorenieratane	open ³
Martinez et al., 2019	L. Famennian - E. Tournaisian	Cleveland Shale	Appalachian Basin, U.S.A.	D/C	isorenieratane, paleorenieratane, aryl isoprenoid fragments	semi-restricted ³
Souza et al., 2022	E. to L. Frasnian ¹⁵	Pimenteiras Fm.	Parnaíba Basin, Brasil (high paleo-latitudes)	None	ND	Intracratonic, semi-restricted
Rakociński et al., 2021b	M. Famennian ¹⁴	Zaręby Beds	Chęciny-Zbrza Basin, Poland	None	isorenieratane, paleorenieratane, diaryl isoprenoids	semi-restricted to restricted based on U/Mo ¹⁴
Lu et al., 2021	E. Frasnian-L. Famennian ¹⁶	Chattanooga Shale	Cincinnati arch within Appalachian Basin, U.S.A.	F/F	aryl isoprenoids throughout the section	open, shallow-water (at or above SWB) ¹⁷

Notes: Data from migrated oils are not included. Major biotic extinctions: (F/F) at the Frasnian-Famennian boundary and (D/C) at the Devonian-Carboniferous boundary. Numerous minor turnovers in marine faunas are not itemized. NED = not enough data. SWB = storm wave base. References to geologic age and paleoceanographic settings: ¹Kabanov (2019); ²Johnston et al. (2010); ³Algeo and Tribouillard (2009); ⁴Nicoll (1984); ⁵Spaak et al. (2018); ⁶Narkiewicz (2007); ⁸Riboulleau et al. (2018); ⁹Wendte and Uyeno (2005); ¹⁰Gatovskii et al. (2016); ¹¹Haddad et al. (2016); ¹²Philp and DeGarmo (2020); ¹³Tulipani et al., 2015; ¹⁴Rakociński et al., 2021b; ¹⁵de Andrade et al., 2020; ¹⁶Over (2007); ¹⁷Li and Schieber (2015).

sediments, and it is currently unknown in the Devonian.

The biomarker fingerprints of PZE were encountered on a paleogeographic high where the section is condensed and seen as overall shallow-water (Lu et al., 2021). This further indicates that the chemocline in Late Devonian seas could have risen at times to quite shallow depths, significantly <100 m, consistent with other indications of episodic chemocline shallowness. Black shales directly onlap erosional unconformities in the distal, epicontinental part of the Appalachian clastic wedge, which historically was seen as evidence of a shallow-water depositional environment (Baird and Brett, 1991; Ettensohn, 1994; Smith et al., 2019). Equally noteworthy, Bond et al. (2013) provide an indication of authigenic U and TOC enrichment at the Upper Kellwasser event level in a very shallow-water setting of a carbonate platform interior.

The marine PZE condition seems to be much less common in icehouse oceanic circulation regimes. For example, no Carboniferous – Lower Permian findings of PZE biomarkers are trackable (French et al., 2015) except for the early-middle Tournaisian (Aderoju and Bend, 2018; Martinez et al., 2019; Rakociński et al., 2021a).

5. Time-specific facies architecture

The concept of time-specific facies (Walliser, 1984, 1996) denotes distinctive facies restricted to a precise time slice when they occur in more than one locality globally, while being totally absent in other intervals of the geologic time (Ferretti et al., 2012; Brett et al., 2012). The Devonian Period was a time of the broadest geographic expanse of carbonate platforms for the Paleozoic (Kiessling et al., 2003), with reef tracts likely reaching high latitudes of about 45° S to 45° N (Copper and Scotese, 2003; Joachimski et al., 2009). These reefs s.l. encompass a broad continuum of carbonate buildups from metazoan reefs to mud mounds. The latter are characterized by extensive *Stromatolites* fabrics and relatively few metazoan remains which are “submerged” within micritic matrix (e.g., Pratt, 1995; Zhou and Pratt, 2019). The mud mound fabrics were particularly widespread during the Devonian and Mississippian, literally vanished from the fossil record during the Late Mississippian transition to the main LPIA phase, and returned in less prominence after the end-Permian mass extinction (Rodríguez-Martínez, 2011). Deep-ramp occurrences of mud mounds suggest a different control over buildup growth, which was conceptualized as a mud mound carbonate factory (Monty, 1995; Pratt, 1995; Schlager, 2003). However, neither mud mounds nor spreads of anoxic sediments make Devonian facies assemblages time specific, as both occur over wide stratigraphic intervals, and the record of mud mounds ranges back to the Proterozoic (Pratt, 1995; Rodríguez-Martínez, 2011). Still, the inventory of facies specific to Devonian time (Brett et al., 2012) is incomplete without inclusion of the *bank-and-trough facies architecture* – extensive co-occurrence of carbonate banks s.l. and interbank hypoxic-anoxic sediments with documented facies transitions between each other (MacKenzie, 1973; Knapp et al., 2017; Shaw and Harris, 2022). The carbonate banks s.l. are variously referred to as patch reefs, mounds, atolls, or pinnacles, and the interbank depressions are sometimes narrow and described in the literature as sags, troughs, or straights. Basins with such facies architecture usually occur on lower shelves off shallower-water zones occupied by main carbonate platforms. Copper and Scotese (2003) conceptualized this abundance and vast geographic expanse of carbonate banks in the pre-Famennian Devonian as “mega-reef belts”. Noteworthy, the pinnacle reef/bank sedimentary architecture was also widespread in the Silurian (e.g., Cramer et al., 2015; McLaughlin et al., 2019).

To add essential arguments for our discussion, below we review two such depositional systems of the Frasnian time.

5.1. Eastern Baltica

The Baltica Craton (a.k.a. Russian Platform or East European Craton)

entered into a phase of continental rifting during late Early to Middle Devonian, which profoundly altered the tectonic structure of the craton (Nikishin et al., 1996). Rifting continued into the Late Devonian, most intensely in south-central and northern parts of Baltica where it was associated with extensive volcanism (Pripyat-Dnieper-Donets and Kola large igneous provinces; Kravchinsky, 2012). Concomitantly with rifting, a broad stripe of shelfal areas along the eastern continental margin, previously uplifted or covered with shallow-water deposits, became overlapped with progressively more offshore sediments, until the anoxic sediments of the Domanik Formation had spread over vast areas now comprising the Timan-Pechora and Volga-Uralian hydrocarbon provinces (Fig. 2A; Ulmishek, 1988). Acceleration of subsidence along the eastern continental margin could have been caused by the accretion of volcanic arc assemblages from the Uralian Ocean which coincides in time with the Givetian-Frasnian transgression, although no significant crustal downwarping and foreland basin development happened until the mid-Carboniferous continent-continent collision (Brown et al., 2006; Puchkov, 2009).

The Domanik black-shale deposition, usually described as a major transgression, commenced nearly simultaneously in both provinces at the base of *punctata* conodont Zone and lasted until upper *hassi* to, locally, *jamieae* zones (Ovnatanova and Kononova, 2008; Gatovskii et al., 2016) thus spanning the entire Middle Frasnian as defined in GTS 2020 (Becker et al., 2020). Late Frasnian-Tournaisian anoxic sediments of interbank depressions occurring stratigraphically above the Domanik Formation are conventionally referred to as domanikoids or domanikites (Liang et al., 2020). The Middle Frasnian was a time of maximum eastward retreat of carbonate platforms, although they did not vanish completely, and isolated carbonate mounds also occur in the Domanik Formation except maybe its basal part (Ulmishek, 1988; House et al., 2000). The thickness of the Domanik Formation is remarkably uniform for such a broad geographic expanse, ranging between 10 and 30 m in its typical condensed anoxic facies and up to 100 m where carbonate mounds are present. The abundance of aryl isoprenoids revealed in Late Devonian domanikoid facies of the Timan-Pechora and Volga-Uralian basins indicates incursion of PZE conditions (Bushnev et al., 2016; Smirnov et al., 2020).

The Domanik transgression initiated a protracted phase of bank-and-trough facies development in both the Timan-Pechora and Volga-Uralian basins, which resulted in the aggradation of carbonate buildups, while progradation was overall slow and mostly limited to larger platforms (House et al., 2000; Zavyalova et al., 2019; Liang et al., 2020). This reduced ability of then-time carbonate platforms to prograde kept anoxic troughs in the sediment-starved regime for millions of years, until they became filled with carbonates and clastics later in the Famennian, Tournaisian, or even Early Viséan in different areas (Fig. 1B). Smaller isolated carbonate buildups were unable to prograde, and many of them retrograded at the late stage of their growth to form characteristic pinnacles extensively mapped in the subsurface (Mirchink et al., 1974; Nikitin et al., 2018; Vilesov et al., 2009, 2019, 2021). Growth of carbonate pinnacles on antecedent topographic highs within anoxic troughs can be locally demonstrated (Liang et al., 2020), while other studies do not reveal such pre-existing highs (Nikitin et al., 2018).

Summing up the extensive knowledge on regional geology, Ulmishek (1988) concluded that differential subsidence along reactivated faults, although repeatedly invoked as a control over this bank-and-trough facies architecture, has fallen short of evidence, specifically in the central part of the Volga-Uralian basin. Tectonic control is obvious where abnormally thick Late Devonian strata fill grabens or constrict into thin shallow-water carbonate platform above uplifted blocks (e.g., Lobkovsky et al., 1996). However, such structural relations are not common. The vast majority of seismic and well-based transects reviewed by the first author in published and proprietary sources indicates rather uniform thickness of Upper Devonian – lower Mississippian strata, essentially excluding tectonic control over this time-specific depositional topography.

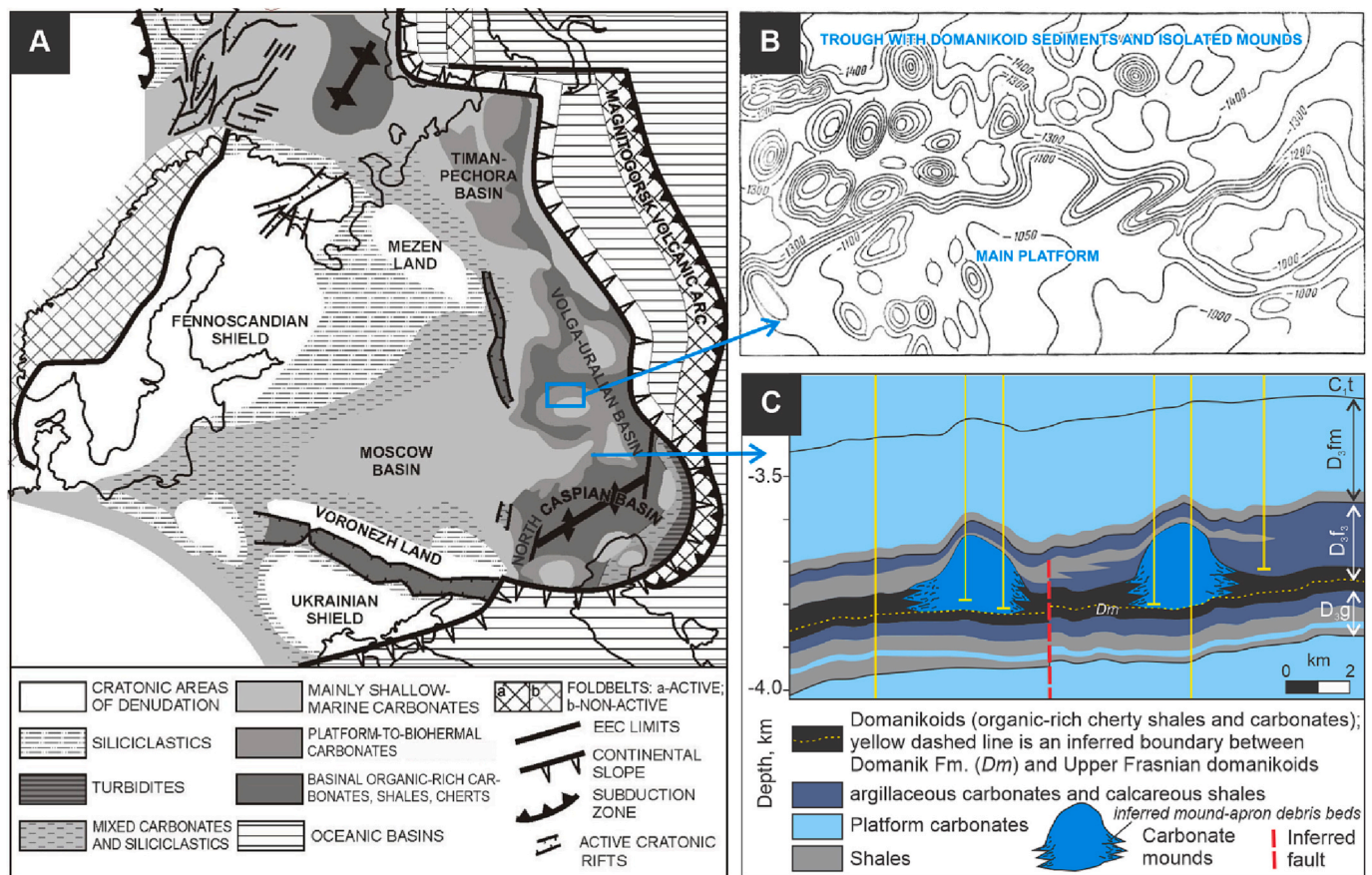


Fig. 2. Timan-Pechora and Volga-Uralian basins of the eastern Baltica Craton with extensive zones of bank-and-trough depositional topography. (A) Middle Frasnian through Famennian palaeogeography (modified from Nikishin et al., 1996). (B) Top-Famennian surface expressing Middle Frasnian-Famennian depositional topography of the main carbonate platform (south) and adjacent trough with numerous large carbonate mounds (Mirchink et al., 1974). (C) Carbonate mounds in southern Volga-Uralian Basin, redrawn from Nikitin et al. (2018). Yellow vertical lines are exploration wells. Age assignments are supported with biostratigraphy: C₁t = Tournaisian, D₃fm = Famennian, D₃f₃ = Late Frasnian, D₂g = Givetian, and D₂e = Eifelian. (For interpretation of the references to colour in this figure legend, the reader is referred to the web version of this article.)

5.2. Western Canada sedimentary basin

Mixed carbonate-siliciclastic deposits accumulated during the Givetian-Frasnian on the western margin of Laurentia, in the area now comprising the main part of Western Canada Sedimentary Basin (WCSB) in the subsurface of Alberta (Fig. 3). A long history of conventional hydrocarbon production (since 1947) has resulted in excellent well control, which permits detailed correlation of surfaces between carbonate buildups and basinal sediments into a robust sequence stratigraphic framework, which is also recognized in the adjacent Rocky Mountains (Wong et al., 2017).

Normal-marine sedimentation had spread over the WCSB in the Late Givetian, giving rise to shallow-water carbonate buildups (reefs and broader platforms). Off-reef sedimentation comprised argillaceous-carbonate oxic sediments (bioturbated wackestones and lime mudstones), until a major change occurred approximately at the base of *punctata* Zone with the spread of organic-rich, mostly laminated shales and lime mudstones of the Duvernay Formation, a major source rock and shale hydrocarbon play (Fowler et al., 2001). It should be noted that the designation “euxinic” to the Duvernay depositional environment (Wong et al., 2017) does not withstand closer facies analysis, which revealed the presence of benthic shelly fossils, bioturbation, and frequent disturbances of seafloor with turbidite and/or contourite currents (Chow et al., 1995; Knapp et al., 2017; Shaw and Harris, 2022). Carbonate buildups and platforms deposited coevally with the Duvernay are known as the Leduc Formation. The Leduc carbonates grew on paleotopographic highs and the edges of underlying platforms (Fig. 3). The

interfingering nature of the Leduc and Duvernay is particularly well documented on the eastern margin of the Redwater reef (Fig. 3C; Wendte, 1994; Chow et al., 1995; Wong et al., 2017). The highest TOC and other signatures of severe oxygen starvation occur within the Duvernay at the early *hassi* Zone interval, which is interpreted as the maximum flooding for the Givetian-Frasnian sequence (Chow et al., 1995; Wong et al., 2017). The greatest retrogradation of Leduc bioherms also occurred at this stratigraphic level (Fig. 3C), as documented in multiple sites across the basin (Wong et al., 2017).

Anoxic sedimentation of the Duvernay was eventually terminated by the introduction of muddy terrigenous siliciclastics (Ireton Formation on Fig. 3), which were largely sourced from the Ellesmerian Orogen in the Canadian Arctic (Boghossian et al., 1996). Contribution of Ellesmerian clastics also manifests in detrital zircon signatures in the younger Devonian (Hauk et al., 2017). By the late Frasnian, clastics of the Ireton Formation filled the inter-buildup basins and eventually suppressed the Leduc carbonate factory completely.

In the Cambrian-Triassic the western margin of Laurentia was dominantly in a passive continental margin regime. Recent research shows that this quiet tectonic regime was interrupted some time in the Devonian, which may be linked to the docking of an oceanic terrane further south in present-day Nevada and/or the establishment of a back-arc setting along the entire western continental margin of Laurentia (Root, 2001; Colpron and Nelson, 2009; Hedhli et al., 2022). The earliest volcanic tuff in the WCSB that indicates the proximity of a volcanic arc is Late Famennian in age (Savoy et al., 2000). However, much of this early tectonism is masked by the heavy overprint of later Mesozoic convergent

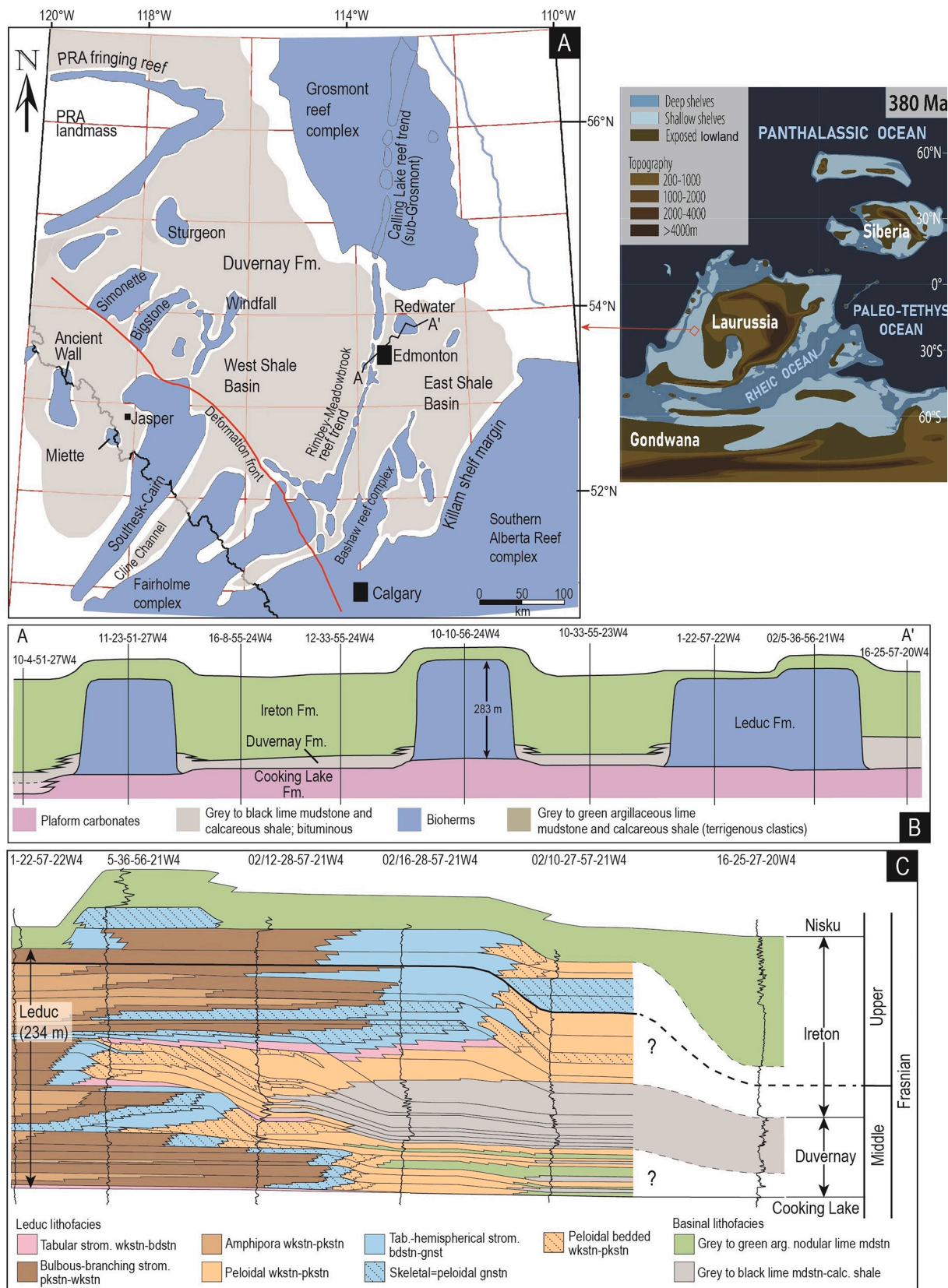


Fig. 3. The Frasnian Duvernay Formation and associated strata in the Western Canada Sedimentary Basin. A) Distribution of the Duvernay Formation (grey) adjacent to Leduc Formation reef complexes (blue). Plate tectonic position and palaeogeography of Laurussia, 380 Myr time slice, rectangular projection, is based on [Marcilly et al. \(2022\)](#). B) Stratigraphic cross-section (datum = base Cooking Lake Formation) running from the West Shale Basin northeastward through various Leduc reef complexes. C) Facies model of the eastern margin of the Redwater Leduc reef (see A)) showing the coeval deposition of Leduc carbonates and the basinal shales of Duvernay and Ireton formations. Modified from [Wong et al. \(2017\)](#). (For interpretation of the references to colour in this figure legend, the reader is referred to the web version of this article.)

tectonics during the Laramide Orogeny. It is unclear what effect, if any, this changing tectonic regime had on the initiation and termination of Duvernay deposits. However, multiple cross-sections intersecting the Leduc-Duvernay facies transition (Chow et al., 1995; Wong et al., 2017), as well as isopach maps, clearly demonstrate persistent thickness of the Late Givetian - Frasnian sequence (300–350 m). As such, no differential subsidence, such as that on a flank of actively subsiding graben or on foreland basin forebulge, can be invoked to explain this pronounced bank-and-trough facies architecture, although the influence of antecedent topography is clear.

5.3. Bank-and-trough facies architecture worldwide

The coeval shelfal basins exhibiting similar facies architecture of carbonate banks and interbank depressions occur in other world regions. Examples are Guangxi in South China (Ma et al., 2016), Lennard Shelf of the Canning Basin in Australia (Playford, 1980; Playford et al., 2009), and the Brabant shelf in Belgium (e.g., Boulvain, 2001, 2007). The long history of geological studies in Belgium made small-scale carbonate mounds and intermound facies in this region particularly well documented. The tectonic control over subsidence manifests in these three examples as involvement in foreland basins (Belgium and Australia) or intracratonic rifting for the Guangxi sedimentary system (Xun et al., 1996). However, in each case, no assumption can be made that carbonate mounds and platforms grew universally on uplifting tectonic blocks. Consequently, oceanographic factors in maintaining this time-specific facies architecture had to be involved.

6. Possible triggers and controls of Devonian events

Formerly popular cosmic impact explanations for mass extinctions (e.g., McLaren, 1983; Arens and West, 2008), are now out of fashion due to the mismatch of the age of known impact structures and biotic crises (Bond and Grasby, 2017), which is amply discussed by Racki (2005, 2020a) in application to Devonian events. Today the end-Cretaceous event remains the only example with a time match between bolide impact and the final phase of mass extinction (e.g., Vellekoop et al., 2016). In recent decades, the Earth-bound mechanisms explaining Devonian events have focused on volcanogenic or large igneous province hypothesis and the land-plant evolution hypothesis.

6.1. Evolution of land plants as a trigger for Devonian anoxia and biotic crises

Algeo et al. (1995) proposed that the spread of anoxic sediments and biotic crises in shelfal seas of the Middle-Late Devonian were induced by the evolutionary spread of vascular plants, and this authentic hypothesis was further expanded on three years later (Algeo and Scheckler, 1998). This “Devonian plant hypothesis” (also referred to as terrestrial-marine teleconnection hypothesis) involves the causal chain of expanding tracheophyte vegetation, root-assisted intensification of weathering leading to thicker soils and greater erodibility of river catchment basins, riverine influx of soil erosion products and plant debris into epeiric seas, resultant eutrophication, planktonic blooms leading to bottom anoxia, and toxic impact of these processes on benthic life habitats. This is currently seen as a leading hypothesis for Devonian anoxic and biotic extinction events (Caplan and Bustin, 2001; Carmichael et al., 2014, 2016; Dahl and Arens, 2020; Chen et al., 2021). Indeed, the late Emsian-Eifelian onset of major atmospheric oxygenation-decarbonization coincided with vigorous radiation of vascular plants leading to the advent of the first forests close to the Eifelian/Givetian boundary (Fig. 1E; Driese et al., 1997; Dahl and Arens, 2020). Positive $\delta^{13}\text{C}$ excursions associated with anoxic events can be interpreted as boosts of primary production which in a cratonic sea setting are normally maintained by riverine runoff. The fossil record of the Devonian also indicates that shallow water faunas were hit by

extinctions more severely than inhabitants of deep water, which suggests that toxicity was spreading from terrigenous sources (review in Bond et al., 2004).

However doubts were raised repeatedly on the ability of land plants to trigger mass extinctions in the Devonian (Hallam and Wignall, 1997; Racki, 2005, 2020a; Percival et al., 2019). As pointed out long ago (e.g., Hallam and Wignall, 1997), the effect of land plant cover on nutrient runoff is ambivalent. Although the increase of depth and density of root penetration certainly increases the depth and efficacy of chemical weathering, nutrients released from parent rock are largely sequestered within plant tissues, soils and wetlands, which also manifests in progressive stabilization of stream banks over the course of Silurian-Carboniferous (e.g., Gibling and Davies, 2012). Thus, on longer-term evolutionary time scale, the net effect should be an increase in nutrient retention rather than nutrient release (D’Antonio et al., 2019). Equally noteworthy, black-shale events with similar signatures of high-amplitude positive $\delta^{13}\text{C}$ excursions occurred in the Late Ordovician - earliest Devonian, long before the mid-Devonian evolutionary boom of vascular plants (e.g., Maikowski and Racki, 2009; Melchin et al., 2013; Smolarek et al., 2016), and the post-Devonian Phanerozoic also features numerous oceanic anoxic pulses which are obviously not associated with the major evolutionary spread of vascular plants. Vegetation had been essentially confined to fluvial corridors and coastal marshes until a seed reproductive strategy emerged in the middle Famennian (Fig. 1E; Prestianni and Gerrienne, 2010). Even after this evolutionary invention it took the entire Mississippian for seed plants to evolve enough to colonize seasonally dry landscapes and uplands, as manifested by fossil floras (DiMichele et al., 2010; Bashforth et al., 2014). This lack of dryland floras is consistent with unvegetated (primary desert, barren land) character of pre-Carboniferous nutrient-lean land surfaces, such as subaerially exposed carbonate platforms (Kabanov, 2021). Furthermore, uplands were barren of vascular plants before the Carboniferous (reviews in Falcon-Lang, 2005; Boyce and Lee, 2017). It follows that most of the land surface was not affected by root-assisted weathering long after this process had shown its effect in coastal marshlands and fluvial corridors under wet climates. This fundamental evolutionary limitation is not adequately addressed in simulations of Devonian vegetation cover. Thus, Le Hir et al. (2011) assume Middle and Late Devonian cordillera were vegetated, whereas Brugger et al. (2019) simulate barren regolith for highlands but vegetated plains for the tropical areas with indications of prevailing aridity (compilation in Boucot et al., 2013). The global character of extinctions cannot be reconciled with local impact of eutrophication, as terrigenous suspension supplied to shelfal seas under arid climates was obviously negligible to that required for a universal killer force.

6.2. Large igneous provinces as triggers for Devonian anoxia and biotic crises

Large igneous provinces (LIPs) are $>0.1 \text{ Mkm}^3$ (frequently $>1 \text{ Mkm}^3$) emplacements of mainly mafic effusives (although silicic LIPs or SLIPs are also recognized) which occur in both continental and oceanic settings. They are geographically extensive ($> 0.1 \text{ Mkm}^2$) basaltic plateaus formed by mantle plumes (Kravchinsky, 2012; Ernst et al., 2020, 2021). A typical mafic LIP consists of volcanic packages (flood basalts, effusives, volcanoclastics) and a plumbing system of dyke swarms, sills, and crustal magmatic underplates (Ernst et al., 2021). Emplacement appears to happen in short (mostly $<1 \text{ Myr}$) pulses accountable for over 75% of LIP effusives, and the total LIP lifespan does not exceed 50 Myr, usually much shorter (Kravchinsky, 2012; Ernst et al., 2020, 2021). Unfortunately, age constraints are still notably poor for pre-Permian LIPs (e.g., Bond and Grasby, 2017), and timing of Devonian LIPs is therefore not constrained on a $< 1 \text{ Myr}$ timescale.

Early ideas linking volcanism, spreads of black shales, and mass extinctions (e.g., Keith, 1982) gained support in recent years (review of Racki, 2020b). Today, LIPs, especially those emplaced in continental

settings, are seen as the main driver of dramatic changes in climate and ocean-atmosphere circulation systems (Wignall, 2001; Bond and Wignall, 2014; Bond and Grasby, 2017; Ernst et al., 2020). Degassing across extensive areas involved in LIPs leads to global warming through massive release of CO₂, and this greenhouse effect may be amplified by methane release from seafloor clathrates in warming oceans (e.g., Archer et al., 2009), and degassing from kerogen cracking of thermally affected rocks within LIP areas (Ganino and Arndt, 2009). At the same time, similarly large-scale volcanic co-emission of SO₂ leads to short-term cooling, which can last several years after major (but still minute comparing to LIP) eruptions (Self, 2015). The multiple toxic effects volcanic pollution exerts on life can amplify into a killer force during LIP eruptions (Bond and Wignall, 2014; Bond and Grasby, 2017; Grasby et al., 2019, 2020).

Several continental LIPs have age constraints partly or completely within the Devonian Period (Kravchinsky, 2012; Ernst et al., 2020; Racki, 2020a). A major issue with tying Devonian volcanism to biotic crises is the lack of high-resolution radiometric ages and detailed mapping. Another issue is that the use of LIP terminology also seems to include rift-related volcanics in the Devonian (e.g. Dniepr-Donets rift; Altay-Sayan rift), which is uncommon for other time periods.

Devonian magmatism accompanying continental rifting all over Baltica Craton had two centres of volcanic activity, one along the Pripyat-Dnieper-Donets aulacogen on the south (Pripyat-Dnieper-Donets LIP of Kravchinsky, 2012) and another in the Kola Peninsula (Kola/Kontogero LIP of Kravchinsky, 2012). Ernst et al. (2020, 2021) consider Baltica to be one igneous province named Kola-Dnieper, Baltica, or East European Craton LIP. Devonian dykes and effusives of this province are predominantly mafic, and associated alkaline rocks, kimberlites and carbonatites occur in the northern part of the craton (*ibid.*). The available age constraints for Devonian magmatism of the Baltica Craton are 380–360 Myr (Ernst et al., 2021). Kravchinsky (2012) lists the volume of Pripyat-Dnieper-Donets basalts as >1.5 Mkm³, but we note that the estimated volume is based entirely on modelling (Kusznir et al., 1996), as the volume of outcropping rocks is extremely limited. Furthermore, no radiometric ages are available for the Dniepr-Donets rift, and ages were determined by biostratigraphy on boreholes (Wilson and Lyashkevich, 1996). The volume of volcanic materials estimated for the Kola LIP is >0.1 Mkm³, although much higher volumes could have been emplaced in Kola but stripped with Baltic shield unroofing. Ernst et al. (2021) provide an estimate of 2.96 Mkm² for the size of the entire Baltica LIP. The third largest magmatic province of Devonian time is the Viluy LIP (a.k.a. Yakutsk-Viluy LIP) of the Siberian Craton with a preserved area of 0.3 Mkm², and volume of the emplaced basalts estimated at 0.1–0.25 Mkm³ (Polyansky et al., 2017), but other estimates as >1.0 Mkm³ of original effusive volume do exist (Kravchinsky, 2012). Two major pulses of eruptions are dated at 374.1 ± 3.5 Ma and 363.4 ± 0.7 Ma (review in Ernst et al., 2021). The fourth continental LIP is the ca. 407–392 Myr Altay-Sayan igneous province of the fragmented southwestern margin of the Siberian Craton, where effusives are represented by a wide range of volcanic rocks. The area of the Altay-Sayan LIP is at least 0.35 Mkm², and the volume of effusives is estimated as 120,000 km³ (Vorontsov et al., 2021).

Smaller magmatic provinces which were potentially able to amplify the global environmental effect of four (or three) LIPs are Magdalen (pulses of 380–370 Myr, ca. 360 Myr, and 330 Myr; Dunning et al., 2002), Kedon (400–345 Myr; may be part of Yakutsk-Viluy LIP), and possibly the Selwyn Basin (Canada) of northwestern Laurentia margin (reviews in Ernst et al., 2020, 2021; Racki, 2020a). Variability in cumulative volcanic arc emissions of CO₂, along with variable rates of its drawdown through weathering, can account for long-term (10–100 Myr) greenhouse-icehouse cycles, whereas LIPs are likely responsible for short-term (~1 Myr and less) and disastrous perturbations (McKenzie et al., 2016; McKenzie and Jiang, 2019).

It was noted that absolute ages available from LIP igneous assemblages are younger than Middle Devonian anoxic events, which is likely

due to an incomplete set of age data, although non-LIP mechanisms for global warming and anoxia prior to the Frasnian should not be completely discounted (Bond and Wignall, 2014; Ernst et al., 2020). Adopting volcanism as a universal driver for Devonian marine events is also confused by reports of time offsets between event levels and Hg loading spikes (Liu et al., 2021).

6.3. Volcanism and expanding land plants as linked drivers of Devonian events

The absence of one unequivocal driver, or controversy in appointing such a driver amongst known candidates, encourages to see Devonian anoxic and biotic events as multicausal or driven by press-pulse mechanisms (Carmichael et al., 2019; Racki, 2020a). This implies that one long-ranging stressor (*i.e.* LIPs, arc volcanism) has to be amplified by another short-term stressor (press-pulse) to knock the ecosystem out of stability, culminating in extinction (Arens and West, 2008).

Racki (2020b) and Piszarska and Racki (2020) summarise one such multicausal pathway under the name R&S (*Retallack/Racki-Schobben*) hypothesis. In this hypothesis, the volcanogenic and land-plant-evolution pathways are bound in a causal loop. This loop involves igneous outbursts associated with massive CO₂ release, which, in addition to driving the ocean into an anoxic event, promotes migration and expansion of plants due to pulsatory expansion of humid climates (Retallack and Huang, 2011). These intermittent spreads of vegetation boost weathering through expanded areas of rooting, which leads to marine anoxia through the teleconnection pathway of Algeo et al. (1995).

The R&S hypothesis also explains a sequence of carbon isotopic deflections from the initial low-amplitude negative δ¹³C swing to higher amplitude positive excursions documented in some Devonian events (Table 1), as well as isotopic events of other ages. The initial enrichment in ¹²C in this model is pushed by massive volcanic degassing, and its reversal into a ¹³C-enriched mode is linked to the succeeding burst of phytoplankton production caused by land-derived eutrophication. As the δ¹³C fingerprint of volcanically emitted CO₂ will not always be highly negative, but could be close to the average mantle source of carbon (−6 ± 2‰; Deines, 2002), the initial abrupt negative δ¹³C excursion characteristic of many Phanerozoic carbon perturbations is sometimes attributed to methane released from decomposing seafloor clathrates (e.g., Gales et al., 2020; Beil et al., 2020). This explanation is also embedded in the R&S hypothesis (Piszarska and Racki, 2020). However, it is unclear how much clathrate would survive in a greenhouse ocean if, as inferred by Kidder and Worsley (2010), its bottom waters will warm to ~15 °C or higher in hothouse conditions. Heating of bottom waters to 20–23 °C would release most methane completely (Buffett and Archer, 2004; Majorowicz et al., 2014). Furthermore, clathrate release is a slow self-limiting endothermic process according to Majorowicz et al. (2014), instead of a rapid outburst as often portrayed.

6.4. Other potential controls over Devonian anoxic and extinction events

More powerful than early land plant expansion, but a much slower (multimillion year range) engine of CO₂ drawdown, is weathering of ophiolite-containing orogens in tropical humid settings (Macdonald et al., 2019; Penman et al., 2020). Mafic effusives emplaced in LIPs, due to their large surface and weatherability comparable to ophiolite slivers in orogens, were also considered as auxiliary or even, at times, main contributors to atmospheric decarbonization (Kent and Muttoni, 2013). However, major Phanerozoic glaciations coincide with rise of orogenic masses in the tropics while showing no correlation with LIP basalts, pointing to tropical orogens as a main CO₂ removal agent (Macdonald et al., 2019). It was also hypothesised that a converse orogenic process of CO₂ degassing through metamorphic decarbonation could contribute to greenhouse conditions during the Devonian, however, this idea has not evolved beyond speculation (e.g., Stewart and Ague, 2018).

Onset of orogenic weathering along with several tropical continental sutures was thought to play a role in abrupt changes (transgressions, regressions, overheating and cooling) characterizing the Frasnian-Famennian event interval (Averbuch et al., 2005). However, this idea also remains conjectural, and this is also less applicable to Devonian events preceding the Frasnian-Famennian crisis. With much more certainty, orogenic weathering was a major agent of gradual CO₂ draw-down during the Famennian, acting in concert with carbon sequestration into anoxic sediments, marine carbonates, and lignitic coals. These processes compensated LIP degassing and induced Late Famennian glaciation as a result (Averbuch et al., 2005; Chen et al., 2021). This is consistent with ⁸⁷Sr/⁸⁶Sr records (Fig. 1F). Intensification of weathering in response to the rise of the tropical Cordillera is thought to exert a major control on the ⁸⁷Sr/⁸⁶Sr balance in seawater, which is imprinted in Phanerozoic ⁸⁷Sr/⁸⁶Sr cycles as measured on unaltered marine calcites (McArthur et al., 2020; Martin and Cárdenas, 2022). Thus, the ⁸⁷Sr/⁸⁶Sr trend towards more radiogenic values (enriched in ⁸⁷Sr) over the Late Devonian coincides with rapid and large-scale (estimated ~10 km) exhumation of the Acadian Cordillera (Fig. 1F; Murphy and Keppie, 2005).

One factor that has recently come into view is the strength and character of the magnetic field in the Devonian (Van der Boon et al., 2022). Particularly during the Middle and Late Devonian, paleomagnetism shows that the magnetic field was extremely weak (e.g., Hawkins et al., 2021; Shcherbakova et al., 2017), and a possible non-dipolar configuration has been suggested (Shatsillo and Pavlov, 2019). Van der Boon et al. (2022) calculate standoff distances of the magnetopause and show that the magnetopause could have been at a distance half of what it is today, possibly up to tens of millions of years. This means that Earth's atmosphere was poorly protected from solar winds, which could have had a profound effect on the biosphere. Findings of increased UV-B radiation during, e.g., the Hangenberg event (Marshall et al., 2020) are in line with an extremely weak magnetic field. However, due to the scarcity in Devonian paleomagnetic data, there are still many unanswered questions about this hypothesis, particularly with regards to timing and duration of the weak field period. If the field was indeed extremely weak and the reduction in magnetic shielding had an influence on life on Earth, there might be more indications for increased UV-B radiation found in the biological record of the Devonian (e.g., Marshall et al., 2020).

It is possible that the Devonian greenhouse ocean was consistently near the tipping point of anoxic events. In this scenario, Milankovitch forcing could regulate periodic incurrence of bottom water anoxia, through fluctuating global mean temperature, at frequencies <1 My (De Vleeschouwer et al., 2014; Lu et al., 2021). This was most compellingly demonstrated for the Lower-Upper Kellwasser cycle which lasted 330–600 Kyr based on astronomical calibration (De Vleeschouwer et al., 2017; Percival et al., 2018; Ma et al., 2022). As reviewed by Da Silva et al. (2016) and Da Silva in Becker et al. (2020), astronomic calibrations of deep geologic time mostly rely on eccentricity orbital variations which are considered stable and remaining close to 405 kyr, and the correctly identified number of these cycles allows an estimated duration of stages or conodont zones during the Devonian. Other Milankovitch periodicities lose their predictability on time ranges extending beyond 50 Myr in the past due to the chaotic diffusion of the inner solar system (Laskar et al., 2011).

7. Ocean circulation on an ice-free Earth

Today's conveyor belt of thermohaline circulation keeps deep ocean water oxygenated and unfavorable for widespread organic carbon accumulation, but this condition is unstable on geologic timescales (Arthur and Sageman, 1994; Meyer and Kump, 2008). The thermohaline circulation in the modern ocean consists of thermal and haline components. The thermal mode is driven by strong temperature gradients between low and high latitudes, which are characteristic of icehouse

climates, when cold brines sink in polar regions. The haline mode describes sinking of warm brines concentrated by evaporation, which mostly occurs in arid mid-latitudes. In addition to thermal and haline drivers, it is possible that geothermal heating from the ocean floor may alone drive circulation, although at a much slower rate, approximately 15,000 years for a complete turnover (Meyer and Kump, 2008), comparing with today's 1000–2000 years under thermohaline regime (Böös et al., 2012).

Ocean stagnation, assumed decades ago to be the main control on global anoxia (e.g., Fischer and Arthur, 1977; Goodfellow and Jonasson, 1984), may not be the chief factor, however, drastic slowdown and partial reversal of ocean circulation has to be a critical component of the greenhouse planetary condition (Meyer and Kump, 2008; Hay and Flögel, 2012). This slowdown is happening today with the ongoing global warming and ice retreats (<https://www.ipcc.ch/srocc/>). The associated changes are ocean acidification due to increasing pCO₂, overall deoxygenation due to water warming, and the slow expansion of oxygen minimum zones (e.g., Ruvalcaba Baroni et al., 2020; Wallmann et al., 2022).

Today the oceanic oxygen minimum zone (OMZ) is a mid-depth (100–900 m) ocean layer depleted in oxygen due to decomposition of planktonic organic matter. The OMZ is overlain by the photic surface layer with thriving phytoplankton-based pelagic life and underlain by an oxygenated bottom layer (Karstensen et al., 2008; Paulmier and Ruiz-Pino, 2009; Stramma et al., 2010; Gilly et al., 2013). Today OMZs develop in areas where surface production is elevated and mixing with oxygenated waters is sluggish (*ibid.*). Four large OMZs persist in the modern Ocean: two between 0 and 30° on both sides of equator in the eastern Pacific and Atlantic oceans (both splitting in two lobes along the equator), one in the northern part of Indian Ocean (Arabian Sea OMZ and the Bay of Bengal), and one higher-latitude OMZ impinges upon the Kurily-Kamchatka-Aleutian volcanic arc.

The northern lobe of the eastern tropical Pacific OMZ is the broadest zone of oxygen depletion in the ocean, where waters with ≤60 μmol/L of dissolved O₂ extend as far west as the eastern Mariana Trench-Arc System (Karstensen et al., 2008; Gilly et al., 2013). The World's largest OMZ in the eastern tropical Pacific occurs beneath the high primary production zone nourished by upwelling of bottom waters off Peru (Humboldt) and Mexico-California advected from polar regions. Oxygen levels in the eastern, most fertile parts of southern and northern lobes of this OMZ do not exceed 20 μmol/L (0.5 ml/l or <1/10 of surface-water O₂ level), and often reach zero, triggering sulphate reduction (Karstensen et al., 2008; Wallmann et al., 2022). Outbreaks of hydrogen sulphide into shallow waters are also recorded in the tropical Atlantic OMZ off Africa (Weeks et al., 2004). Biochemical activity in the present-day eastern tropical OMZs is dominated by anaerobic non-sulfidic processes via denitrification and anammox pathways (Fig. 4), amplified by electron scavenger from the lean inventory of dissolved trace metals. Once these energy reservoirs are exhausted without resupply, the system is driven into sulphate reduction, which is only the intermittent state in present-day OMZs. The OMZ thickness is quite dynamic on decadal and even diurnal time scales. Many decades of monitoring reveal a worldwide thickening trend of OMZs, a switch to nitrogen-limited conditions, and expansion of toxic sulfidic waters in OMZ cores. Denitrification is currently in full swing in the world's thickest OMZ of the Arabian Sea (Lachkar et al., 2019; Rixen et al., 2020), and the likely great extent of denitrification is simulated for the near future in the Peruvian OMZ if the current trend towards enhanced productivity and deoxygenation continues (Paulmier and Ruiz-Pino, 2009; Wallmann et al., 2022). These processes increase pressure on sea life, most obviously, by reducing migration ranges of pelagic species and colonisable seafloors for benthic life forms (Stramma et al., 2010).

Kidder and Worsley (2004, 2010) conceptualized three principal states of the Phanerozoic World Ocean (Fig. 5) where greenhouse conditions are set as a default state accounting for >70% of Phanerozoic time. The icehouse mode with its characteristic strong thermal

circulation lasted about 20–25% of the Phanerozoic, and the remainder was hothouse conditions. Greenhouse oceans are characterized by weakened thermal sinking in polar regions, with consequently less oxygen injection into the deep ocean leading to expansion of OMZs (Fig. 5). Simulation of the ocean circulation for the end-Permian Pangea-Panthalassa Earth indicates that deep-ocean anoxia is achievable when the thermal mode becomes dominant (Zhang et al., 2001). Expanded anoxic factories, in turn, promote loss of nitrogen from the biochemical cycle into the atmosphere in the form of N_2 and N_2O (Fig. 4). The hothouse condition of Kidder and Worsley (2004, 2010) is a disastrous, usually short-term (≤ 1 Myr, rarely up to 3 Myr) planetary condition accounting for $<4\%$ of the Phanerozoic and frequently coincides with mass extinctions. Hothouse Earth features ice-free polar regions, weak oceanic haloclines, and haline-mode ocean convection that drives polar and equatorial upwellings of warm anoxic waters (Fig. 4). As no sinking of cold brines occurs, the water turnover is sluggish, which allows geothermal heat to warm bottom waters. The OMZ expands dramatically under hothouse climates and transfers into a euxinic state while its upper boundary shallows to the photic zone (Fig. 4). The hothouse is an unstable condition requiring forcing mechanisms, such as degassing by LIPs.

According to Kidder and Worsley (2010), icehouse-greenhouse-hothouse transitions are coupled with a profound change in atmospheric circulation (Fig. 5). The planetary wind belt speed is predicted to wane to 0.83 of the present-day in a greenhouse and 0.67 in a hothouse. This calming should contribute to slowdown of wind-driven oceanic currents (including upwelling), temper physical weathering, and reduce aeolian delivery of iron and other nutrients to surface waters. At the same time, Kidder and Worsley (2010) speculate that cyclonic storms will likely strengthen and reach out to high latitudes, which will push the storm wave base to greater depths, entrap euxinic waters, and release H_2S into upper productive oceanic layer and the atmosphere. These large-scale breakthroughs of hydrogen sulphide would cause a major stress to biota and possibly contribute to mass extinctions (Fig. 4). Even without involvement of strong cyclonic storms, dramatic shallowing of the chemocline and decreased pO_2 (an aggressive H_2S oxidant) in heated surface waters would cause H_2S release in upwelling zones that is >2000 times higher than the small flux from modern volcanoes (Kump et al., 2005).

Kidder and Worsley (2010)'s prediction for oceanic response to

ultimate global warming is compelling, and corroborative simulations of almost totally ($\sim 90\%$) anoxic ocean condition at the peaks of most severe OAEs exist (e.g. Flögel et al., 2011). However, expanding knowledge on Mesozoic OAEs refutes expansions of OMZs into a continuous euxinic layer during hothouse crises (review in Robinson et al., 2017). For example, the southern deeper portion of the proto-Atlantic Ocean remained oxygenated during the Toarcian OAE (Ruvalcaba Baroni et al., 2017), and deoxygenation during the severe OAE2 at the Cenomanian/Turonian boundary varied between suboxic and euxinic in the Atlantic and Tethys (Westermann et al., 2014) while much of the Pacific oceanic floor and slopes remained variously oxygenated (Takashima et al., 2011). Estimates from isotope proxies (primarily $\delta^{98}Mo$, $\delta^{238}U$, and $\epsilon^{205}Tl$) compiled by Reershemius and Planavsky (2021) indicate that anoxia (both non-sulfidic and sulfidic) rarely, if ever, expanded to the excess of 50% of the total ocean floor during severe OAEs of the Phanerozoic. The Hirnantian anoxic event (HOAE) seems to be one exception with its prevalently or almost completely anoxic ocean floors, but the Early Paleozoic ocean, including HOAE, is very different from more recent OAEs due to manifold differences in the Earth-surface system, such as much lower content of free oxygen and profound difference in nutrient runoff due to the lack of vascular-plant modulation of land surface. The End Permian extinction also shows evidence for transient euxinia in the abyssal plains of Panthalassa Ocean (Grasby et al., 2021) that could be too brief to be imprinted in isotope proxies. Nevertheless, slowdown in watermass turnover leading to drastic expansion and shallowing of OMZs, coupled with the reversal of deep ocean circulation, is a well-founded prediction helping to understand Devonian shelfal seas and biotic/environmental/carbon cycle perturbations imprinted in them.

8. Devonian anoxic events in NW Canada

8.1. Geologic and paleogeographic context

The Horn River Group (HRG) of the latest Eifelian – Frasnian age is an excellent archive of oxic and anoxic facies (Fig. 6). The HRG consists of the Hare Indian, Ramparts, and Canol formations (Fig. 6). This stratigraphic succession and its geochemical signatures were characterized in several recent studies (Pyle and Gal, 2016; Kabanov and Gouwy, 2017, 2021; Morrow, 2018; Kabanov, 2019, 2022; Kabanov,

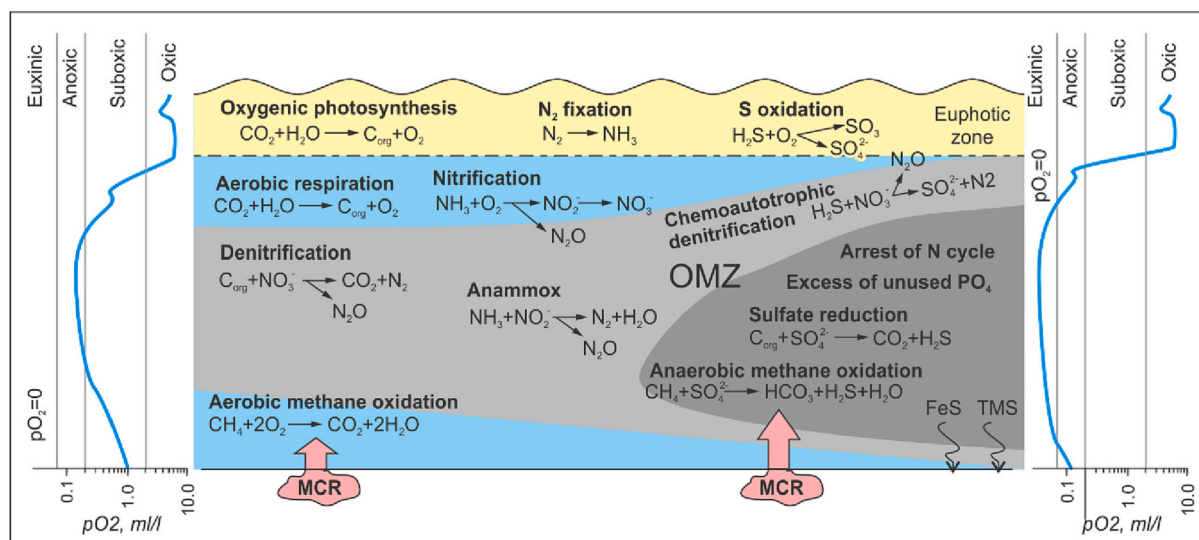


Fig. 4. Biochemical element cycling in OMZ from mildly anoxic (left-hand) to severe euxinic (right-hand). Note that expansion of the OMZ biochemical factory boosts production of greenhouse gases, ultimately arrests N cycle, and removes iron and trace metals as sulphide precipitates; TMS is trace metal sulphides; MCR are methane clathrate reservoirs. Graphic summary from Caldwell et al. (2008), Jenkyns (2010), Seibel (2011), and Gilly et al. (2013). Boundaries of redox environments (euxinic, anoxic, suboxic and oxic) reproduced from Tribouillard et al. (2006).

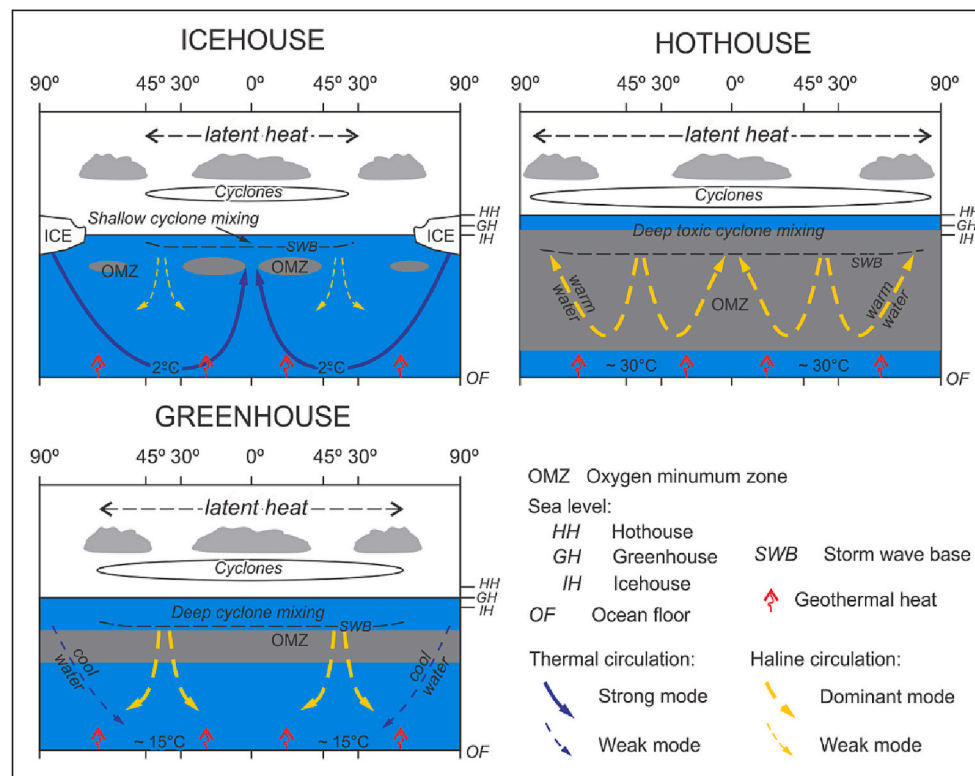


Fig. 5. Critical characteristics of icehouse, greenhouse and hothouse ocean-atmosphere circulation systems (Kidder and Worsley, 2010, with slight modifications).

2021). Three exploration wells and the Prohibition Creek composite outcrop section are chosen to discuss here (Fig. 6). They occur in the easternmost Laramide Cordillera in the Northwest Territories, Canada. Paleogeographically, these sections were deposited on the western continental shelf of Laurentia, in the southern hemisphere close to paleo-equator (Torsvik and Cocks, 2017). All four sections are located in the southern off-bank facies zone (Fig. 6) where the HRG is dominated by dark, organic-rich laminated shales and subdivided into the Hare Indian Formation (40–60 m) and the Canol Formation (60–90 m). The Hare Indian Formation is composed of partly calcareous shales and siltstones, and the Canol Formation is composed of siliceous shales and cherts with intervals enriched in authigenic dolomite. The chert beds are especially abundant in the upper Canol Formation (Dodo Canyon Member) where they form thin (1–7 cm) couplets with siliceous shale. Upwards, the Canol Formation grades into the Imperial Formation (Fig. 6), a thick stratigraphic succession composed of soft shales, siltstones and very fine-grained sandstones deposited in the distal foreland setting of the north-easterly located Ellesmerian Orogen (Hadlari et al., 2009).

The review of Cordilleran tectono-sedimentary history suggests the lack of effective oceanographic barriers between the HRG seaway and Panthalassa until at least Late Frasnian or even Famennian (Colpron et al., 2007; Colpron and Nelson, 2009; Cobbett et al., 2021). The geochemical signatures with strong U/Mo covariation and high enrichment of black shales in authigenic Mo and V are consistent with unrestricted supply of trace-metal ions from the dissolved ocean inventory (Kabanov, 2019). Further west of the study area within the same shelfal basin, thin (1–10 cm) hyper-enriched metalliferous (Ni-Mo-Zn-PGE-...Au-Re) horizons occur in the Middle Devonian (latest Eifelian to Middle Givetian?), which is also interpreted as precipitation of metals from the oceanic watermass under the regime of extreme sediment starvation (Gadd et al., 2020, 2022). This oceanographically open regime with a minor and uneven supply of siliciclastics from the distant Laurentian sourceland lasted in the study area until the end of the HRG deposition near the Middle-Late Frasnian boundary (~373.4

My). During the Famennian and especially across the Devonian/Carboniferous boundary, actively rising volcanic arcs converted the NW margin of Laurentia into back-arc sea, thus ending the Ordovician – Devonian period of passive-margin tectonic regime (Colpron et al., 2007; Colpron and Nelson, 2009; Cobbett et al., 2021).

Kabanov (2019) provided first evidence for anoxic events in the HRG, preceded by globally traced carbon isotope excursions at the Trail River section, ~400 km NW of the study area, within the same shelfal basin (Fraser and Hutchison, 2017).

8.2. Intermittent PZE in the HRG basin

The basinal black-shale units of the HRG (Fig. 5B) are characterized by a strong presence of isorenieratane and aryl isoprenoids at and between the levels of anoxic events (Table 2; Kabanov and Jiang, 2020). The Carcajou horizon is a marker level within the Ramparts Formation with a relatively high content of *in-situ* kerogen (Fig. 6B). At the same time, several lines of evidence attest for the fluctuating chemocline in the water column. First, the unstable presence of gammacerane and the variation of the gammacerane/hopane ratio in the organic extracts (*ibid.*) indicates a lack of permanent water-column stratification (Sinninghe Damsté et al., 1995). Secondly, the black laminated shales and cherts of the HRG contain minute pyritized spicules of hyalosponges, sometimes in the form of collapsed and obviously *in-situ* sponge sacks (Braun, 1966; Kabanov and Jiang, 2020). Moreover, these overall anoxic facies preserve minute disruptions of lamination identified as trace fossils (Biddle et al., 2021). Collectively this indicates that seafloor oxygenation episodes were sufficient in duration for benthic metazoans with very low oxygen demand to colonize seafloor until the next advent of sulfidic conditions (Kabanov and Jiang, 2020).

8.3. Chemostratigraphic data and proxies

Since the off-bank HRG is a superficially monotonous black-shale succession, carbon-cycle perturbation events can be revealed only

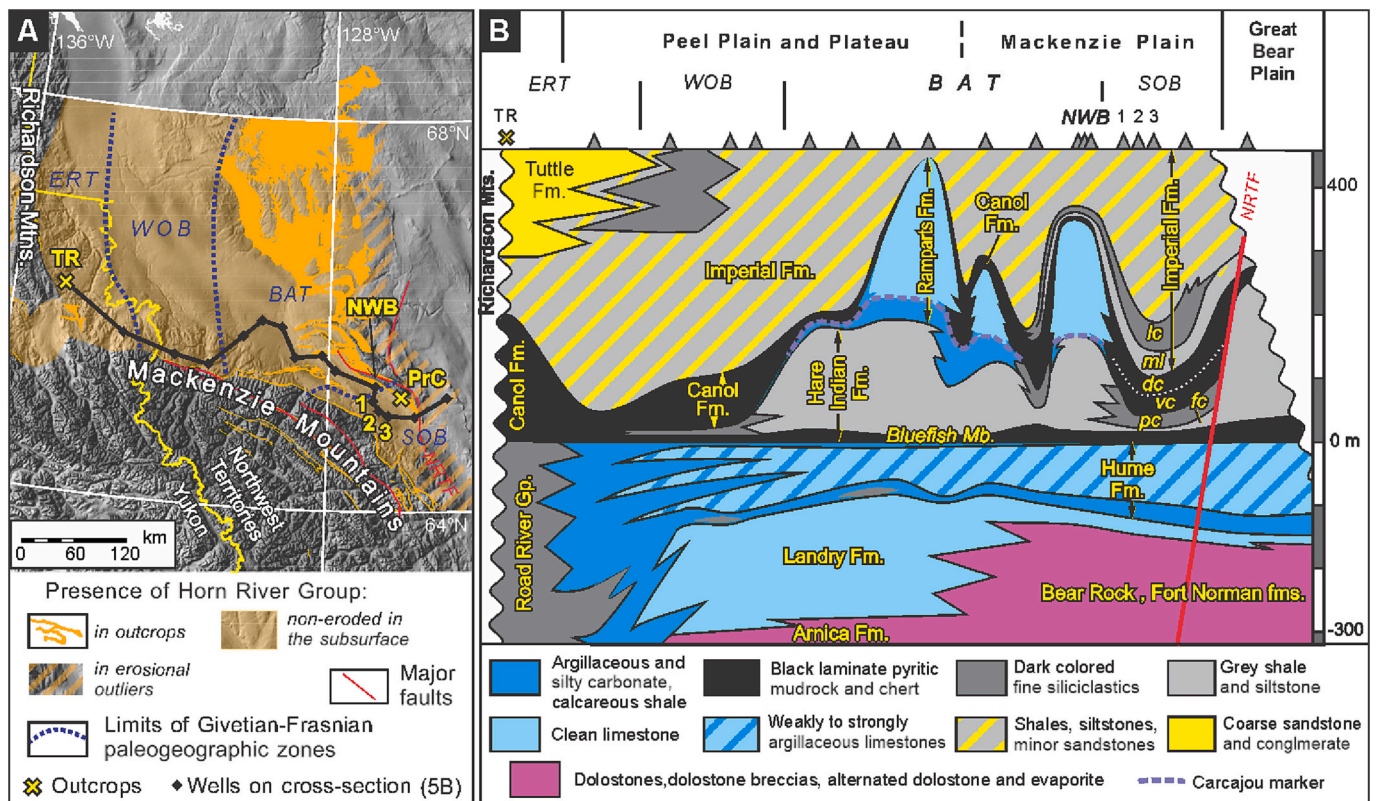


Fig. 6. Geographic extent and stratigraphy of the Horn River Group (HRG) between 64°N and 68°N, NW Canada (simplified from Kabanov, 2019). (A) HRG occurrence in outcrops and the subsurface. (B) West-east cross-section based on exploration wells, traced on (5A). Givetian-Frasnian facies zones: (ERT) West Peel - East Richardson Trough zone; (WOB) Western off-bank zone; (BAT) bank and trough zone; (SOB) Southern off-bank zone. Sections discussed in this study: (TR) Trail River outcrop; (NWB) Norman Wells carbonate bank (oilfield) with hundreds of wells; (1) Loon Creek O-06 well; (2) Mirror Lake N-20 well; (3) Little Bear N-09 well; (PrC) Prohibition Creek outcrop. NRTF is Norman Range thrust fault at the eastern limit of Laramide Cordillera. Abbreviations of lithostratigraphic units in the southern off-bank area: (fc) Francis Creek Member; (pc) Prohibition Creek Member; (vc) Vermillion Creek Member; (dc) Dodo Canyon Member; (ml) Mirror Lake Member; and (lc) Loon Creek Member.

with instrumental proxies. Data acquisition methods and proxies are summarized in sufficient detail by Kabanov (2019), Kabanov and Gouwy (2021), and Kabanov et al. (in review). Tabulated data are available in Kabanov (2019) and Kabanov et al. (2023). A selection of proxies employed herewith includes, first of all, the gamma spectrometry proxies U_n ($U_n = 0.29 \times U[\text{ppm}] \times K[\text{wt}\%]^{-1}$) and KTH ($KTH[\text{gAPI}] \approx 4 \times Th[\text{ppm}] + 16 \times K[\text{wt}\%]$). In the HRG, the U_n is mimicking the U/Al ratio based on strong covariation of Al and K in the large data set of elemental geochemistry (Kabanov and Gouwy, 2021). The KTH is the uranium-stripped potassium-thorium signal characterizing the input of terrigenous fines. The acronym KTH, as accustomed in North American well logging, stands for potassium + thorium. This proxy is also known as CGR (computed or clay gamma-ray signal; e.g., Bábek et al., 2018). Other proxies are TOC (total organic carbon content), hydrogen index (HI), and oxygen index (OI) from pyrolysis-combustion analyses using Rock-Eval 6 and HAWK instrumentation; high-accuracy major + trace elemental data acquired with ICP-MS/ES and LECO instrumentation; and stable carbon isotope data of bulk organic matter made on acid-treated samples ($\delta^{13}\text{C}_{\text{org}}$ vs. VPDB notation).

The HI and OI are TOC-normalized pyrolysis peaks S2 (mg HC/g) and S3 (mg CO_2 /g), respectively (Lafargue et al., 1998). In recent sediments and Phanerozoic rocks of relatively low thermal maturity (oil window and less), high HI and low OI characterizes marine kerogen of mostly algal origin, whereas elevated OI traces input of oxygen-rich kerogen, mainly polysaccharide-rich remains of land plants which often constitutes the bulk of “coaly detritus” in siliciclastic sediments (e.g., Hansen et al., 2022).

8.4. Mid-Devonian events

The benthic limestone of the Hume Formation is overlapped abruptly by the black laminated calcareous shale of the basal Hare Indian Formation (Fig. 6), producing a prime well log and seismic marker of regional significance. Conodont data place this contact within the *ensis* Zone of the uppermost Eifelian (Uyeno et al., 2017; Gouwy, 2022), thus indicating that cessation of benthic carbonate production and switch to pelagic sedimentation may be related to the Kačák event (Table 1).

Unless tectonically displaced, the top of the Hume limestone in the study area appears flat across the study area (Fig. 6). The character of this surface changes further south in the Northwest Territories, in proximity to the Presqu’île carbonate platform (Fig. 7). This carbonate platform, also referred to as the reefal barrier (Meijer Drees, 1993; Morrow, 2018), is the shallow-water equivalent of the Horn River Formation, the black anoxic shale is correlated with the HRG of the study area (Fig. 7). The Presqu’île carbonate barrier thus represents a major mid-Devonian stepback of the shallow-water carbonate sedimentation. This carbonate paleo-escarpment is outposted by carbonate pinnacles of Givetian age named the Horn Plateau reefs (Meijer Drees, 1993; Corlett and Jones, 2011). Although flank facies of Horn Plateau reefs are undocumented, and no outcrops are available, they presumably interfinger with the Horn River anoxic sediments just like the Frasnian carbonate buildups of WCSB and eastern Baltica (Figs. 2 and 3).

Upon closer look, the Hume/Bluefish contact appears as a rugged pyritized and chertified hardground in some sections, whereas in others it is a condensed transitional limestone of 0.5 to 2.6 m thick (Kabanov

and Gouwy, 2017; Kabanov, 2022). This transitional limestone is usually argillaceous, bioturbated, and ranges in texture from bioclastic packstone to carbonate mudstone (core face on Fig. 8). As a sign of transition to pelagic sedimentation, tentaculitids (predominantly dactyloconarids) appear in the upper-most Hume limestone and grow in abundance to rock-forming amounts in the base of the Bluefish Member. The basal few centimetres of the Bluefish Member are limestone with imbricated brachiopod shells mixed with tentaculitids, sometimes dominated by tentaculitids with rare brachiopod fragments. As seen on the core face (Fig. 8), the degree of bioturbation in this basal Bluefish limestone diminishes from base to top, and right above this basal bed it declines to zero. Given the collective evidence, the Hume-Bluefish contact is interpreted as a drowning unconformity *sensu* Schlager (1989) with no evidence of a geologically appreciable hiatus (Kabanov and Gouwy, 2017).

The elemental logs across the Hume/Bluefish contact reveal overall gradual increase in siliciclastic content (Al log on Fig. 8) and gradual buildup of authigenic trace metals (Mo, V, and U) from moderate at the contact to a major spike in 2.0–4.0 m above the contact (Fig. 8). Kabanov (2019) named this horizon of high trace-metal enrichment “the first anoxic horizon of the Horn River Group” (AH-I). The siliciclastic content increases significantly just above the AH-I, while the calcareousness decreases. This lithochemical change marks the transition to the upper Bluefish Member, a fissile black shale with abundant acritarchs historically known as the “spore bearing member”. Further up the section, this latter grades into the soft shale and siltstone of the Francis Creek Member (Fig. 8; Kabanov and Gouwy, 2017).

Our new high-resolution (~ 0.3 m) $\delta^{13}\text{C}_{\text{org}}$ log through the Bluefish – Francis Creek interval (Fig. 8) reveals a consistent negative trend from -28.7% at the Hume/Bluefish contact to -29.8% above the AH-I (Fig. 7). An abrupt swing to heavier carbon values of $\sim 1.2\%$ amplitude occurs in the uppermost Bluefish – Francis Creek interval (Fig. 8). This is the positive isotopic excursion A revealed by Kabanov and Jiang

(2020) in Little Bear N-09. It was inferred that this $\delta^{13}\text{C}_{\text{org}}$ deflection may result from the influx of coaly detritus based on a moderate spike of OI (*ibid.*). However, data plots from Loon Creek O-06 do not reveal the same oxygen index (OI) spike, and the strong dominance of planktonic kerogen at this stratigraphic interval is indicated by uniformly high hydrogen index (Fig. 8). These considerations suggest that the isotopic excursion A likely reflects an oceanic perturbation. Awareness that the top of the Bluefish Member occurs within the *rhenanus-varcus* Zone (upper part of the lower *varcus* Zone) (Gouwy, 2022) makes the isotopic excursion A too young for the Kačák event. Correlation of the excursion A with the *pumilio* isotopic event is most likely (Table 1).

The carbon isotopic signature of the Kačák event is a pronounced negative excursion which varies greatly in amplitude, reaching $\sim 3\%$ in $\delta^{13}\text{C}_{\text{org}}$ (van Hengstum and Gröke, 2008) and an extreme of $\sim 8\%$ in $\delta^{13}\text{C}_{\text{carb}}$ (Ellwood et al., 2011). The Eifelian/Givetian boundary occurs within the negative $\delta^{13}\text{C}$ excursion (Ellwood et al., 2011), or the negative excursion can be entirely within the *ensensis* Zone (e.g., Königshof et al., 2015). It should be noted that the conodont age constraints presented by van Hengstum and Gröke (2008) are not conclusive and may rather suggest that their negative isotopic excursion in the northern Appalachian basin is slightly younger (*timorensis* Zone) than the Kačák event in its type area. Our data from the Hume/Bluefish contact and the basal part of the HRG (Fig. 8) do not fit unequivocally into this isotopic pattern, although the position of the Hume/Bluefish contact within the *ensensis* Zone is of little doubt (Uyeno et al., 2017; Gouwy, 2022).

8.5. Latest Givetian – Middle Frasnian events

The thick (~ 75 – 100 m) Canol Formation of the off-bank sections (WOB and SOB facies zones on Fig. 6) reveals three main horizons of the highest authigenic U and Mo enrichment marked on Fig. 9 as AH-II, AH-III, and AH-IV. Using gamma spectrometry, these AHs (Anoxic Horizons) are traceable in multiple sections, including those located remotely

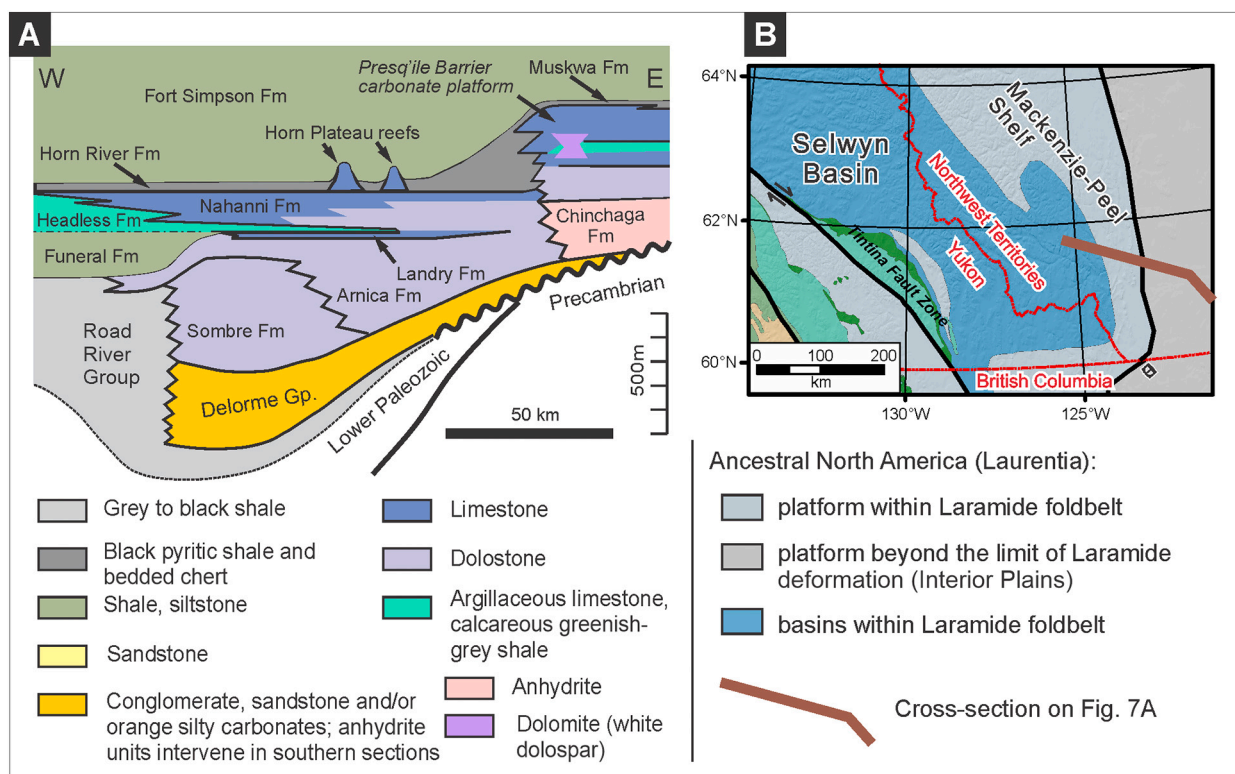


Fig. 7. Conceptual cross-section in the southeastern Horn River shale basin (A) showing backstepped carbonate shelf (Presqu'île barrier) outposted by Horn Plateau carbonate buildups (modified from Morrow, 2018). (B) The map of Cordilleran terranes representative of the Lower-Middle Paleozoic (Colpron and Nelson, 2011) with trace of cross-section on Fig. 7A.

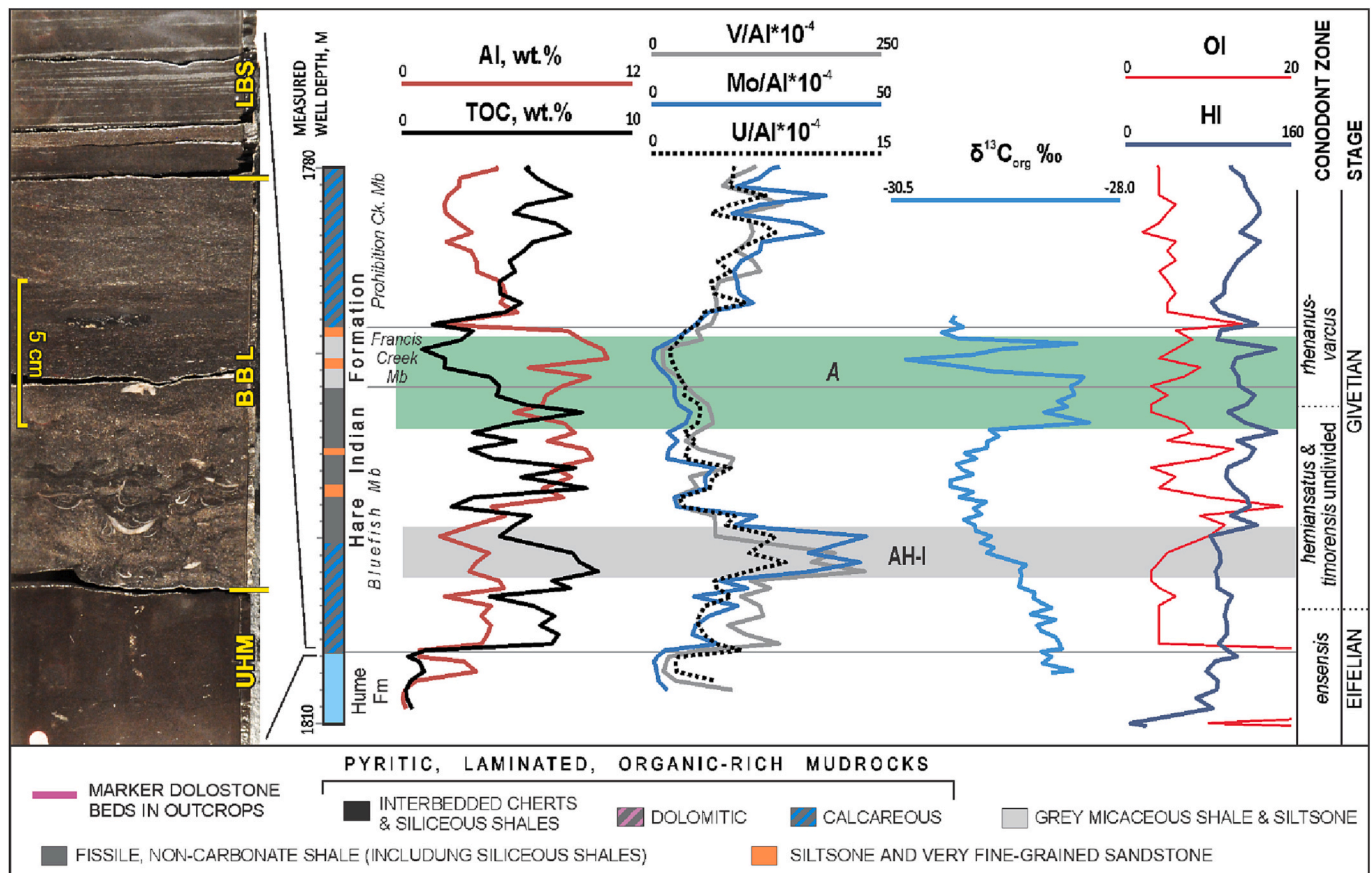


Fig. 8. Elemental and $\delta^{13}\text{C}_{\text{org}}$ logs through the Kačák-pumilio event interval in Loon Creek O-06 core. Grey stripe is the anoxic event AH-I and green stripe is the carbon isotopic excursion A (Kabanov and Jiang, 2020). OI: oxygen index (mg CO_2/g TOC). HI: Hydrogen index (mg HC/g TOC). Labels on core face: (UHLM) lime mudstone in top of Hume Formation; (BBL) basal Bluefish limestone; (LBS) laminated calcareous shale of the lower Bluefish Member. Conodont age of this stratigraphic interval is based on Kabanov and Gouwy (2017) and Gouwy (2022). (For interpretation of the references to colour in this figure legend, the reader is referred to the web version of this article.)

within the same basin (Kabanov, 2019; Kabanov and Gouwy, 2021; Kabanov et al., in review). These AHs are marked by the elevated TOC and lows in fine siliciclastics as approximated by KTH (Fig. 9). These siliciclastic lows are especially distinct at AH-III and AH-IV.

The $\delta^{13}\text{C}_{\text{org}}$ data from three sections reveal multiple positive isotope excursions coincident with the highest TOC content (Kabanov et al., in review). These carbon isotopic trends are best resolved in the Prohibition Creek section due to the high sampling density (Fig. 9). A major shift of +2.5‰ in the basal Canol Formation is characterized by gradual buildup of heavier values occurring at 4–8 m of the section from its inception to acme; the reversal to more negative background is even more gradual (excursion B on Fig. 9). An abrupt $\delta^{13}\text{C}_{\text{org}}$ swing of up to +2.3‰ occurs just underneath AH-III (excursion B2), and a similar deflection to heavier isotope values occurs at the base of AH-IV (excursion B3).

Conodont data from the Prohibition Creek section correlate the $\delta^{13}\text{C}$ excursion B with the Frasnian anoxic event at the Givetian-Frasnian boundary (Kabanov et al., in review). The abrupt $\delta^{13}\text{C}$ excursion in the base of AH-III is characteristic of the “basal punctata” sub-event in the upper *transitans* Zone, and this correlation is validated with conodonts (*ibid.*). The $\delta^{13}\text{C}$ excursion B3 is placed within the *punctata* Zone and identified as the late pulse of the global *punctata* event. Minor isotopic excursions B1, B4 and B5 may correlate with other global isotopic perturbations in the Late Givetian-Frasnian interval of geologic time which was particularly eventful (Becker et al., 2020). Assignment of the excursion B1 to the Timan isotopic event is very likely within the available conodont age constraints (Fig. 9). These age constraints allow estimation of the average sedimentation rate in the Canol Formation at

Prohibition Creek and nearby well sections of ~ 0.19 mm/yr based on calibration to the Geologic Time Scale 2020 (Kabanov et al., in review). This sedimentation rate is not corrected for compaction (*i.e.*, was originally higher), but estimates of time values of events further down the text are independent of such correction.

Fig. 10 zooms in on event horizons in the upper Canol Formation and visualises finer-scale chemostratigraphic patterns using slightly different proxies than on Fig. 9. Firstly, it is clearly seen that the high content of authigenic U, Mo and V is a signature of the entire Dodo Canyon Member. Within this trace metal rich interval, expression of AH-III and AH-IV as high Mo and U horizons is rather muffled at Prohibition Creek, however, it is more pronounced in two nearby cored sections, Little Bear N-09 and Loon Creek O-06 (Kabanov et al., in review). Further, the stratigraphic pattern of vanadium enrichment is different from U and Mo. Instead of an abrupt swing to higher values at the base of the Dodo Canyon Member like U/Al and Mo/Al, the content of authigenic vanadium increases gradually up the section to attain the highest values between AH-III and AH-IV, which is also a feature in the two aforementioned borehole cores (Kabanov, 2019). Fig. 10 also shows that the minor $\delta^{13}\text{C}_{\text{org}}$ excursion B4 is associated with the modest spike of authigenic U, Mo, and V. The downsection offsets of major carbon isotopic excursions B2 and B3 relative to AH-III and AH-IV are very clear at Prohibition Creek. Conversely, the minor isotopic excursion B4 post-dates the associated trace-metal spike (Fig. 10).

The elemental mercury data from Prohibition Creek reveal an interesting pattern. The interval of AH-II and up to the base of AH-III shows overall Hg enrichment and wide data scatter. LOWESS fitting manifests a possible Hg spike of up to 0.48 ppm (the second highest Hg

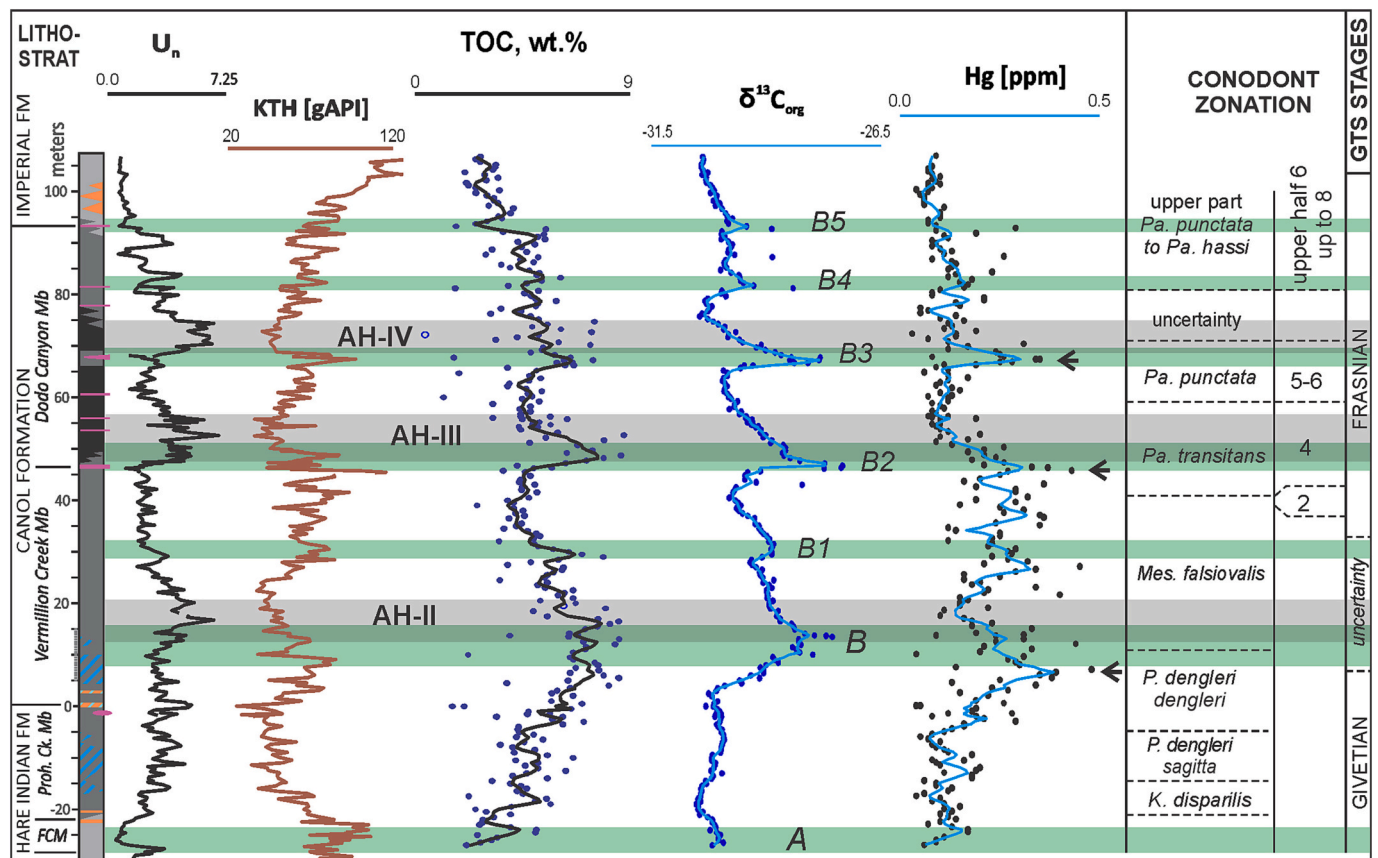


Fig. 9. Geochemical expression and conodont age of Late Givetian-Frasnian anoxic events at Prohibition Creek. Horizons of severe anoxia (AHs), traced by grey stripes, overlap with carbon isotopic excursions (green stripes). Arrows on the mercury log point at Hg spikes below main event horizons. FCM is Francis Creek Member. The isotopic excursions are labelled in italics. The TOC, $\delta^{13}\text{C}_{\text{org}}$ and Hg scatterplots are clipped at outliers (96–99 percentile). Smoother is LOWESS with sliding window 2.5% of data. Match of isotopic excursions: A = ?*pumilio*; B = Frasnian/*Manticoceras*; B1 = ?Timan; B2 = early *punctata*; B3 = late *punctata*. (For interpretation of the references to colour in this figure legend, the reader is referred to the web version of this article.)

value in the entire section) in the base of the $\delta^{13}\text{C}$ excursion B (lower arrow on Fig. 9). Nonetheless, this cannot be treated as a Hg enrichment horizon due to high data scatter and the fact that normalisation to TOC and Al muffs this spike. Mercury enrichment horizons are more pronounced higher in the section (two upper arrows on Fig. 9). Mercury and Hg/TOC logs on Fig. 10 further resolve details of these enrichments. A distinct spike of up to 0.43 ppm occurs in the very base of the isotopic excursion B2, and normalisation to TOC inflates it to the highest Hg/TOC value in the entire section. A similar spike coincident with the isotopic excursion B3, however, is muffled by TOC normalisation. An enhanced Hg/TOC signal is also detectable in the base of the isotopic excursion B4 (Fig. 10). The column “Event signals” on Fig. 10 makes it easy to see that two distinct Hg/TOC spikes occur in the basal portions of isotopic excursions B2 and B4. Unfortunately, currently available sampling density seems to be insufficient to resolve records of other potential Hg enrichment horizons.

Although with a significant age uncertainty, conodont data from the Prohibition Creek section are consistent with the identity of the $\delta^{13}\text{C}$ excursion B as the Frasnian event at the Givetian-Frasnian boundary (Kabanov et al., in review). The abrupt $\delta^{13}\text{C}$ excursion in the base of AH-III is characteristic of the “basal *punctata*” sub-event in the upper *transitans* Zone, and this correlation is validated with conodonts. The $\delta^{13}\text{C}$ excursion B3 is placed within the *punctata* Zone and identified as the late pulse of the global *punctata* event. Minor isotopic excursions B1, B4 and B5 may correlate with other global isotopic perturbations in the Late Givetian-Frasnian interval (Becker et al., 2020). Assignment of the excursion B1 to the Timan isotopic event is very likely within the available conodont age constraints (Fig. 9). These age constraints allow

estimation of the average sedimentation rate in the Canol Formation at Prohibition Creek based on time calibration in GTS 2020 (Becker et al., 2020). Position of the Givetian/Frasnian boundary at 10.5 m and the base of *punctata* zone at 59.0 m (Fig. 9) yields 0.19 mm/yr as an average sedimentation rate through the Early Frasnian (2.55 My), and relative facies homogeneity translates this value up the section to the top of the Canol Formation.

Total phosphorus and proxies (P/Al, P/TOC) are used as tracers of nutrient inflow at Devonian anoxic event levels (Percival et al., 2020; Smart et al., in press), and we explore P distribution in our case study (Fig. 10). It is known that the HRG is severely depleted in phosphorus (average 342 ppm) against reference values such as the average P content in the surface of Laurentian Shield (655 ppm; Shaw et al., 1986) or post-Archean Australian shale (700 ppm; Taylor and McLennan, 1985). It is also known that bottom redox conditions were fluctuating between mildly oxygenated and euxinic (Kabanov and Jiang, 2020; Biddle et al., 2021), which would be conducive for episodes of seafloor phosphogenesis if sedimentation were slow and waters were enriched in dissolved phosphorus. Both P and P/Al logs on Fig. 10 indicate no outstanding spikes coincident with isotopic excursions B2 and B3. Moreover, most prominent spikes of P and P/Al occur between siliciclastic highs, consistently with near-zero covariance of P and Al at this interval (Pearson $r = -0.02$).

It is also noteworthy that OI is very low (mostly <10), except for rare spikes made up of single datapoints (Fig. 10). Neither OI, nor OI/Al show a response to major events in the Canol Formation, and no significant covariance of OI with Al or P exists in the Prohibition Creek data (Pearson $r = -0.12$ and -0.15 , respectively). Meanwhile, HI is mostly

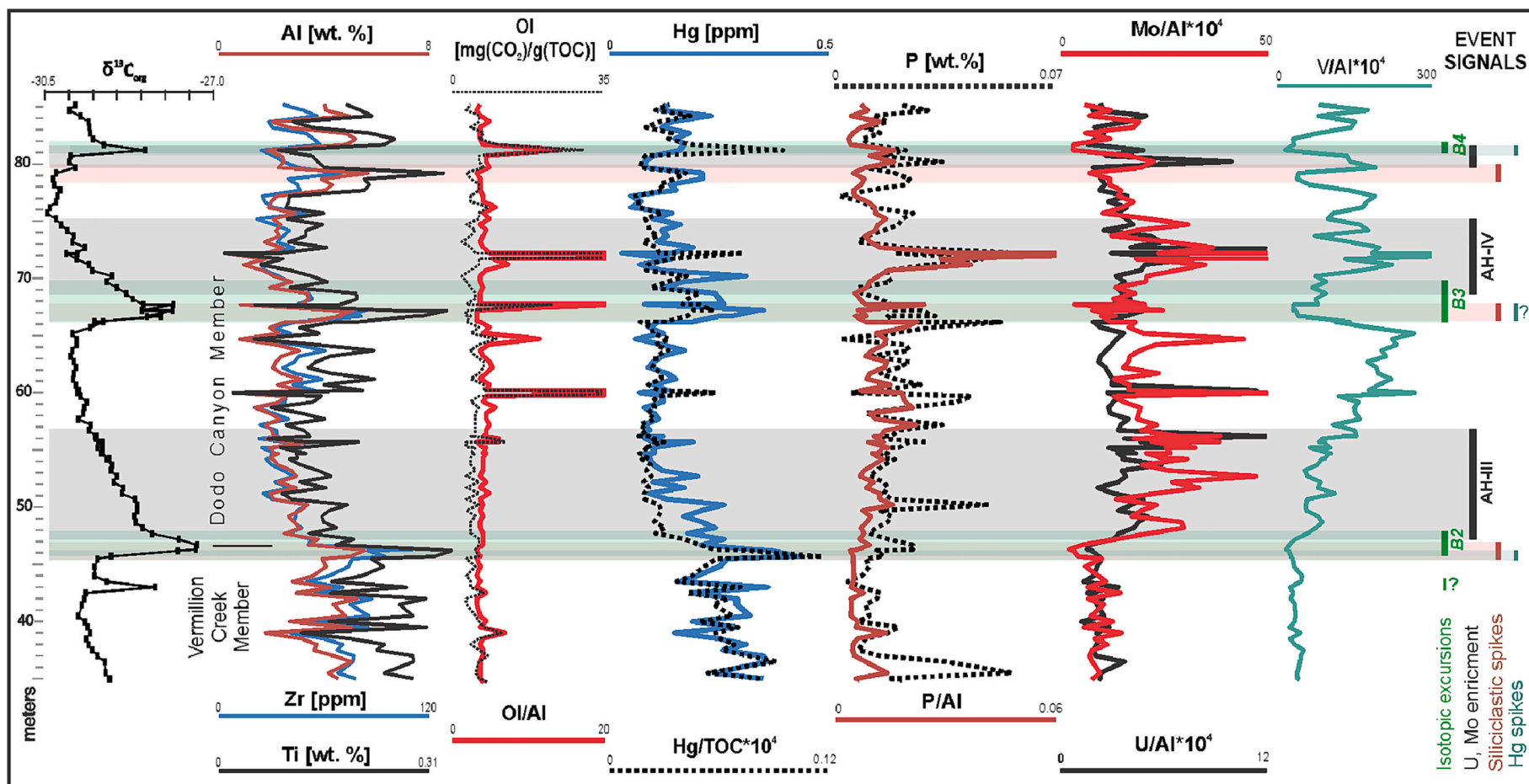


Fig. 10. Geochemical expression of the *punctata* event interval in the composite Prohibition Creek section. Recognized event signals are bracketed with colour bars on the right and traced across geochemical logs with high-transparency stripes of same colour. Excessively high values of OI, OI/Al, P/Al, Mo/Al, U/Al, and V/Al are clipped.

over 200 (data in Kabanov et al., 2023). Low thermal maturity at Prohibition Creek (median $T_{\max} = 430^\circ\text{C}$) makes this signature trustworthy and in line with the larger dataset indicating a planktogenic origin of organic matter in the HRG (Pyle et al., 2015; Kabanov, 2017).

It seems remarkable that chemostratigraphic signals array in repeating sequences at three main events within the Canol Formation. This sequence is best resolved at the basal *punctata* event interval (Fig. 10). The early phase of isotopic excursion B2 is coupled with a very thin (≤ 1 m) Hg spike and the spike in siliciclastic content as revealed with the KTH proxy (Fig. 9) and scatterplots of siliciclastics-residing elements (Al, Ti, Zr on Fig. 10). This siliciclastic spike reverses to lows abruptly at the onset of the late phase of B2, when $\delta^{13}\text{C}$ just starts trending back to lighter values, and this reversal coincides with the onset of severe anoxia in AH-III. Such sequences of signals also characterize Frasnian and late *punctata* events, although initial Hg enrichments there are less clear.

9. Discussion

9.1. OAE identity of Devonian anoxic events

Many oceanic anoxic events, major biotic extinctions, and other environmental crises through the Phanerozoic have an associated sedimentary Hg anomaly. Hg anomalies are commonly interpreted as fingerprints of catastrophic pulses of volcanism, such as those expected from LIP eruptions (Grasby et al., 2019). Although Hg loading into marine sediments may not occur directly from volcanic eruptions, but rather as recycled Hg from temporary reservoirs in siliciclastic source land, the robust correlation of Hg anomalies with episodes of enhanced volcanic activity exists (Grasby et al., 2019). In particular, it is typical of Mesozoic OAEs that pulses of increased volcanic activity manifest themselves as spikes of Hg or other proxies, such as negative deflections of $^{187}\text{Os}/^{188}\text{Os}$, in the basal part or just below the isotopic excursion and buildup of TOC content. Such signals are very well documented in many OAEs, for example at the onset of the Jurassic T-OAE and the Cretaceous OAE2 (e.g., Jenkyns, 2010; Du Vivier et al., 2014; Them et al., 2019). The $^{187}\text{Os}/^{188}\text{Os}$ proxy (Os_i) reflects mass balance between two osmium isotopes: the primitive (non-radiogenic) ^{188}Os from mantle or extraterrestrial sources, and ^{187}Os as the product of radiogenic decay of ^{187}Re in upper continental crust. The fairly short seawater residence time (≤ 10 kyr) makes osmium isotopic balance sensitive to geologically brief events. Negative $^{187}\text{Os}/^{188}\text{Os}$ anomalies thus trace inputs of primitive osmium from enhanced volcanism (submarine and/or continental LIPs), unless other evidence (such as a coincident iridium anomaly and large-scale impact ejecta) indicates ^{188}Os enrichment from a major bolide impact (Peucker-Ehrenbrink and Ravizza, 2000).

World records corroborate the assumption that Hg enrichment spikes found in the Canol Formation (Figs. 9 and 10) are of the same nature as those extensively reported in association with Mesozoic OAEs. Pisarzowska et al. (2020a) report a high-amplitude (up to 1.1 ppm) Hg spike just underneath the uppermost *transitans* Zone (referred by these authors to as *Ancyrodella nodosa* Zone), the stratigraphic level close to isotope excursion B2 in the Canol Formation (Fig. 9). Mercury spikes are also known from just before other Late Devonian anoxic events. The Hg excursions preceding the LKW and UKW in Laurussian records (Racki et al., 2018; Liu et al., 2021) are close in amplitude to the Hg spike underneath the excursion B2 (Fig. 10). In the Anti-Atlas region of Morocco, the Hg and Hg/TOC enrichment horizon at UKW is nearly triple these values (Racki et al., 2018). Multiple Hg and Hg/TOC spikes characterize the upper *triangularis* Zone in the Timan-Pechora Basin of eastern Baltica, up to the top of the UKW-equivalent black shale (*ibid.*). Even higher-amplitude Hg enrichment spikes are reported from the Devonian-Carboniferous boundary interval (Pisarzowska et al., 2020b; Rakociński et al., 2021a). At the Hangenberg event level, $^{187}\text{Os}/^{188}\text{Os}$ and biomarkers are in favor of volcanic emissions as a press-pulse for extreme global warming and biotic crises (Percival et al., 2019;

Rakociński et al., 2020; Kaiho et al., 2021; Zhang et al., 2021). A tentative indication of the volcanic trigger for the Frasnian event is provided by Kaiho et al. (2021) who report a low (0.09–0.1 ppm) yet distinct Hg enrichment spike just below the Frasnian event in Belgium, at the stratigraphic level of the Hg spike that may be present underneath the isotopic excursion B in the Canol Formation (Fig. 9).

The sequence of chemostratigraphic signals at our three major events in the Canol Formation (Figs. 9 and 10) seems to fit very well into the Earth-surface perturbation loop characteristic of Meso-Cenozoic OAEs (Jenkyns, 2010; Föllmi, 2012; Lowery et al., 2021; Chen et al., 2022). A volcanic press-pulse triggered global overheating (progression towards hothouse condition of Kidder and Worsley, 2010) and intensified hydrological cycling in humid areas, thus boosting terrigenous flux into shelfal seas. These boosts are imprinted in the siliciclastic spikes. In a chain reaction, eutrophication-induced planktonic overproduction pushed the $^{13}\text{C}/^{12}\text{C}$ to heavier values and increased shower of dead organic matter, resulting in the highest TOC concentration in sediments (Fig. 9). This is recorded in the early phases of isotopic anomalies B, B2, and B3.

During the late phase of the three major events, the volcanic CO_2 reinforcement wanes, and the system gradually reverts to more oligotrophic condition, which is recorded in gradual $^{13}\text{C}/^{12}\text{C}$ reversal towards lighter values. It is not yet clear why this decrease in primary production is coupled with enhanced anoxia (buildup of trace metals into AHs). Earlier ideas that siliciclastic lows at AHs indicate retreats of source land in response to thermal transgressions (Kabanov, 2019) is invalidated by a geologically momentary response of the oceanic watermass to fluctuating global temperatures (see review above). Meanwhile, the onset of a Hg anomaly and siliciclastic spike at the earliest stage of *punctata* event occurred ~ 87 kyr prior to the onset of AH-III based on a sedimentation rate of 0.19 mm/yr. Similarly, the time lag between the onset of the late *punctata* event and the AH-IV was ~ 125 kyr. It is thus obvious that fitting of signal sequences into an ideal OAE loop is an oversimplification of complex environmental dynamics over protracted time spans, also because such signals do not align the same way on other event levels such as the one marked by the isotopic excursion B3 (Fig. 10).

The expression of the Kačák event is different from younger events in the Canol Formation (Fig. 8). The AH-I is not associated with a carbon isotope excursion and siliciclastic low. Our data from the base of the HRG do not reveal a clear $\delta^{13}\text{C}_{\text{org}}$ excursion. However, in other records of the Kačák event, a major negative $\delta^{13}\text{C}$ excursion is extensively documented, and it is succeeded by a moderate positive excursion of $\leq 1\text{‰}$ amplitude (Buggisch and Joachimski, 2006; van Hengstum and Gröke, 2008; Ellwood et al., 2011; Königshof et al., 2015). This carbon isotopic signature is similar to the Toarcian OAE (T-OAE; McArthur et al., 2008; Jenkyns, 2010; Léonide et al., 2012; Suan et al., 2015; Them et al., 2017) and the mid-Aptian OAE-1a (e.g., Bellanca et al., 2002). The major stepback of the carbonate platform in the HRG at the Kačák event level (Fig. 7), and shutdown of the Ramparts carbonate banks at some level within the *punctata* event interval (Fig. 6B; Kabanov, 2022), exemplify the link between Devonian anoxic events and shrinking of benthic carbonate production, which is a well-known signature of Mesozoic OAEs (Föllmi and Gainon, 2008; Jenkyns, 2010; Léonide et al., 2012; Han et al., 2018).

One takeaway message from this review and the HRG case study is that geochemical fingerprints of Middle-Late Devonian events are highly variable, just like in Mesozoic OAEs. These variations include presence/absence of negative $\delta^{13}\text{C}$ excursion and variable sequence of geochemical signals, and depletion-enrichment in redox-sensitive trace metals. Trace metal depletion is rare in the Devonian (e.g., Algeo, 2004) but well established at Mesozoic OAEs where it is interpreted to indicate oceanwide exhaustion of trace-metal inventory, which is especially likely with regards to dissolved ions having the longest seawater residence time: Mo, U, and V (Algeo and Rowe, 2012; Bennett and Canfield, 2020). Most severe depletion is traced at OAE2 within the proto-Atlantic

(*ibid.*). However, in the Tethys, trace-metal depletion is not so severe and partially inverted to enrichment, despite broad connections between the Tethys and proto-Atlantic (Algeo and Rowe, 2012; Owens et al., 2016; Siebert et al., 2021).

Another feature in common is the development of intermittent photic-zone euxinia in oceanographically open settings, which is now widely recognized based on chlorobi biomarkers in the Mesozoic (review above) and in the Middle-Late Devonian (Table 2). In the black-shale HRG facies, such biomarkers were identified at and between the event levels, consistent with the black-shale, dominantly anoxic character of these strata (Kabanov and Jiang, 2020).

9.2. Top-down vs. bottom-up nutrient flux

The latest Devonian – earliest Mississippian suboxic-anoxic sediments of western Laurentia (Exshaw Formation and equivalents) have signatures of intermittent phosphogenesis, which supports “bottom-up” nutrient flux maintained through tropical oceanic upwelling (Caplan and Bustin, 2001; Li et al., 2022). The physical evidence for limited ice caps in the latest Famennian and a cooling trend in sea-surface temperatures (Fig. 1G) further support hypothetical enforcement of thermohaline oceanic circulation as a driver of such upwelling (Hedhli et al., 2022). In a similar way, upwelling has also been invoked to explain spread of anoxia in the pre-Famennian Devonian, including the Frasnian anoxic sediments in western Laurentia and eastern Baltica that are part of our review (Harris et al., 2018; Bushnev et al., 2016). However, in neither of these two regions do Frasnian black shales exhibit signatures of phosphogenesis, and instead it is typical to see these strata depleted in phosphorus. The overall phosphorus-lean character of Frasnian black shales is consistent with qualitative palaeontological observations indicating the paucity of fish remains and conodonts, as well as the absence of any reports indicating phosphorite occurrence in time equivalent strata anywhere across the Mackenzie Shelf. The condensed sections and hardgrounds at the drowning unconformity in the top of Hume Formation were never found affected by phosphatization either (Kabanov and Gouwy, 2017). Most obviously, tropical oceanic upwelling is not applicable to the Late Devonian shelves of eastern (in modern coordinates) Baltica which were open northeast (or north) to Uralian Ocean between equator and 30° N (Domeier and Torskvik, 2014; Golonka, 2020). In this paleogeographic position, eastern Baltica must have been under Hadley Cell circulation with dominantly westward, onshore advection of surface watermass (e.g., simulation in De Vleeschouwer et al., 2014).

Eutrophication of shelfal seas through a top-down pathway in response to increased weathering is seen as part of the OAE loop. As argued above, this also applies to Devonian events. Further in favor of this pathway, Smart et al. (2022, in press) reveal two pulses of phosphorus supply in the near-source lacustrine succession of the Cordilleran foreland basin now located in Eastern Greenland. These two pulses, best expressed as P/Al, are correlated with the Lower Kellwasser (LKW) and Upper Kellwasser (UKW) anoxic events and interpreted as related to intensified soil formation under expanding vegetation (*ibid.*), by analogy with the Quaternary-Holocene pulsations of P supply into sediments (Filippelli, 2002), although in the Devonian case a volcanically forced overheating rather than orbitally driven interglacial was a culprit (Smart et al., in press). The UKW phosphorus enrichment is the strongest. Smart et al. (in press) simulate such strong inflow of nutrients at global scale using the Carbon Oxygen Phosphorus Sulfur Evolution (COPSE) model and find it adequate to explain the Frasnian-Famennian mass extinction. However, as discussed above, persistence or even expansion of arid belts during overheating crises makes globally strong inflow of nutrients a false assumption (e.g., Hay and Flögel, 2012; Davies et al., 2020). In Devonian marine sediments, the far-field response of phosphorus to the onset of anoxic events varies between depletion and no response to high enrichment. This is clearly seen on P_{tot} , P/Al, and TOC/P logs from six sites of the LKW-UKW interval presented by Percival et al. (2020).

Phosphorus enrichment is also encountered on other Devonian event levels (*ibid.*). We assume that lack of P response to the onsets of major events in the Canol Formation (Fig. 10) reflects depletion of siliciclastic plumes in nutrients as they reached offshore to the distal site of our case study. Distinct phosphorus enrichment is also known in association with the latest Ordovician HOAE which occurred long before the advent of tracheophytes and root-assisted weathering (Qui et al., 2022).

We concur that drastic slowdown of ocean watermass turnover was the underlying condition to maintain expanded OMZs impinged upon continental shelves (Meyer and Kump, 2008). Moreover, deep-ocean circulation reversed towards a haline mode (Fig. 5) is not compliant with the bottom-up scenario by which bottom oxygenated waters advect from high latitudes and upwell to nourish primary production in tropical shelfal seas. This lends more credit to the top-down eutrophication during the Middle-Upper Devonian except for maybe the Late Famennian when thermohaline circulation, and therefore bottom-up supply of nutrients, could have been enforced by glacial caps. However, there is a very limited spread of Famennian glaciers compared to the LPIA, and the sea-surface temperatures were much warmer than today (Fig. 1G; Isaacson et al., 2008; Montañez, 2021). This suggests that these oxygenated upwellings were much weaker than in modern settings.

Finally, a bottom-up flux should have been also operational in the pre-Late Famennian ocean through the release of dissolved phosphorus from anoxic bottom waters into overlying oxygenated waters (Fig. 4), as conventionally perceived for the greenhouse ocean (Meyer and Kump, 2008; Kidder and Worsley, 2010). This bottom-up flux of P was likely the highest in the anoxic/euxinic upwelling zones. Perhaps the chief factor in greenhouse ocean oligotrophy was the shortage of bioavailable nitrogen caused by drastically expanded denitrification/annamox (Meyer and Kump, 2008; Schoepfer et al., 2016), although this is also not devoid of controversy (Algeo et al., 2014).

9.3. Land plants did not trigger Devonian mass extinctions

If boosts of weathering in response to volcanic CO₂ emissions were due to rapid expansions of vascular plants (R&S pathway of Grzegorz Racki), one would expect an inflow of coaly detritus at event levels. It is not unusual to see driftwood impressions in carbonate banks and black shales of the HRG (e.g., Kabanov, 2017), but a robust proxy, such as the oxygen index (OI), is required to assess the scale of plant debris inflow. The OI shows zero response at event levels (Fig. 10), just like in two nearby drillhole cores (Kabanov et al., in review). As a cautionary note, OI response to Mesozoic carbon-cycle perturbations is not known well, and in documented cases it varies between sections from no response to distinct enrichment (e.g., Suan et al., 2015).

Collective evidence discussed above converges on a volcanic driver of Devonian carbon-cycle perturbations, anoxic events, and mass extinctions, which aligns these events with many other prominent environmental-biotic crises of the Phanerozoic. Dramatic contraction of the habitable seafloor between the eutrophicated shallow shelf and the expanded OMZ probably exerted major stress on benthic metazoans. However, shrinking habitats would not decimate marine faunas alone, as clearwater seas offshore extensive deserts and copious isolated carbonate platforms located away from river deltas had sufficient space to form refugia for faunas. Mass extinctions were likely driven by a combined killer force involving several major amplifiers such as the fast pace of transition into hothouse, heat stress, seawater deoxygenation and acidification (Bond and Grasby, 2017). The hypothesis of Algeo et al. (1995), on the other hand, does not find unequivocal support in any proxies discussed herein. It is still assumable that root-assisted weathering could act as a minor amplifier of biotic crises operating more likely at a regional than on a global scale.

9.4. Water-column chemocline as a major control on Devonian facies and cyclicity

One of the pieces in the Middle-Late Devonian puzzle is the time-specific “bank and trough” facies architecture (megareef tracts of [Copper and Scotese, 2003](#)), which was most widespread during the Givetian-Frasnian, the time known for its warmest climate and highest frequency of carbon-cycle perturbations ([Fig. 1](#)). Collective evidence suggests that this facies architecture was controlled by a water-column redox boundary in combination with siliciclastics-starved regime and sufficient subsidence rate. Benthic carbonate production maintained tops of carbonate banks above the chemocline, while lateral expansion was suppressed by ambient anoxic waters, thus producing a bank or atoll-like shape of carbonate buildups (e.g., [Fig. 3B](#)). A pinnacle shape is also common (e.g., [Fig. 2C](#)) and can be interpreted as a gradual advance of an oxygen-deficient environment onto bank flanks until the complete demise and drowning under anoxic waters. This suppression of progradation made survival of inter-bank anoxic troughs over millions of years possible. As summarized by [Kabanov and Jiang \(2020\)](#), another factor in suppressed lateral expansion was a reduced ability for sediment dispersal from carbonate bank tops. This is attested by the thinness and dominantly fine-grained character of carbonate-bank aprons, which are often hard to pinpoint with subsurface data. These fine-grained (calcarenes, calcisiltites), thin (mostly <10 m) off-bank sequences are documented in case studies from Western Canada ([MacKenzie, 1973](#); [Wendte, 1994](#); [Knapp et al., 2017](#); [Shaw and Harris, 2022](#)). Other indications of reduced hydrodynamic activity are the rarity of coarse reef rubble and the paucity of acicular cements in shallow-water carbonate facies relative to equivalent facies of Miocene-Quaternary and LPIA time (summary in [Kabanov and Jiang, 2020](#)). [Whalen et al. \(2000\)](#) provided a detailed description of what appears to be the greatest known carbonate-platform escarpments of Frasnian age. Their two examples of a platform-to-basin transition (Ancient Wall and Miette) exhibit thick (up to 150 m) successions of toe-of-slope debris interbedded with basinal sediments. Cobbly wedges are present there, including megabreccias (clasts ≥ 1 m). However, such coarse-grain expression of the off-reef debris is rare. In the subsurface of Alberta, intraclastic and breccia beds within the Duvernay Formation are thin (10–20 cm) and mostly occur adjacent to Leduc reefs where they constitute only a minute portion of examined cores ([Knapp et al., 2017](#)). Coarse debris on carbonate bank – shale basin transitions seem to be rare globally, although reports of such facies exist. Thus, slope calcarenites and rubble accumulations occur in the Late Devonian pinnacle reefs of eastern Baltica ([Viles et al., 2009, 2019](#)), but materials presented in cited works do not allow to estimate how thick are these reef-apron sequences. Relatively quiet-water sedimentation was likely a norm for the broad expanse of bank-and-trough shelfal basins. This seems consistent with reduction of wind strength predicted for greenhouse and hothouse Earth conditions ([Kidder and Worsley, 2010](#)) and was likely a factor in sustaining water-column stratification.

The redox boundary in stratified shelfal basins was in turn maintained by expanded greenhouse OMZs which were fundamentally different from today's OMZs in their nutrient and water mass cycling. In a representative uranium isotope record through the Devonian, [Elrick et al. \(2022\)](#) demonstrate broad scatter of $\delta^{238}\text{U}$ during Givetian – early Famennian which shows occasional reversals to low (–8 to –4 ‰) values characteristic of largely anoxic deep ocean of the earlier Paleozoic. This is consistent with pulsatory expansions of anoxic watermass in the deep ocean during that time known for its warmest sea-surface temperatures, frequent carbon-cycle perturbations and multitude of anoxic events ([Fig. 1](#)). However, anoxic pulses in shelfal seas and in deep ocean might have had a complex relation, or were even decoupled, as suggested by heavier $\delta^{238}\text{U}$ values at the Frasnian-Famennian boundary that apparently indicate more oxygenated deep oceans during the UKL anoxic event ([White et al., 2018](#)).

The bank-and-trough depositional architecture is uncommon in Mesozoic shelfal seas, despite the parallelism in climatic conditions, the multitude of anoxic events and the carbon-cycle perturbations. We

speculate that this difference is due to the evolutionary advent of calcareous phytoplankton in Late Triassic and the progressive increase of its biomass over the later Mesozoic ([Bown et al., 2004](#)). Calcareous phytoplankton channelled CO_2 sequestration into new carbonate pathways which partly took over massive production of benthic microcrystalline calcites (“microbial carbonates”) and filled seafloor depressions with pelagic calcareous ooze ([Hay, 2008](#)), thus producing chalk successions in loci that would host thin anoxic sediments between carbonate buildups in the Devonian.

Fluctuations of the water-column chemocline, combined with pulsations of siliciclastic influx, can adequately explain sedimentary cycles which are revealed with magnetic susceptibility, gamma spectrometry, and elemental geochemistry. Our review elucidates how controversial is translation of such sedimentary cycles into sea level changes without confirmation from verified coastal onlaps, stacked subaerial exposure surfaces, incised valleys, and unambiguous facies progressions from deep to shallow-water. We also point out that in an ice-free world, $\delta^{18}\text{O}$ signatures in marine biogenic minerals possibly require different interpretations than in the Quaternary-like world where pulsating ice volumes control eustasy at < 1 Myr time scales. As such, spreads of anoxic facies put by [Johnson et al. \(1985\)](#) in the heart of “Devonian eustatic sea-level curve” may just emulate transgressions, but in fact record expansions of anoxia in response to overheating and ocean deoxygenation with no or minimal eustatic effect. However, this latter idea applies to the idealistic ice-free greenhouse world, whereas advanced simulations suggest that the input of glacio-eustasy is unavoidable even at some hottest episodes of greenhouse time spans (e.g., [Davies et al., 2020](#)). This sea-level puzzle clearly calls for new scrutiny, in the meantime justifying serious scepticism with regards to Devonian eustatic amplitudes as routinely exceeding ~25 m for 3rd and 4th order cycles ([Haq and Shutter, 2008](#)).

10. Conclusions

This paper reviews global records of anoxic events of the Middle Devonian – earliest Carboniferous. These anoxic events are complex multistage paleoenvironmental disturbances manifested through multiple proxies. We provide a case study on the latest Eifelian – Frasnian black-shale succession named the Horn River Group (HRG). Our review and case study elucidate a number of remarkable aspects and controversies of the Devonian: (1) widespread black-shale sedimentation with pulsatory expansions of anoxic environments historically recognized as anoxic events; (2) multiple $\delta^{13}\text{C}$ excursions and associated geochemical signatures; (3) widespread intermittent photic-zone euxinia in oceanographically open shelfal seas; (4) time-specific facies architecture with aggrading isolated carbonate buildups (reefs, banks, pinnacles, mud mounds) interspersing oxygen-deficient (severely anoxic at times) seafloor areas; (5) lack of rigorous evidence for high-amplitude eustatic sea level fluctuations; (6) controversy on marine nutrient flow through top-down (terrigenous eutrophication) or bottom-up (nurtured by oceanic upwelling) pathways; and (7) whether or not evolutionary expansion of vascular plants could drive marine ecosystems into mass extinctions. In this sequence, we conclude that:

- (1) Drastically expanded oxygen minimum zones (OMZs) of the Devonian greenhouse ocean maintained water-column stratification in shelfal seas, which explains thick anoxic successions in oceanographically open settings; the HRG provides a good example of redox dynamics in such an OMZ in a shelfal sea that was likely broadly open to eastern tropical Panthalassa.
- (2) The clearest fingerprint of the middle Devonian Kačák event is a regional backstepping of the benthic carbonate factory and a rapid switch to anoxic sedimentation at the HRG base. Higher in the section, three major events of the latest Givetian-Middle Frasnian interval display repeating sequences of signals: $\delta^{13}\text{C}_{\text{org}}$ shifts to heavier values coupled with mercury and siliciclastic

enrichment spikes; $\delta^{13}\text{C}$ reversals to background values, coincident with onsets of severe anoxia (authigenic trace metal enrichment) and weakening of the siliciclastic supply. This sequence fits in the hothouse loop induced by massive volcanic eruptions. These signatures are similar to those of Mesozoic oceanic anoxic events (OAEs).

- (3) Shallowness of sulfidic episodes in the water column is attested by a widespread presence of chlorobi biomarkers indicating photic-zone euxinia (Table 2).
- (4) The shallow chemocline in the expanded OMZ fluctuated with a high frequency and likely suppressed lateral expansion of carbonate buildups, thus controlling bank-and-trough facies architecture. We hypothesize that the absence of such facies architecture in otherwise similar Cretaceous sediments is partly or completely due to the advent of calcareous phytoplankton which filled basinal depressions with chalk instead.
- (5) Just like in the better understood super-greenhouse sedimentary archive of the Cretaceous, direct evidence of high-frequency (< 1 My) sea-level fluctuations is suspiciously meager in the Devonian. Our review of proxies usually employed to interpret Devonian eustasy shows that none of them confidently translate into eustatic fluctuations in an ice-free world. However, simulations of hydrological dynamics signal that glacioeustatic forcing was likely operational even during the hottest episodes of the Cretaceous greenhouse. This sea-level puzzle clearly calls for new scrutiny. In the meantime, this justifies strong scepticism with regards to the validity of the classical eustatic sea-level curve of the Devonian and estimates of eustatic amplitudes in excess of ~25 m for 3rd and 4th order cycles.
- (6) The reversal of deep-ocean circulation into thermal mode during a model ice-free greenhouse is not compatible with a bottom-up nutrient supply though oceanic upwelling at the scale we see it today, which is consistent with signatures from the HRG and worldwide. Collective evidence converges on a prevalent top-down nutrient flow possibly combined with a bottom-up supply of dissolved P from anoxic bottom waters.
- (7) Not a single proxy assessed in this paper unequivocally supports the hypothesis that holds expanding vascular vegetation accountable for anoxic events and biotic crises in the marine realm. Intolerance of pre-Pennsylvanian plants to dry seasons and upland climates implies that root-assisted weathering was geographically limited, and hence only locally impacted nutrient flows. It is nevertheless assumable that vascular plants, through root-assisted weathering, were one of multiple amplifiers of biotic crises in the Devonian.

Declaration of Competing Interest

None.

Data availability

Data for the Horn River Group case study are available in (Kabanov et al., 2023).

Acknowledgements

Analytical results for this study were obtained through GeoMapping for Energy and Minerals Program of Natural Resources Canada (NRCan) with management support from Carl Ozyer and Michel Plouffe. The 2019 field work at Prohibition Creek was conducted in large part within Sahtu Indigenous Land under the Northwest Territories Scientific Research Licence No. 16545 (issued by Aurora Research Institute on May 17, 2019); funds for this field came from the Geoscience for New Energy Supplies Project of NRCan. Sampling of cores was conducted with OROGO approvals SR-2017-004 (Mirror Lake N-20 and Little Bear

N-09 wells) and SR-2020-002 (Loon Creek O-06 well). The editor Christopher Fielding and three anonymous reviewers are cordially thanked for hard work on this manuscript, which resulted in profound improvements. We also thank Chloé Marcilly (U of Oslo, Norway) for last-minute help with Devonian paleogeography simulation. This work is a contribution to the UNESCO project IGCP-652 "Reading geological time in Palaeozoic sedimentary rocks". This is GSC/LMS/NRCan contribution no. 20220354.

References

- Aboussalam, S.Z., 2003. Das «Taghanic-Event» im höheren Mittel-Devon von West-Europa und Marokko. *Münster. Forschungen Geol. Paläontol.* 97, 1–332.
- Aboussalam, S.Z., Becker, R.T., 2011. The Global Taghanic biocrisis (Givetian) in the eastern Anti-Atlas, Morocco. *Palaeogeogr. Palaeoclimatol. Palaeoecol.* 304, 136–164. <https://doi.org/10.1016/j.palaeo.2010.10.015>.
- Aderoju, T., Bend, S., 2018. Reconstructing the palaeoecosystem and palaeodepositional environment within the Upper Devonian-lower Mississippian Bakken Formation: a biomarker approach. *Org. Geochem.* 119, 91–100.
- Algeo, T.J., 2004. Can marine anoxic events draw down the trace element inventory of seawater? *Geology* 32, 1057–1060. <https://doi.org/10.1130/G20896.1>.
- Algeo, T.J., Fisk, N.H., Berner, R.A., Maynard, J.B., Scheckler, S.E., 1995. Late Devonian oceanic anoxic events and biotic crises: 'Rooted' in the evolution of vascular land plants? *GSA Today* 5, 64–66.
- Algeo, T.J., Rowe, H., 2012. Paleooceanographic applications of trace-metal concentration data. *Chem. Geol.* 324–325, 6–18. <https://doi.org/10.1016/j.chemgeo.2011.09.002>.
- Algeo, T.J., Scheckler, S.E., 1998. Terrestrial-marine teleconnections in the Devonian: Links between the evolution of land plants, weathering processes, and marine anoxic events. *Phil. Trans. R. Soc. B Biol. Sci.* 353, 113–130. <https://doi.org/10.1098/rstb.1998.0195>.
- Algeo, T.J., Tribouillard, N., 2009. Environmental analysis of paleooceanographic systems based on molybdenum-uranium covariation. *Chem. Geol.* 268, 211–225. <https://doi.org/10.1016/j.chemgeo.2009.09.001>.
- Algeo, T.J., Meyers, P.A., Robinson, R.S., Rowe, H., Jiang, G.Q., 2014. Icehouse-greenhouse variations in marine denitrification. *Biogeosciences* 11, 1273–1295. <https://doi.org/10.5194/bg-11-1273-2014>.
- Archer, D., Buffett, B., Brovkin, V., 2009. Ocean methane hydrates as a slow tipping point in the global carbon cycle. *PNAS* 106, 20596–20601. www.pnas.org/cgi/doi/10.1073/pnas.0800885105.
- Arens, N.C., West, I.D., 2008. Press-pulse: a general theory of mass extinction? *Paleobiology* 34, 456–471. <https://doi.org/10.1666/07034.1>.
- Arthur, M.A., Sageman, B.B., 1994. Marine black shales: depositional mechanisms and environments of ancient deposits. *Annu. Rev. Earth Planet. Sci.* 22, 499–551.
- Averbuch, O., Tribouillard, N., Devleeschouwer, X., Riquier, L., Mistiaen, B., van Vliet-Lanoe, B., 2005. Mountain building-enhanced continental weathering and organic carbon burial as major causes for climatic cooling at the Frasnian-Famennian boundary (c. 376 Ma)? *Terra Nova* 17, 25–34. <https://doi.org/10.1111/j.1365-3121.2004.00580.x>.
- Bábek, O., Faméra, M., Šimfček, D., Weinerová, H., Hladil, J., Kalvoda, J., 2018. Sea-level changes vs. Organic productivity as controls on early and Middle Devonian bioevents: Facies- and gamma-ray based sequence-stratigraphic correlation of the Prague Basin, Czech Republic. *Glob. Planet. Chang.* 160, 75–95. <https://doi.org/10.1016/j.gloplacha.2017.11.009>.
- Bambach, R.K., Knoll, A.H., Wang, S.C., 2004. Origination, extinction, and mass depletions of marine diversity. *Paleobiology* 30, 522–542.
- Baird, G.C., Brett, C.E., 1991. Submarine erosion on the anoxic sea floor: Stratigraphic, palaeoenvironmental, and temporal significance of reworked pyrite-bone deposits. In: Tyson, R.V., Pearson, T.H. (Eds.), *Modern and Ancient Continental Shelf Anoxia*, 58. Geological Society of London Special Publication, pp. 233–257. <https://doi.org/10.1144/GSL.SP.1991.058.01.16>.
- Bashforth, A.R., Cleal, C.J., Gibling, M.R., Falcon-Lang, H.J., 2014. Paleoecology of early Pennsylvanian vegetation on a seasonally dry tropical landscape (Tynemouth Creek Formation, New Brunswick, Canada). *Rev. Palaeobot. Palynol.* 200, 229–263. <https://doi.org/10.1016/j.revpalbo.2013.09.006>.
- Becker, R.T., 1993a. Stratigraphische Gliederung und Ammonoiten-Faunen im Nehdenium (Oberdevon II) von Europa und Nord-Afrika. *Cour. Forsch. Inst. Senckenb.* 155, 1–353.
- Becker, R.T., 1993b. Anoxia, eustatic changes, and Upper Devonian to lowermost Carboniferous global ammonoid diversity. *Syst. Assoc. Spec. Vol. Ser.* 47, 115–163.
- Becker, R.T., House, M.R., 1997. Sea-level changes in the Upper Devonian of the Canning Basin, Western Australia. *Courier Forschungsinstitut Senckenberg* 199, 129–146.
- Becker, R.T., House, M.R., Kirchgasser, W.T., 1993. Devonian goniatite biostratigraphy and timing of facies movements in the Frasnian of the Canning Basin. *Geol. Soc. London Spec. Publ.* 70, 293–321.
- Becker, R.T., Marshall, J.E.A., Da Silva, A.-C., 2020. The Devonian period. In: Gradstein, F.M., Ogg, J.G., Schmidt, M.D., Ogg, G.M. (Eds.), *Geologic Time Scale 2020*, 1st edition. Elsevier, pp. 733–810. <https://doi.org/10.1016/B978-0-12-824360-2.00022-X>.
- Beil, S., Kuhnt, W., Holbourn, A., Scholz, F., Oxmann, J., Wallmann, K., Lorenzen, J., Aquit, M., Chellai, H., 2020. *Clim. Past* 16, 757–782. <https://doi.org/10.5194/cp-16-757-2020>.
- Bellanca, A., Erba, E., Neri, R., Premoli Silva, I., Sprovieri, M., Tremolada, F., Verga, D., 2002. Palaeoceanographic significance of the Tethyan 'Livello Selli' (early Aptian)

- from the Hybla Formation, northwestern Sicily: Biostratigraphy and high-resolution chemostratigraphic records. *Palaeogeogr. Palaeoclimatol. Palaeoecol.* 185, 175–196. [https://doi.org/10.1016/S0031-0182\(02\)00299-7](https://doi.org/10.1016/S0031-0182(02)00299-7).
- Biddle, S., LaGrange, M., Harris, B., Fiess, K., Terlaky, V., MacQuaker, J., Gingras, M.K., 2021. A fine detail physiochemical depositional model for Devonian organic-rich mudstones: a petrographic study of the Hare Indian and Canol Formations, Central Mackenzie Valley, Northwest Territories. *Sediment. Geol.* 414, 105838 <https://doi.org/10.1016/j.sedgeo.2020.105838>.
- Boghossian, N.D., Patchett, P.J., Ross, G.M., Gehrels, G.E., 1996. Nd isotopes and the source of sediments in the miogeocline of the Canadian Cordillera. *J. Geol.* 104, 259–277. <https://www.jstor.org/stable/30068191>.
- Bond, D.P.G., Wignall, P.B., Racki, G., 2004. Extent and duration of marine anoxia during the Frasnian-Famennian (Late Devonian) mass extinction in Poland, Germany, Austria, and France. *Geol. Mag.* 141, 173–193. <https://doi.org/10.1017/S0016756804008866>.
- Bond, D., Wignall, P.B., 2005. Chapter 9. Evidence for Late Devonian (Kellwasser) anoxic events in the Great Basin, western United States. In: Over, D.J., Morrow, J.R., Wignall, P.B. (Eds.), *Understanding Late Devonian and Permian-Triassic Biotic and Climatic Events: Towards an Integrated Approach*. Elsevier, pp. 225–262.
- Bond, D.P.G., Wignall, P.B., 2008. The role of sea-level change and marine anoxia in the Frasnian-Famennian (Late Devonian) mass extinction. *Palaeogeogr. Palaeoclimatol. Palaeoecol.* 263, 107–118. <https://doi.org/10.1016/j.palaeo.2008.02.015>.
- Bond, D.P.G., Zatoň, M., Wignall, P.B., Marynowski, L., 2013. Evidence for shallow water 'Upper Kellwasser' anoxia in the Frasnian-Famennian reefs of Alberta, Canada. *Lethaia* 46, 355–368. <https://doi.org/10.1111/let.12014>.
- Bond, D.P.G., Wignall, P.B., 2014. Large igneous provinces and mass extinctions: An update. In: Keller, G., Kerr, A.C. (Eds.), *Volcanism, Impacts, and Mass Extinctions: Causes and Effects*, 505. Geological Society of America Special Paper, pp. 29–55. [https://doi.org/10.1130/2014.2505\(02\)](https://doi.org/10.1130/2014.2505(02)).
- Bond, D.P.G., Grasby, S.E., 2017. On the causes of mass extinctions. *Palaeogeogr. Palaeoclimatol. Palaeoecol.* 478, 3–29. <https://doi.org/10.1016/j.palaeo.2016.11.005>.
- Böös, K., Nilsson, J., Nycander, J., Brodeau, L., Ballarotta, M., 2012. The World Ocean thermohaline circulation. *J. Phys. Oceanogr.* 42, 1445–1460. <https://doi.org/10.1175/JPO-D-11-0163.1>.
- Boucot, A.J., Xu, C., Scotese, C.R., Morley, R.J., 2013. Phanerozoic Paleoclimate: an Atlas of Lithological Indicators of climate. SEPM Concepts Sedimentol. Paleontol. 11 <https://doi.org/10.2110/sepmcsp.11>.
- Boulvain, F., 2001. Facies architecture and diagenesis of Belgian late Frasnian carbonate mounds (Petit-Mont Member). *Sediment. Geol.* 145, 269–294.
- Boulvain, F., 2007. Frasnian carbonate mounds from Belgium: sedimentology and palaeoceanography.
- Bown, P.R., Lees, J.A., Young, J.R., 2004. Calcareous nannoplankton evolution and diversity through time. In: Thierstein, H.R., Young, J.R. (Eds.), *Coccolithophores: From Molecular processes to Global Impact*. Springer, Berlin, pp. 481–508.
- Boyce, C.K., Lee, J.-E., 2017. Plant evolution and climate over geological timescales. *Annu. Rev. Earth Planet. Sci.* 45, 61–87. <https://doi.org/10.1146/annurev-earth-063016-015629>.
- Brady, M., Bowie, C., 2017. Discontinuity surfaces and microfacies in a storm dominated shallow Epeiric Sea, Devonian Cedar Valley Group, Iowa. *Depos. Rec.* 3, 136–160. <https://doi.org/10.1002/dep2.26>.
- Braun, W.K., 1966. Stratigraphy and microfauna of Middle and Upper Devonian formations, Norman Wells area, Northwest Territories, Canada. Available from: *Neues Jahrbuch für Geologie und Paläontologie*, vol. 125, pp. 247–264 [Accessed on 19 March 2020]. <https://www.schweizerbart.de/journals/njgpa>.
- Brett, C.E., Baird, G.C., 1996. Middle Devonian sedimentary cycles and sequences in the northern Appalachian Basin. In: *Geological Society of America Special Paper*, 306, pp. 213–241.
- Brett, C.E., Baird, G.C., Bartholomew, A.J., Desantis, M.K., Ver Straeten, C.A., 2011. Sequence stratigraphy and a revised sea-level curve for the Middle Devonian of eastern North America. *Palaeogeogr. Palaeoclimatol. Palaeoecol.* 304, 21–53. <https://doi.org/10.1016/j.palaeo.2010.10.009>.
- Brett, C.E., McLaughlin, P.I., Histon, K., Schindler, E., Ferretti, A., 2012. Time-specific aspects of facies: State of the art, examples, and possible causes. *Palaeogeogr. Palaeoclimatol. Palaeoecol.* 367–368, 6–18. <https://doi.org/10.1016/j.palaeo.2012.10.009>.
- Britton, G., Liaaen-Jensen, S., Pfander, H., Mercadante, A., Egeland, E., 2004. *Carotenoids: Handbook*. Springer Science & Business Media.
- Brown, T.C., Kenig, F., 2004. Water column structure during deposition of Middle Devonian-lower Mississippian black and green/gray shales of the Illinois and Michigan Basins: a biomarker approach. *Palaeogeogr. Palaeoclimatol. Palaeoecol.* 215, 59–85.
- Brown, D., Spadea, P., Puchkov, V., Alvarez-Marron, J., Herrington, R., Willner, A.P., Hetzel, R., Gorozhanina, Y., Juhlin, C., 2006. Arc-continent collision in the Southern urals. *Earth Sci. Rev.* 79, 261–287.
- Brugger, J., Hofmann, M., Petri, S., Feulner, G., 2019. On the Sensitivity of the Devonian climate to Continental Configuration, Vegetation Cover, Orbital Configuration, CO₂ Concentration, and Insolation. *Paleoceanogr. Paleoclimatol.* 34, 1375–1398. <https://doi.org/10.1029/2019PA003562>.
- Buffett, B., Archer, D., 2004. Global inventory of methane clathrate: sensitivity to changes in the deep ocean. *Earth Planet. Sci. Lett.* 227, 185–199. <https://doi.org/10.1016/j.epsl.2004.09.005>.
- Buggisch, W., Mann, W., 2004. Carbon isotope stratigraphy of Lochkovian to Eifelian limestones from the Devonian of central and southern Europe. *Int. J. Earth Sci.* 93, 521–541. <https://doi.org/10.1007/S00531-004-0407-6>.
- Buggisch, W., Joachimski, M.M., 2006. Carbon isotope stratigraphy of the Devonian of Central and Southern Europe. *Palaeogeogr. Palaeoclimatol. Palaeoecol.* 240, 68–88. <https://doi.org/10.1016/j.palaeo.2006.03.046>.
- Bushnev, D.A., Burdakov, N.S., Ponomarenko, E.S., Zubova, T.A., 2016. Anoxia in the Domanik basin of the Timan-Pechora region. *Lithol. Miner. Resour.* 51, 283–289. <https://doi.org/10.1134/S0024490216040027>.
- Caldwell, S.L., Laidler, J.R., Brewer, E.A., Eberly, J.O., Sandborgh, S.C., Colwell, F.S., 2008. Anaerobic Oxidation of Methane- Mechanisms, Bioenergetics, and the Ecology of Associated Microorganisms. *Environ. Sci. Technol.* 42, 6791–6799.
- Capel, E., Cleal, C.J., Xue, J., Monnet, C., Servais, T., Cascales-Miñana, B., 2022. The Silurian-Devonian terrestrial revolution: Diversity patterns and sampling bias of the vascular plant macrofossil record. *Earth Sci. Rev.* 231, 104085 <https://doi.org/10.1016/j.earscirev.2022.104085>.
- Caplan, M.L., Bustin, R.M., 2001. Palaeoenvironmental and palaeoceanographic controls on black, laminated mudrock deposition: example from Devonian-Carboniferous strata, Alberta, Canada. *Sediment. Geol.* 145, 45–72. [https://doi.org/10.1016/S0037-0738\(01\)00116-6](https://doi.org/10.1016/S0037-0738(01)00116-6).
- Carmichael, S.K., Waters, J.A., Suttner, T.J., Kido, E., DeReuil, A.A., 2014. A new model for the Kellwasser anoxia events (Late Devonian): shallow water anoxia in an open oceanic setting in the central Asian Orogenic belt. *Palaeogeogr. Palaeoclimatol. Palaeoecol.* 399, 394–403. <https://doi.org/10.1016/j.palaeo.2014.02.016>.
- Carmichael, S.K., Waters, J.A., Batchelor, C.J., Coleman, D.M., Suttner, T.J., Kido, E., Moore, L.M., Chadimová, L., 2016. Climate instability and tipping points in the Late Devonian: detection of the Hangenberg event in an open oceanic island arc in the central Asian Orogenic Belt. *Gondwana Res.* 32, 213–231. <https://doi.org/10.1016/j.jgr.2015.02.009>.
- Carmichael, S.K., Waters, J.A., Königshof, P., Suttner, T.J., Kido, E., 2019. Palaeogeography and paleoenvironments of the Late Devonian Kellwasser event: a review of its sedimentological and geochemical expression. *Glob. Planet. Chang.* 183 <https://doi.org/10.1016/j.gloplacha.2019.102984>.
- Cascales-Miñana, B., 2016. Apparent changes in the Ordovician-Mississippian plant diversity. *Rev. Palaeobot. Palynol.* 227, 19–27. <https://doi.org/10.1016/j.revpalbo.2015.10.005>.
- Chen, B., Ma, X., Mills, B.J.W., Qie, W., Joachimski, M.M., Shen, S., Wang, C., Xu, H., Wang, X., 2021. Devonian paleoclimate and its drivers: a reassessment based on a new conodont δ18O record from South China. *Earth Sci. Rev.* 222, 103814 <https://doi.org/10.1016/j.earscirev.2021.103814>.
- Chen, D., Tucker, M., 2004. Palaeokarst and its implication for the extinction event at the Frasnian-Famennian boundary (Guilin, South China). *J. Geol. Soc. Lond.* 161, 895–898. <https://doi.org/10.1144/0016-764904-034>.
- Chen, H., Xu, Z., Bayon, G., Lim, D., Batenburg, S.J., Petrizzo, M.R., Hasegawa, T., Li, T., 2022. Enhanced hydrological cycle during Oceanic Anoxic Event 2 at southern high latitudes: New insights from IODP Site U1516. *Glob. Planet. Chang.* 209, 103735. <https://doi.org/10.1016/j.gloplacha.2022.103735>.
- Chow, N., Wendte, J., Stasiuk, L.D., 1995. Productivity versus preservation controls on two organic-rich carbonate facies in the Devonian of Alberta: sedimentological and organic petrological evidence. *Bull. Can. Petrol. Geol.* 43, 433–460.
- Chlupáč, I., Kukal, Z., 1988. Possible global events and the stratigraphy of the Palaeozoic of the Barrandian (Cambrian-Middle Devonian, Czechoslovakia). *Sborník Geologických Ved Geologie* 43, 83–146.
- Chow, N., George, A.D., Trinajstić, K.M., 2004. Tectonic control on development of a Frasnian-Famennian (Late Devonian) palaeokarst surface, Canning Basin reef complexes, northwestern Australia. *Aust. J. Earth Sci.* 51, 911–917. <https://doi.org/10.1111/j.1400-0952.2004.01493.x>.
- Colpron, M., Nelson, J.L., Murphy, D.C., 2007. Northern Cordilleran terranes and their interactions through time. *GSA Today* 17, 4–10. <https://doi.org/10.1130/GSAT01704-5A.1>.
- Colpron, M., Nelson, J.L., 2009. A Palaeozoic Northwest Passage: Incursion of Caledonian, Baltic and Siberian terranes into eastern Panthalassa, and the early evolution of the North American Cordillera. In: Cawood, P.A., Kröner, A. (Eds.), *Earth Accretionary Systems in Space and Time*, 318. Geological Society of London Special Publication, pp. 273–307. <https://doi.org/10.1144/SP318.10>.
- Colpron, M., Nelson, J.L., 2011. A Digital Atlas of Terranes for the Northern Cordillera. *Brit. Columb. Geol. Surv. GeoFile*, 2011-11.
- Connock, G.T., Nguyen, T.X., Philp, R.P., 2018. The development and extent of photic-zone euxinia concomitant with Woodford Shale deposition. *AAPG Bull.* 102, 959–986.
- Copper, P., 2002. Reef development at the Frasnian-Famennian mass extinction boundary. *Palaeogeogr. Palaeoclimatol. Palaeoecol.* 181, 27–66. [https://doi.org/10.1016/S0031-0182\(01\)00472-2](https://doi.org/10.1016/S0031-0182(01)00472-2).
- Copper, P., Scotese, C.R., 2003. Megareefs in Middle Devonian super-greenhouse climates. *Geol. Soc. Am. Spec. Pap.* 370, 209–230. <https://doi.org/10.1130/0-8137-2370-1.209>.
- Le Cotonnec, A., Ventra, D., Hudson, S., Moscardelli, A., 2020. Systematically variable geometry and architecture of incised-valley fills controlled by orbital forcing: a conceptual model from the Pennsylvanian Breathitt Group (Kentucky, USA). *Sedimentology* 67, 2149–2188. <https://doi.org/10.1111/sed.12698>.
- Cramer, B.D., Vandenbroucke, T.R.A., Ludvigson, G.A., 2015. High-Resolution Event Stratigraphy (HiRES) and the quantification of stratigraphic uncertainty: Silurian examples of the quest for precision in stratigraphy. *Earth Sci. Rev.* 141, 136–153. <https://doi.org/10.1016/j.earscirev.2014.11.011>.
- Cramer, B.D., Jarvis, I., 2020. Chapter 11. Carbon isotope stratigraphy. In: Gradstein, F. M., Ogg, J.G., Schmidt, M.D., Ogg, G.M. (Eds.), *Geologic Time Scale 2020*, 1st edition. Elsevier, pp. 309–343. <https://doi.org/10.1016/B978-0-12-824360-2.00011-5>.

- Da Silva, A.-C., Boulvain, F., 2006. Upper Devonian carbonate platform correlations and sea level variations recorded in magnetic susceptibility. *Palaeogeogr. Palaeoclimatol. Palaeoecol.* 240, 373–388. <https://doi.org/10.1016/j.palaeo.2006.02.012>.
- Da Silva, A.C., De Vleeschouwer, D., Boulvain, F., Claeys, P., Fagel, N., Humblet, M., Mabilille, C., Michel, J., Sardar Avadi, M., Pas, D., Dekkers, M.J., 2013. Magnetic susceptibility as a high-resolution correlation tool and as a climatic proxy in Paleozoic rocks – Merits and pitfalls: examples from the Devonian in Belgium. *Mar. Pet. Geol.* 46, 173–189. <https://doi.org/10.1016/j.marpetgeo.2013.06.012>.
- Da Silva, A.C., Hladil, J., Chadimová, L., Slavík, L., Hilgen, F.J., Bábek, O., Dekkers, M.J., 2016. Refining the early Devonian time scale using Milankovitch cyclicity in Lochkovian-Pragian sediments (Prague Synform, Czech Republic). *Earth Planet. Sci. Lett.* 455, 125–139. <https://doi.org/10.1016/j.epsl.2016.09.009>.
- Da Silva, A.C., Sinnesael, M., Claeys, P., Davies, J.H.F.L., de Winter, N.J., Percival, L.M.E., et al., 2020. Anchoring the late Devonian mass extinction in absolute time by integrating climatic controls and radioisotopic dating. *Sci. Rep.* 10, 12940, 12 pp. <https://doi.org/10.1038/s41598-020-69097-6>.
- Dahl, T.W., Arens, S.K.M., 2020. The impacts of land plant evolution on Earth's climate and oxygenation state—an interdisciplinary review. *Chem. Geol.* 547, 119665. <https://doi.org/10.1016/j.chemgeo.2020.119665>.
- D'Antonio, M., Ibarra, D.E., Boyce, C.K., 2003. Land plant evolution decreased, rather than increased, weathering rates. *Geology*. <https://doi.org/10.1130/G46776.1>.
- Davies, A., Grésle, B., Hunter, S.J., Baines, G., Robson, C., Haywood, A.M., Ray, D.C., Simmons, M.D., van Buchem, F.S.P., 2020. Assessing the impact of aquifer-eustasy on short-term cretaceous sea-level. *Cretac. Res.* 112, 104445. <https://doi.org/10.1016/j.cretres.2020.104445>.
- de Andrade, C.L.N., Cardoso, T.R.M., Santos, R.R., Dino, R., Machado, A.J., 2020. Organic facies and paleontology from the Middle to late Devonian of the Pimenteira formation, Parnaíba Basin, Brazil. *J. S. Am. Earth Sci.* 99, 102481. <https://doi.org/10.1016/j.jsames.2019.102481>.
- De Vleeschouwer, D., Crucifix, M., Bounceur, N., Claeys, P., 2014. The impact of astronomical forcing on the late Devonian greenhouse climate. *Glob. Planet. Chang.* 120, 65–80. <https://doi.org/10.1016/j.gloplacha.2014.06.002>.
- De Vleeschouwer, D., Da Silva, A.-C., Sinnesael, M., Chen, D., Day, J.E., Whalen, M.T., Guo, Z., Claeys, P., 2017. Timing and pacing of the late Devonian mass extinction event regulated by eccentricity and obliquity. *Nat. Commun.* 8, 2268. <https://doi.org/10.1038/s41467-017-02407-1>.
- Deines, P., 2002. The carbon isotope geochemistry of mantle xenoliths. *Earth-Sci. Rev.* 58, 247–278. [https://doi.org/10.1016/S0012-8252\(02\)00064-8](https://doi.org/10.1016/S0012-8252(02)00064-8).
- DeSantis, M.K., Brett, C.E., 2011. Late Eifelian (Middle Devonian) bioevents: Timing and signature of the pre-Kacák Bakoven and Stony Hollow Events in eastern North America. *Palaeogeogr. Palaeoclimatol. Palaeoecol.* 304, 113–135. <https://doi.org/10.1016/j.palaeo.2010.10.013>.
- DiMichele, W.A., Cecil, C.B., Montañez, I.P., Falcon-Lang, H.J., 2010. Cyclic changes in Pennsylvanian paleoclimate and effects on floristic dynamics in tropical Pangaea. *Int. J. Coal Geol.* 83, 329–344. <https://doi.org/10.1016/j.coal.2010.01.007>.
- Domeier, M., Torsvik, T.H., 2014. Plate tectonics in the late Paleozoic. *Geosci. Front.* 5, 303–350. <https://doi.org/10.1016/j.gsf.2014.01.002>.
- Dong, T., Harris, N.B., Ayranci, K., 2018. Relative Sea-level cycles and organic matter accumulation in shales of the Middle and Upper Devonian Horn River Group, northeastern British Columbia, Canada: Insights into sediment flux, redox conditions, and bioproductivity. *GSA Bull.* 130, 859–880.
- Dopieralska, J., Belka, Z., Walczak, A., 2016. Nd isotope composition of conodonts: an accurate proxy of sea-level fluctuations. *Gondwana Res.* 22, 1102–1109. <https://doi.org/10.1016/j.gr.2015.02.022>.
- Driese, S.G., Mora, C.I., Elick, J.M., 1997. Morphology and taphonomy of root and stump casts of the earliest trees (Middle to Late Devonian), Pennsylvania and New York, U. S.A. *Palaos* 12, 524–537.
- Du Vivier, A.D., Selby, D., Sageman, B.B., Jarvis, I., Gröcke, D.R., Voigt, S., 2014. Marine 187Os/188Os isotope stratigraphy reveals the interaction of volcanism and ocean circulation during Oceanic Anoxic Event 2. *Earth Planet. Sci. Lett.* 389, 23–33. <https://doi.org/10.1016/j.epsl.2013.12.024>.
- Dunning, G.R., Barr, S.M., Giles, P.S., McGregor, D.C., Pe-Piper, G., Piper, D.J.W., 2002. Chronology of Devonian to early Carboniferous rifting and igneous activity in southern Magdalen Basin based on U-Pb (zircon) dating. *Can. J. Earth Sci.* 39. <https://doi.org/10.1139/e02-037>.
- Dyni, J.R., 2006. Geology and resources of some World oil-shale deposits. USGS Scientific Investigations Report 2005–5294, 42 p. [accessed on 2021-07-26 at. <http://www.usgs.gov/sir/2006/5294>].
- Ellwood, B.B., Crick, R.E., El Hassani, A., 1999. Magnetostratigraphy (MSEC) method used in geological correlation of Devonian rocks from Anti-Atlas Morocco. *AAPG Bull.* 83, 1119–1134. <https://doi.org/10.1306/E4FD2E8D-1732-11D7-8645000102C1865D>.
- Ellwood, B.B., Algeo, T.J., El Hassani, A., Tomkin, J.H., Rowe, H.D., 2011. Defining the timing and duration of the Kacák Interval within the Eifelian/Givetian boundary GSSP, Mech Irdane, Morocco, using geochemical and magnetic susceptibility patterns. *Palaeogeogr. Palaeoclimatol. Palaeoecol.* 304, 74–84. <https://doi.org/10.1016/j.palaeo.2010.10.012>.
- Elrick, M., 1995. Cyclostratigraphy of Middle Devonian carbonates of the eastern Great Basin. *J. Sediment. Res.* B65, 61–79. <https://doi.org/10.1306/D42681E4-2B26-11D7-8648000102C1865D>.
- Elrick, M., Berkýová, S., Klapper, G., Sharp, Z., Joachimski, M., Frýda, J., 2009. Stratigraphic and oxygen isotope evidence for My-scale glaciation driving eustasy in the Early-Middle Devonian greenhouse world. *Palaeogeogr. Palaeoclimatol. Palaeoecol.* 276, 170–181. <https://doi.org/10.1016/j.palaeo.2009.03.008>.
- Elrick, M., Scott, L.A., 2010. Carbon and oxygen isotope evidence for high-frequency (104–105 yr) and My-scale glacio-eustasy in Middle Pennsylvanian cyclic carbonates (Gray Mesa Formation), Central New Mexico. *Palaeogeogr. Palaeoclimatol. Palaeoecol.* 285, 307–320. <https://doi.org/10.1016/j.palaeo.2009.11.023>.
- Elrick, M., Witzke, B., 2016. Orbital-scale glacio-eustasy in the Middle Devonian detected using oxygen isotopes of conodont apatite: Implications for long-term greenhouse-icehouse climatic transitions. *Palaeogeogr. Palaeoclimatol. Palaeoecol.* 445, 50–59. <https://doi.org/10.1016/j.palaeo.2015.12.019>.
- Elrick, M., Gilleaudeau, G.J., Romaniello, S.J., Algeo, T.J., Morford, J.L., Sabbatino, M., Goepfert, T.J., Cleal, C., Cascales-Miñana, B., Chernyavskiy, P., 2022. Major Early-Middle Devonian oceanic oxygenation linked to early land plant evolution detected using high-resolution U isotopes of marine limestones. *Earth Planet. Sci. Lett.* 581, 117410. <https://doi.org/10.1016/j.epsl.2022.117410>.
- Ernst, R.E., Roddygin, S.A., Grinev, O.M., 2020. Age correlation of large Igneous Provinces with Devonian biotic crises. *Glob. Planet. Change* 185 (103097), 1–13. <https://doi.org/10.1016/j.gloplacha.2019.103097>.
- Ernst, R.E., Bond, D.P.G., Zhang, S.-H., Buchan, K.L., Grasby, S.E., Youbi, N., El Bilali, H., Bekker, A., Doucet, L.S., 2021. Large igneous province record through time and implications for secular environmental changes and geological time-scale boundaries. In: Ernst, R.E., Dickson, A.J., Bekker, A. (Eds.), *Large Igneous Provinces: A Driver of Global Environmental and Biotic Changes*, 255. Geophysical Monograph. <https://doi.org/10.1002/9781119507444.ch1>.
- Eriksson, K.A., McClung, W.S., Simpson, E.L., 2019. Sequence stratigraphic expression of greenhouse, transitional and icehouse conditions in siliciclastic successions: Paleozoic examples from the central Appalachian basin, USA. *Earth Sci. Rev.* 188, 176–189. <https://doi.org/10.1016/j.earscirev.2018.11.010>.
- Ettensohn, F.R., 1994. Tectonic control on formation and cyclicity of major Appalachian unconformities and associated stratigraphic sequences. In: Dennison, J.M., Ettensohn, F.R. (Eds.), *Tectonic and Eustatic Controls on Sedimentary Cycles: SEPM (Society for Sedimentary Geology) Concepts in Sedimentology and Paleontology*, 4, pp. 217–242.
- Evans, J.E., Maurer, J.T., Holm-Denoma, C.S., 2019. Recognition and significance of Upper Devonian fluvial, estuarine, and mixed siliciclastic-carbonate nearshore marine facies in the San Juan Mountains (southwestern Colorado, USA): Multiple incised valleys backfilled by lowstand and transgressive systems tracts. *Geosphere* 15, 1479–1507. <https://doi.org/10.1130/GES02085.1>.
- Falcon-Lang, H.J., 2005. Earliest mountain forests. *Geol. Today* 21, 178–181. <https://doi.org/10.1111/j.1365-2451.2005.00526.x>.
- Ferretti, A., Histon, K., McLaughlin, P.I., Brett, C.E., 2012. Time-specific facies: The color and texture of biotic events. *Palaeogeogr. Palaeoclimatol. Palaeoecol.* 367–368, 1–2. <https://doi.org/10.1016/j.palaeo.2012.10.010>.
- Filer, J.K., 2002. Late Frasnian sedimentation cycles in the Appalachian basin—possible evidence for high frequency eustatic sea-level changes. *Sediment. Geol.* 154, 31–52. [https://doi.org/10.1016/S0037-0738\(02\)00159-8](https://doi.org/10.1016/S0037-0738(02)00159-8).
- Filippelli, G.M., 2002. The global phosphorus cycle. *Rev. Mineral. Geochem.* 48, 391–425. <https://doi.org/10.2138/rmg.2002.48.10>.
- Fischer, A.G., Arthur, M.A., 1977. Secular variations in the pelagic realm. In: Cook, H.E., Enos, P. (Eds.), *Deep-Water Carbonate Environments*, 25. SEPM Special Publication, pp. 19–50.
- Flögel, S., Wallmann, K., Poulsen, C.J., Zhou, J., Oschlies, A., Voigt, S., Kuhnt, W., 2011a. Simulating the biogeochemical effects of volcanic CO₂ degassing on the oxygenate of the deep ocean during the Cenomanian/Turonian Anoxic Event (OAE2). *Earth Planet. Sci. Lett.* 305, 371–384. <https://doi.org/10.1016/j.epsl.2011.03.018>.
- Föllmi, K., 2012. Early cretaceous life, climate and anoxia. *Cretac. Res.* 35, 230–257. <https://doi.org/10.1016/j.cretres.2011.12.005>.
- Föllmi, K., Weissert, H., Bispin, M., Funk, H., 1994. Phosphogenesis, carbon-isotope stratigraphy, and carbonate-platform evolution along the lower cretaceous northern Tethyan margin. *Geol. Soc. Am. Bull.* 106, 729–746. [https://doi.org/10.1130/0016-7606\(1994\)106<0729:PCISAC>2.3.CO;2](https://doi.org/10.1130/0016-7606(1994)106<0729:PCISAC>2.3.CO;2).
- Föllmi, K.B., Gairola, F., 2008. Demise of the northern Tethyan Urogenian carbonate platform and subsequent transition towards pelagic conditions: the sedimentary record of the Col de la Plaine Morte area, Central Switzerland. *Sediment. Geol.* 205, 142–159.
- Fowler, M.G., Stasiuk, L.D., Hearn, M., Obermajer, M., 2001. Devonian hydrocarbon source rocks and their derived oils in the Western Canada Sedimentary Basin. *Bull. Can. Petrol. Geol.* 49, 117–148. <https://doi.org/10.2113/49.1.117>.
- Fraser, T.A., Hutchison, M.P., 2017. Lithogeochemical characterization of the Middle-Upper Devonian Road River Group and Canol and Imperial formations on Trail River, East Richardson Mountains, Yukon: age constraints and a depositional model for fine-grained strata in the lower Paleozoic Richardson trough. *Can. J. Earth Sci.* 54, 731–765. <https://doi.org/10.1139/cjes-2016-0216>.
- French, K.L., Rocher, D., Zumberge, J.E., Summons, R.E., 2015. Assessing the distribution of sedimentary C40 carotenoids through time. *Geobiology* 13, 139–151. <https://doi.org/10.1111/gbi.12126>.
- Freyemueller, N.A., Moore, J.R., Myers, C.E., 2019. An analysis of the impacts of cretaceous oceanic anoxic events on global molluscan diversity dynamics. *Paleobiology* 2019, 1–16. <https://doi.org/10.1017/pab.2019.10>.
- Gadd, M.G., Peter, J.M., Hnatyshin, D., Creaser, R., Gouwy, S.A., 2020. A Middle Devonian basin-scale precious metal enrichment event across northern Yukon (Canada). *Geology* 48, 242–246. <https://doi.org/10.1130/G46874.1>.
- Gadd, M.G., Peter, J.M., Fraser, T.A., Layton-Matthews, D., 2022. Paleoredox and lithogeochemical indicators of the environment of formation and genesis of the Monster River hyper-enriched black shale showing, Yukon. In: Peter, J., Gadd, M. (Eds.), *Geological Survey of Canada Bulletin* 617, pp. 113–127. <https://doi.org/10.4095/328004>.

- Gale, A.S., Mutterlose, J., Batenburg, S., Gradstein, F.M., Agterberg, F.P., Ogg, J.G., Petrizzo, M.R., 2020. Chapter 27 - The Cretaceous period. In: Gradstein, F.M., Ogg, J.G., Schmidt, M.D., Ogg, G.M. (Eds.), *Geologic Time Scale 2020*, 1st edition. Elsevier, pp. 1023–1086. <https://doi.org/10.1016/B978-0-12-824360-2.00027-9>.
- Gales, E., Black, B., Elkins-Tanton, L.T., 2020. Carbonates as a record of the carbon isotope composition of large igneous province outgassing. *Earth Planet. Sci. Lett.* 535, 116076. <https://doi.org/10.1016/j.epsl.2020.116076>.
- Ganino, C.G., Arndt, N.T., 2009. Climate changes caused by degassing of sediments during the emplacement of large igneous provinces. *Geology* 37, 323–326. <https://doi.org/10.1130/G25325A.1>.
- Ganopolski, A., Winkelmann, R., Schellnhuber, H.J., 2016. Critical insolation-CO₂ relation for diagnosing past and future glacial inception. *Nature* 592, 200–203. <https://doi.org/10.1038/nature16494>. + suppl. Materials.
- Gatovskii, Y.A., Stupakova, A.V., Kalmykov, G.A., Korobova, N.Y., Suslova, A.A., Sautkin, R.S., Kalmykov, D.G., 2016. New data on the biostratigraphy and facies types of upper carboniferous Domanik sections in the.
- Gibling, M.R., Davies, N.S., 2012. Palaeozoic landscapes shaped by plant evolution. *Nat. Geosci.* 5. <https://doi.org/10.1038/NGEO1376>.
- Gilly, W.F., Beman, J.M., Litvin, S.Y., Robison, B.H., 2013. Oceanographic and biological effects of shoaling of the oxygen minimum zone. *Annu. Rev. Mar. Sci.* 5, 393–420.
- Golonka, J., 2020. Late Devonian paleogeography in the framework of global plate tectonics. *Glob. Planet. Chang.* 186, 103129. <https://doi.org/10.1016/j.gloplacha.2020.1031>.
- Goodfellow, W.D., Jonasson, I.R., 1984. Ocean stagnation and ventilation defined by 834S secular trends in pyrite and barite, Selwyn Basin. *Yukon Geol.* 12, 583–586.
- Goodfellow, W.D., Geldsetzer, H.H.J., McLaren, D.J., Orchard, M.J., Klapper, G., 1989. The Frasnian-Famennian extinction: The current results and possible causes. In: McMillan, N.J., Embry, A.F., Glass, D.J. (Eds.), *Devonian of the World, v. III: Canadian Society of Petroleum Geologists Memoir 14*, pp. 9–21.
- Gouwy, S.A., 2022. Devonian conodont biostratigraphy of the Mackenzie Mountains, western part of the Northwest Territories. In: Lavoie, D., Dewing, K. (Eds.), *Sedimentary Basins of the Canadian North - Contributions to a 1 000 Ma Geological Journey and Insight on Resource Potential*. Geological Survey of Canada, Bulletin 609, pp. 159–184. <https://doi.org/10.4095/326098>.
- Gradstein, F.M., Ogg, J.G., 2020. Chapter 2. The chronostratigraphic scale. In: Gradstein, F.M., Ogg, J.G., Schmidt, M.D., Ogg, G.M. (Eds.), *Geologic Time Scale 2020*, 1st edition. Elsevier, pp. 21–32. <https://doi.org/10.1016/B978-0-12-824360-2.00002-4>.
- Grasby, S.E., Rhem II, T.R., Chen, Z., Yin, R., Ardakani, O.H., 2019. Mercury as a proxy for volcanic emissions in the geologic record. *Earth Sci. Rev.* 196. <https://doi.org/10.1016/j.earscirev.2019.102880>.
- Grasby, S.E., Liu, X., Yin, R., Ernst, R., Chen, Z., 2020. Toxic mercury pulses into late Permian terrestrial and marine environments. *Geology* 48 (8), 830–833. <https://doi.org/10.1130/G47295.1>.
- Grasby, S.E., Bond, D.P.G., Wignall, P.B., Yin, R., Strachan, L.J., Takahashi, S., 2021. Transient Permian-Triassic euxinia in the southern Panthalassa deep ocean. *Geology* 49, 889–893. <https://doi.org/10.1130/G48928.1>.
- Grice, K., Cao, C., Love, G.D., Böttcher, M.E., Twitcheit, R.J., Grosjean, E., Summons, R.E., Turgeon, S.C., Dunning, W., Jin, Y., 2005. Photic zone euxinia during the Permian-Triassic superanoxic event. *Science* 307 (5710), 706–709. <https://doi.org/10.1126/science.1104323>.
- Grossman, E.L., Joachimski, M.M., 2020. Chapter 10. Oxygen isotope stratigraphy. In: Gradstein, F.M., Ogg, J.G., Schmidt, M.D., Ogg, G.M. (Eds.), *Geologic Time Scale 2020*, 1st edition. Elsevier, pp. 279–307. <https://doi.org/10.1016/B978-0-12-824360-2.00010-3>.
- Haddad, E.E., Tuite, M.L., Martinez, A.M., Willford, K., Boyer, D.L., Droser, M.L., Love, G.D., 2016. Lipid biomarker stratigraphic records through the late Devonian Frasnian/Famennian boundary: comparison of high- and low-latitude epicontinental marine settings. *Org. Geochem.* 98, 38–53. <https://doi.org/10.1016/j.orggeochem.2016.05.007>.
- Hadlari, T., Tylosky, S.A., Lemieux, Y., Zantvoort, W.G., Catuneanu, O., 2009. Slope and submarine fan turbidite facies of the Upper Devonian Imperial Formation, northern Mackenzie Mountains NWT. *Bull. Can. Pet. Geol.* 57, 192–208.
- Hallam, A., Wignall, P.B., 1997. In: *Mass Extinctions and their Aftermath*. Oxford University Press, p. 328 p..
- Hallam, A., Wignall, P.B., 1999. Mass extinctions and sea-level changes. *Earth-Sci. Rev.* 48, 217–250. [https://doi.org/10.1016/S0012-8252\(99\)00055-0](https://doi.org/10.1016/S0012-8252(99)00055-0).
- Han, Z., Hu, X., Kemp, D.B., Li, J., 2018. Carbonate-platform response to the Toarcian Oceanic Anoxic Event in the southern hemisphere: Implications for climatic change and biotic platform demise. *Earth Planet. Sci. Lett.* 489, 59–71. <https://doi.org/10.1016/j.epsl.2018.02.017>.
- Hansen, K.E., Giraudeau, J., Limoges, A., Massé, L., Massé, G., Rudra, A., Wacker, L., Sanei, H., Pearce, C., Seidenkrantz, M.-S., 2022. Characterization of organic matter in marine sediments to estimate age offset of bulk radiocarbon dating. *Quat. Geochronol.* 67, 101242. <https://doi.org/10.1016/j.quageo.2021.101242>.
- Hancock, J.M., Kauffman, E.G., 1979. The great transgressions of the late Cretaceous. *J. Geol. Soc. Lond.* 136, 175–186. <https://doi.org/10.1144/gsjgs.136.2.0175>.
- Haq, B.U., Shutter, S.R., 2008. A chronology of Paleozoic Sea-level changes. *Science* 322, 64–68. <https://doi.org/10.1126/science.1161648>.
- Haq, B.U., 2014. Cretaceous eustasy revisited. *Glob. Planet. Chang.* 113, 44–58. <https://doi.org/10.1016/j.gloplacha.2013.12.007>.
- Harris, B.S., LaGrange, M.T., Biddle, S.K., Playter, T.L., Fiess, K.M., Gingras, M.K., 2021. Chemostratigraphy as a tool for sequence stratigraphy in the Devonian Hare Indian Formation in the Mackenzie Mountains and Central Mackenzie Valley, Northwest Territories, Canada. *Can. J. Earth Sci.* 59. <https://doi.org/10.1139/cjes-2020-0198>.
- Harris, N.B., McMillan, J.M., Knapp, L.J., Mastalerz, M., 2018. Organic matter accumulation in the Upper Devonian Duvernay Formation, Western Canada Sedimentary Basin, from sequence stratigraphic analysis and geochemical proxies. *Sediment. Geol.* 376, 185–203.
- Hartenfels, S., Becker, R.T., 2009. Timing of the global Dasberg Crisis - implications for Famennian eustasy and chronostratigraphy. In: Over, D.J. (Ed.), *Studies in Devonian Stratigraphy: Proceedings of the 2007 International Meeting of the Subcommittee on Devonian Stratigraphy and IGCP 499*, 63. *Palaeontographica Americana*, pp. 69–95.
- Hauck, T.E., Paná, D., DuFrane, S.A., 2017. Northern Laurentian provenance for Famennian clastics of the Jasper Basin (Alberta, Canada): a Sm-Nd and U-Pb detrital zircon study. *Geosphere* 13 (4), 1149–1172. <https://doi.org/10.1130/GES01453.1>.
- Hawkins, L.M.A., Grappone, J.M., Sprain, C.J., Saengduan, P., Sage, E.J., Thomas-Cunningham, S., Kugabalan, B., Biggin, A.J., 2021. Intensity of the Earth's magnetic field: evidence for a Mid-Paleozoic dipole low. *Proc. Natl. Acad. Sci. U. S. A.* 118. <https://doi.org/10.1073/pnas.2017342118>.
- Hay, W.W., Leslie, M.A., 1990. Could possible changes in global groundwater reservoir cause eustatic sea-level fluctuations? In: Revelle, R. (Ed.), *Panel Chairman, Sea-Level Change*. National Academy Press, Washington D.C., pp. 161–170.
- Hay, W.W., 2008. Evolving ideas about the Cretaceous climate and ocean circulation. *Cretac. Res.* 29, 725–753. <https://doi.org/10.1016/j.cretres.2008.05.025>.
- Hay, W.W., Flögel, S., 2012. New thoughts about the Cretaceous climate and oceans. *Earth Sci. Rev.* 115, 262–272. <https://doi.org/10.1016/j.earscirev.2012.09.008>.
- Heath, M.N., Cramer, B.D., Stolfus, B.M., Barnes, G.L., Clark, R.J., Day, J.E., Barnett, B.A., Witzke, B.J., Hogancamp, N.J., Tassier-Surine, S., 2021. Chemoautotrophy as the driver of decoupled organic and carbonate carbon isotope records at the onset of the Hangenberg (Devonian-Carboniferous Boundary) Oceanic Anoxic Event. *Palaeogeogr. Palaeoclimatol. Palaeoecol.* 577, 110540. <https://doi.org/10.1016/j.palaeo.2021.110540>.
- Heckel, P.H., 2008. Chapter 19: Pennsylvanian cyclothem in Midcontinent North America as far-field effects of waxing and waning of Gondwana ice sheets. In: Fielding, C.R., Frank, T.D., Isbell, J.L. (Eds.), *Resolving the Late Paleozoic Ice Age in Time and Space*, 441. Geological Society of America Special Paper, pp. 275–289.
- Hedhli, M., Dewing, K., Beauchamp, B., Grasby, S.E., Meyer, R., 2022. Devonian to Carboniferous continental-scale carbonate turnover in Western Laurentia (North America): upwelling or climate cooling? *Facies* 68. <https://doi.org/10.1007/s10347-022-00653-4>.
- Holmden, C., Braun, W.K., Patterson, W.P., Eglinton, B.M., Prokopiuk, T.C., Whittaker, S., 2006. Carbon isotope chemostratigraphy of Frasnian sequences in western Canada. In: *Summary of Investigations 2006, Volume 1*, Saskatchewan Geological Survey, Sask. Industry Resources, Misc. Rep. 2006-4.1, CD-ROM, Paper A-8, 6p.
- House, M.R., 1983. Devonian eustatic events. *Proc. Ussher Society* 5, 396–405.
- House, M.R., 1985. Correlation of mid-Paleozoic ammonoid evolutionary events with global sedimentary perturbations. *Nature* 313, 17–22.
- House, M.R., 1996. In: *The Middle Devonian Kačák Event*, vol. 9. *Proceedings of the Ussher Society*, pp. 79–84.
- House, M.R., 2002. Strength, timing, setting and cause of mid-Paleozoic extinctions. *Palaeogeogr. Palaeoclimatol. Palaeoecol.* 181, 5–25. [https://doi.org/10.1016/S0031-0182\(01\)00471-0](https://doi.org/10.1016/S0031-0182(01)00471-0).
- House, M.R., Menner, V.V., Becker, R.T., Klapper, G., Ovnatanova, N.S., Kuzmin, A.V., 2000. Reef episodes, anoxia and sea-level changes in the Frasnian of the southern Timan (NE Russian Platform). In: Insalaco, E., Skelton, P.W., Palmer, T.J. (Eds.), *Carbonate Platform Systems: Components and Interactions*, 178. Geological Society, London, pp. 147–176. <https://doi.org/10.1144/GSL.SP.2000.178.01.11>.
- Huang, C., Joachimski, M.M., Gong, Y., 2018. Did climate changes trigger the Late Devonian Kellwasser Crisis? Evidence from a high-resolution conodont $\delta^{18}\text{O}_{\text{PO}_4}$ record from South China. *Earth Planet. Sci. Lett.* E. 495, 174–184. <https://doi.org/10.1016/j.epsl.2018.05.016>.
- Imhoff, J.F., Thiel, V., 2010. Phylogeny and taxonomy of Chlorobiaceae. *Photosynth. Res.* 104, 123–136.
- Immenhauser, A., 2005. High-rate Sea-level change during the Mesozoic: new approaches to an old problem. *Sediment. Geol.* 175, 277–296. <https://doi.org/10.1016/j.sedgeo.2004.12.016>.
- Isaacson, P.E., Diaz-Martinez, E., Grader, G.W., Kalvoda, J., Babek, O., Devuyst, F.X., 2008. Late Devonian-earliest Mississippian glaciation in Gondwanaland and its biogeographic consequences. *Palaeogeogr. Palaeoclimatol. Palaeoecol.* 268, 126–142. <https://doi.org/10.1016/j.palaeo.2008.03.047>.
- Isbell, J.L., Vesely, F.F., Rosa, E.L.M., Pauls, K.N., Fedorchuk, N.D., Ives, L.R.W., McNall, N.B., Litwin, S.A., Borucki, M.K., Malone, J.E., Kusick, A.R., 2021. Evaluation of physical and chemical proxies used to interpret past glaciations with a focus on the late Paleozoic Ice Age. *Earth Sci. Rev.* 221, 103756. <https://doi.org/10.1016/j.earscirev.2021.103756>.
- Jenkyns, H.C., 2010. Geochemistry of oceanic anoxic events. *Geochim. Geophys. Geosyst.* 11, Q03004. <https://doi.org/10.1029/2009GC002788>.
- Jiang, C., Li, M., Osadetz, K.G., Snowdon, L.R., Obermajer, M., Fowler, M.G., 2001. Bakken/Madison petroleum systems in the Canadian Williston Basin. Part 2: molecular markers diagnostic of Bakken and Lodgepole source rocks. *Org. Geochem.* 32, 1037–1054.
- Joachimski, M.M., Buggisch, W., 1993. Anoxic events in the late Frasnian — causes of the Frasnian-Famennian faunal crisis? *Geology* 21, 675–678. [https://doi.org/10.1130/0091-7613\(1993\)021<0675:AEITLF>2.3.CO;2](https://doi.org/10.1130/0091-7613(1993)021<0675:AEITLF>2.3.CO;2).
- Joachimski, M.M., Ostertag-Henning, C., Pancost, R.D., Strauss, H., Freeman, K.H., Littke, R., Damste, J.S.S., Racki, G., 2001. Water column anoxia, enhanced productivity and concomitant changes in $\delta^{13}\text{C}$ and in 834S across the Frasnian-

- Famennian boundary (Kowala Holy Cross Mountains/Poland). *Chem. Geol.* 175, 109–131.
- Joachimski, M.M., Breisig, S., Buggisch, W., Day, J., van Geldern, R., 2004. Oxygen isotope evolution of biogenic calcite and apatite during the Middle and late Devonian. *Int. J. Earth Sci.* 93, 542–553. <https://doi.org/10.1007/s00531-004-0405-8>.
- Joachimski, M.M., Breisig, S., Buggisch, W., Talent, J.A., Mawson, R., Gereke, M., Morrow, J.R., Day, J., Weddige, K., 2009. Devonian climate and reef evolution: Insights from oxygen isotopes in apatite. *Earth Planet. Sci. Lett.* 284, 599–609. <https://doi.org/10.1016/j.epsl.2009.05.028>.
- Johnson, J.G., 1971. Timing and coordination of orogenic, epeirogenic, and eustatic events. *Geol. Soc. Am. Bull.* 82, 3263–3298.
- Johnson, J.G., Klapper, G., Sandberg, C.A., 1985. Devonian eustatic fluctuations in Euramerica. *Geol. Soc. Am. Bull.* 96, 567–587. [https://doi.org/10.1130/0016-7606\(1985\)96<567:DEFIE>2.0.CO;2](https://doi.org/10.1130/0016-7606(1985)96<567:DEFIE>2.0.CO;2).
- Johnston, D.L., Henderson, C.M., Schmidt, M.J., 2010. Upper Devonian to lower Mississippian conodont biostratigraphy of uppermost Wabamun Group and Palliser Formation to lowermost Banff and Ledgepole formations, southern Alberta and southeastern British Columbia, Canada: Implications for correlations and sequence stratigraphy. *Bull. Can. Petrol. Geol.* 58 (4), 295–341.
- Kabanov, P.B., 2014. Landry Formation of Kugaluk N-02 well (Devonian, northern mainland NWT): insight into formation's boundaries, lithofacies, and stratal stacking patterns. *Bull. Can. Petrol. Geol.* 62, 105–124. <https://doi.org/10.2113/gscpgbull.62.2.105>.
- Kabanov, P., 2017. Geological and geochemical data from Mackenzie Corridor. Part VII: new geochemical, Rock-Eval 6, and field data from the Ramparts and Canol formations of northern Mackenzie Valley, Northwest Territories. <https://doi.org/10.4095/306299>.
- Kabanov, P., 2019. Devonian (c. 388–375 my) Horn River Group of Mackenzie Platform (northwestern Canada) is an open-shelf succession recording oceanic anoxic events. *J. Geol. Soc. Lond.* 176, 29–45.
- Kabanov, P., 2021. Early-Middle Devonian paleosols and palustrine beds of NW Canada in the context of land plant evolution and global spreads of anoxia. *Glob. Planet. Change* 204, 103573. <https://doi.org/10.1016/j.gloplacha.2021.103573>.
- Kabanov, P., 2021. Early-Middle Devonian paleosols and palustrine beds of NW Canada in the context of land plant evolution and global spreads of anoxia. *Glob. Planet. Change* 204, 103573. <https://doi.org/10.1016/j.gloplacha.2021.103573>.
- Kabanov, P., 2022. Devonian of the Mackenzie. In: Lavoie, D., Dewing, K. (Eds.), *Sedimentary Basins of the Canadian North - Contributions to a 1000 Ma Geological Journey and Insight on Resource Potential*, 609. Geological Survey of Canada, Bulletin, pp. 129–158. <https://doi.org/10.4095/326094>.
- Kabanov, P., Alekseeva, T., Alekseev, A., Alekseeva, V., Gubin, S., 2010. Paleosols in late Moscovian (Carboniferous) marine carbonates of east European Craton revealing “Great Calcimagnesian Plain” paleolandscapes. *J. Sediment. Res.* 80, 195–215. <https://doi.org/10.2110/jsr.2010.026>.
- Kabanov, P., Gouvy, S., 2017. The Devonian Horn River Group and the basal Imperial Formation of the Central Mackenzie Plain, N.W.T., Canada: Multiproxy stratigraphic framework of a black shale basin. *Can. J. Earth Sci.* 54, 409–429. <https://doi.org/10.1139/cjes-2016-0096>.
- Kabanov, P., Gouvy, S.A., van der Boon, A., Grasby, S.E., in review. Nature of Devonian anoxic events based on multiproxy records from Panthalassa, NW Canada. *Glob. Planet. Change*.
- Kabanov, P., Jiang, C., 2020. Photoc-zone euxinia and anoxic events in a Middle-late Devonian shelfal sea of Panthalassan continental margin, NW Canada: changing paradigm of Devonian Ocean and sea level fluctuations. *Glob. Planet. Change* 188. <https://doi.org/10.1016/j.gloplacha.2020.103153>.
- Kabanov, P.B., Gouvy, S.A., 2021. The type section of the Canol Formation (Devonian black shale) at Powell Creek: critical assessment and correlation in the northern Cordillera, NWT, Canada. *Bull. Can. Petrol. Geol.* 68, 123–140. <https://doi.org/10.35767/gscpgbull.68.4.123>.
- Kabanov, P., Abdi, W., Biggin, A.J., Bilot, I., van der Boon, A., Gouvy, S.A., Grasby, S.E., Minions, N., Percival, J.B., Thallner, D., Twemlow, C., 2023. Geological and geochemical data from Mackenzie corridor. Part XI: New geochemical, magnetic susceptibility, and X-ray diffraction data from the Horn River Group (Devonian) in cores and outcrops south of Norman Wells, Northwest Territories. <https://doi.org/10.4095/331201>. Geological Survey of Canada, Open File 8940.
- Kaiho, K., Miura, M., Tezuka, M., Hayashi, N., Jines, D.S., Oikawa, K., Casier, J.-G., Fujibayashi, M., Hen, Z.-Q., 2021. Coronene, mercury, and biomarker data support a link between extinction magnitude and volcanic intensity in the Late Devonian. *Glob. Planet. Change* 199, 103452. <https://doi.org/10.1016/j.gloplacha.2021.103452>.
- Kaiser, S.I., Aretz, M., Becker, R.T., 2016. The global Hangenberg Crisis (Devonian–Carboniferous transition): review of a first-order mass extinction. In: Becker, R.T., Königshof, P., Brett, C.E. (Eds.), *Devonian Climate, Sea Level and Evolutionary Events*, 423. Geological Society, London, pp. 387–437. <https://doi.org/10.1144/SP423.9>. Special Publications.
- Karstensen, J., Stramma, L., Visbeck, M., 2008. Oxygen minimum zones in the eastern tropical Atlantic and Pacific oceans. *Prog. Oceanogr.* 77, 331–350. <https://doi.org/10.1016/j.pocean.2007.05.009>.
- Keith, M.L., 1982. Violent volcanism, stagnant oceans and some inferences regarding petroleum, strata-bound ores and mass extinctions. *Geochim. Cosmochim. Acta* 46, 2621–2637.
- Kendall, B., Wang, J., Zheng, W., Romaniello, S.J., Over, D.J., Bennett, Y., Xing, L., Kunert, A., Boyes, C., Liu, J., 2020. Inverse correlation between the molybdenum and uranium isotope compositions of Upper Devonian black shales caused by changes in local depositional conditions rather than global ocean redox variations. *Geochim. Cosmochim. Acta* 287, 141–164. <https://doi.org/10.1016/j.gca.2020.01.026>.
- Kennedy, K., Gibling, M., Elbe, C.F., Gastaldo, R.A., Gensel, P.G., Werner-Zwanziger, U., Wilson, R.A., 2013. Lower Devonian coaly shales of northern New Brunswick, Canada: plant accumulations in the early stages of terrestrial colonization. *J. Sediment. Res.* 83, 1202–1215. <https://doi.org/10.2110/jsr.2013.86>.
- Kent, D.V., Muttoni, G., 2013. Modulation of Late Cretaceous and Cenozoic climate by variable drawdown of atmospheric pCO₂ from weathering of basaltic provinces on continents drifting through the equatorial humid belt. *Clim. Past* 9, 525–546. <https://doi.org/10.5194/cp-9-525-2013>.
- Kidder, D.L., Worsley, T.R., 2004. Causes and consequences of extreme Permo-Triassic warming to globally equable climate and relation to the Permo-Triassic extinction and recovery. *Palaeogeogr. Palaeoclimatol. Palaeoecol.* 203, 207–237.
- Kidder, D.L., Worsley, T.R., 2010. Phanerozoic large Igneous Provinces (LIPs), HEATT (Haline Euxinic Acidic thermal Transgression) episodes, and mass extinctions. *Palaeogeogr. Palaeoclimatol. Palaeoecol.* 295, 162–191. <https://doi.org/10.1016/j.palaeo.2010.05.036>.
- Kidder, D.L., Worsley, T.R., 2012. A human-induced hothouse climate? *GSA Today* 22, 4–11. <https://doi.org/10.1130/G131A.1>.
- Kiessling, W., Flügel, E., Golonka, J., 2003. Patterns of Phanerozoic carbonate platform sedimentation. *Lethaia* 36. <https://doi.org/10.1080/00241160310004648>.
- Klemme, H.D., Ulmishak, G.F., 1991. Effective petroleum source rocks of the world: stratigraphic distribution and controlling depositional factors. *AAPG Bull.* 75, 1809–1851. <https://doi.org/10.1306/0C9B2A47-1710-11D7-8645000102C1865D>.
- Knapp, L.J., McMillan, J.M., Harris, N.B., 2017. A depositional model for organic-rich Duvernay Formation mudstones. *Sediment. Geol.* 347, 160–182. <https://doi.org/10.1016/j.sedgeo.2016.11.012>.
- Königshof, P., Da Silva, A.C., Suttner, T.J., Kido, E., Waters, J., Carmichael, S.K., Jansen, U., Pas, D., Spassov, S., 2015. Shallow-water facies setting around the Kačák Event: a multidisciplinary approach. In: Becker, R.T., Königshof, P., Brett, C.E. (Eds.), *Devonian Climate, Sea Level and Evolutionary Events*. Geological Society, London. <https://doi.org/10.1144/SP423.4>. Special Publications, 423.
- Koopmans, W.P., Köster, J., van Kaam-Peters, H.M.E., Kenig, F., Schouten, S., Hartgers, W.A., de Leeuw, J.W., Sinnighe Damsté, J.S., 1996. Diagenetic and catagenetic products of isorenieratene; molecular indicators for photic zone anoxia. *Geochim. Cosmochim. Acta* 60, 4467–4496.
- Kopp, R.E., Kirschvink, J.L., 2008. The identification and biogeochemical interpretation of fossil magnetotactic bacteria. *Earth Sci. Rev.* 86, 42–61. <https://doi.org/10.1016/j.earscirev.2007.08.001>.
- Krause, A.J., Mills, B.J.W., Zhang, S., Planavsky, N.J., Lenton, T.M., Poulton, S.W., 2018. Stepwise oxygenation of the Paleozoic atmosphere. *Nat. Commun.* 9, 4081. <https://doi.org/10.1038/s41467-018-06383-y>.
- Kravchinsky, V.A., 2012. Paleozoic large igneous provinces of Northern Eurasia: correlation with mass extinction events. *Glob. Planet. Change* 86–87, 31–36.
- Kump, L.R., Pavlov, A., Arthur, M.A., 2005. Massive release of hydrogen sulfide to the surface ocean and atmosphere during intervals of oceanic anoxia. *Geology* 33, 397–400.
- Kuszniir, N.J., Stovba, S.M., Stephenson, R.A., Poplavskii, K.N., 1996. The formation of the northwestern Dniepr-Donets Basin: 2-D forward and reverse syn-rift and post-rift modelling. *Tectonophysics* 268, 237–255. [https://doi.org/10.1016/S0040-1951\(96\)00230-2](https://doi.org/10.1016/S0040-1951(96)00230-2).
- Lachkar, Z., Lévy, M., Smith, K.S., 2019. Strong intensification of the Arabian Sea Oxygen Minimum Zone in response to Arabian Gulf warming. *Geophys. Res. Lett.* 46, 5420–5429. <https://doi.org/10.1029/2018GL081631>.
- Lafargue, E., Marquis, F., Pillot, D., 1998. Rock-Eval 6 applications in hydrocarbon exploration, production, and soil contamination studies. *Inst. Français Pétrole* 53, 421–437.
- Lash, G.G., 2019. A global biogeochemical perturbation during the Middle Frasnian punctata event: evidence from muted carbon isotope signature in the Appalachian Basin, New York State (USA). *Glob. Planet. Change* 177, 239–254. <https://doi.org/10.1016/j.gloplacha.2019.01.006>.
- Laskar, J., Fienga, A., Gastineau, M., Manche, H., 2011. La2010: a new orbital solution for the long-term motion of the Earth. *Astron. Astrophys.* 532 (A89), 1–15.
- Leckie, R., Bralower, T., Cashman, R., 2002. Oceanic anoxic events and planktonic evolution: biotic response to tectonic forces during the mid-Cretaceous. *Paleoceanography* 17, 1–29. <https://doi.org/10.1029/2001PA000623>.
- Le Hir, G., Donnadieu, Y., Goddérès, Y., Meyer-Berthaud, B., Ramstein, G., Blackey, R.C., 2011. The climate change caused by the land plant invasion in the Devonian. *Earth Planet. Sci. Lett.* 310, 203–212. <https://doi.org/10.1016/j.epsl.2011.08.042>.
- Léonide, P., Floquet, M., Durlot, C., Baudin, F., Pittet, B., Lécuyer, C., 2012. Drowning of a carbonate platform as a precursor stage of the early Toarcian global anoxic event (Southern Provence sub-Basin, South-east France). *Sedimentology* 59, 156–184. <https://doi.org/10.1111/j.1365-3091.2010.01221.x>.
- Li, S., Wignall, P.B., Poulton, S.W., Hedhli, M., Grasby, S.E., 2022. Carbonate shutdown, phosphogenesis and the variable style of marine anoxia in the late Famennian (Late Devonian) in western Laurentia. *Palaeogeogr. Palaeoclimatol. Palaeoecol.* 589, 110835. <https://doi.org/10.1016/j.palaeo.2022.110835>.
- Liang, X., Jin, Z., Philippov, V., Obryadchikov, O., Zhong, D., Liu, Q., Quspensky, B., Morozov, V., 2020. Sedimentary characteristics and evolution of Domanik facies from the Devonian-Carboniferous regression in the southern Volga-Ural Basin. *Mar. Pet. Geol.* 119. <https://doi.org/10.1016/j.marpetgeo.2020.104438>.
- Liu, Z., Percival, L.M.E., Vandeputte, D., Selby, D., Glaeys, P., Over, D.J., Gao, Y., 2021. Upper Devonian mercury record from North America and its implications for the Frasnian-Famennian mass extinction. *Palaeogeogr. Palaeoclimatol. Palaeoecol.* 576, 110502. <https://doi.org/10.1016/j.palaeo.2021.110502>.

- Lobkovsky, L.I., Cloetingh, S., Nikishin, A.M., Volozh, Yu.A., Lankreijer, A.C., Belyakov, S.L., Groshev, V.G., Fokin, P.A., Milanovsky, E.E., Pevzner, L.A., Gorbachev, V.I., Korneev, M.A., 1996. Extensional basins of the former Soviet Union — structure, basin formation mechanisms and subsidence history. *Tectonophysics* 266, 251–285. [https://doi.org/10.1016/S0040-1951\(96\)00193-X](https://doi.org/10.1016/S0040-1951(96)00193-X).
- Lottmann, J., 1990. Die pumilio events (Mittel-Devon). *Gött. Arb. Geol. Paläontol.* 44, 1–98.
- Lu, M., Lu, Y., Ikejiri, T., Sun, D., Carroll, R., Blair, E.H., Algeo, T.J., Sun, Y., 2021. Periodic oceanic euxinia and terrestrial fluxes linked to astronomical forcing during the late Devonian Frasnian-Famennian mass extinction. *Earth Planet. Sci. Lett.* 562 <https://doi.org/10.1016/j.epsl.2021.116839>.
- Lüning, S., Wendt, J., Belka, Z., Kaufmann, B., 2004. Temporal-spatial reconstruction of the early Frasnian (Late Devonian) anoxia in NW Africa: new field data from the Ahnet Basin (Algeria). *Sediment. Geol.* 163, 237–264. [https://doi.org/10.1016/S0037-0738\(03\)00210-0](https://doi.org/10.1016/S0037-0738(03)00210-0).
- Ma, J., Cui, X., 2022. Aromatic carotenoids: Biological sources and geological implications. *Geosyst. Geoenviron.* 1, 100045 <https://doi.org/10.1016/j.geogeo.2022.100045>.
- Ma, K., Hinnov, L., Zhang, X., Gong, Y., 2022. Astronomical climate changes trigger late Devonian bio- and environmental events in South China. *Glob. Planet. Chang.* 215, 103874 <https://doi.org/10.1016/j.gloplacha.2022.103874>.
- Ma, X., Gong, Y., Chen, D., Racki, G., Chen, X., Liao, W., 2016. The late Devonian Frasnian-Famennian event in South China - patterns and causes of extinctions, sea level changes, and isotope variations. *Palaeogeogr. Palaeoclimatol. Palaeoecol.* 448, 224–244. <https://doi.org/10.1016/j.palaeo.2015.10.047>.
- Macdonald, F.A., Swanson-Hysell, N.L., Park, Y., Lisiecki, L., Jagoutz, O., 2019. Arc-continent collisions in the tropics set Earth's climate state. *Science* 364 (6436), 181–184.
- MacKenzie, W.S., 1973. Upper Devonian Echinoderm Debris Beds with Graded Texture, District of Mackenzie, Northwest Territories. *Can. J. Earth Sci.* 10, 519–528. <https://doi.org/10.1139/e73-051>.
- Majorowicz, J., Grasby, S.E., Safanda, J., Beauchamp, B., 2014. Gas hydrate contribution to late Permian global warming. *Earth Planet. Sci. Lett.* 393, 243–253. <https://doi.org/10.1016/j.epsl.2014.03.003>.
- Małkowski, K., Racki, G., 2009. A global biogeochemical perturbation across the Silurian-Devonian boundary: Ocean-continent-biosphere feedbacks. *Palaeogeogr. Palaeoclimatol. Palaeoecol.* 276, 244–254. <https://doi.org/10.1016/j.palaeo.2009.03.010>.
- Marcilly, C.M., Torsvik, T.H., Conrad, C.P., 2022. Global Phanerozoic sea levels from paleogeographic flooding maps. *Gondwana Research* 110, 128–142. <https://doi.org/10.1016/j.gr.2022.05.011>.
- Marshall, J.E.A., Lakin, J., Troth, I., Wallace-Johnson, S.M., 2020. UV-B radiation was the Devonian-Carboniferous boundary terrestrial extinction kill mechanism. *Sci. Adv.* 6, 1–9. <https://doi.org/10.1126/sciadv.aba07>.
- Martin, R.E., Cárdenas, A.L., 2022. Terrestrial forcing of marine biodiversification. *Sci. Rep.* 12, 8309. <https://doi.org/10.1038/s41598-022-12384-1>.
- Martinez, A.M., Boyer, D.L., Droser, M.L., Barrie, C., Love, G.D., 2019. A stable and productive marine microbial community was sustained through the end-Devonian Hangenberg Crisis within the Cleveland Shale of the Appalachian Basin, United States. *Geobiology* 17, 27–42. <https://doi.org/10.1111/gbi.12314>.
- Marynowski, L., Filipiak, P., 2007. Water column euxinia and wildfire evidence during deposition of the Upper Famennian Hangenberg event horizon from the Holy Cross Mountains (central Poland). *Geol. Mag.* 144, 569–595.
- Marynowski, L., Filipiak, P., Piszczowska, A., 2008. Organic geochemistry and palynofacies of the Early-Middle Frasnian transition (Late Devonian) of the Holy Cross Mountains, Southern Poland. *Palaeogeogr. Palaeoclimatol. Palaeoecol.* 268, 152–165. <https://doi.org/10.1016/j.palaeo.2008.04.033>.
- Marynowski, L., Zatoń, M., Rakociński, M., Filipiak, P., Kurkiewicz, S., Pearce, T.J., 2012. Deciphering the upper Famennian Hangenberg Black Shale depositional environments based on multi-proxy record. *Palaeogeogr. Palaeoclimatol. Palaeoecol.* 346–347, 66–86.
- McArthur, J.M., Algeo, T.J., van de Schootbrugge, B., Li, Q., Howarth, R.J., 2008. Basinal restriction, black shales, and the early Toarcian (Jurassic) oceanic anoxic event. *Paleoceanography* 23, PA4217. <https://doi.org/10.1029/2008PA001607>.
- McArthur, J.M., Howarth, R.J., Shields, G.A., Zhou, Y., 2020. Chapter 7. Strontium isotope stratigraphy. In: Gradstein, F.M., Ogg, J.G., Schmidt, M.D., Ogg, G.M. (Eds.), *Geologic Time Scale 2020*, 1st edition. Elsevier, pp. 211–238. <https://doi.org/10.1016/B978-0-12-824360-2.00007-3>.
- McGhee, G.R., Orth, C.J., Quintana, L.R., Gilmore, J.S., Olsen, E.J., 1986. Late Devonian "Kellwasser Event" mass extinction horizon in Germany: no geochemical evidence for a large-body impact. *Geology* 14, 776–779. [https://doi.org/10.1130/0091-7613\(1986\)14<776:LDKMH>2.0.CO;2](https://doi.org/10.1130/0091-7613(1986)14<776:LDKMH>2.0.CO;2).
- McClung, W.S., Cuffey, C.A., Eriksson, K.A., Terry Jr., D.O., 2016. An incised valley fill and lowland wedges in the Upper Devonian Foreknobs Formation, central Appalachian Basin: implications for Famennian glacioeustasy. *Palaeogeogr. Palaeoclimatol. Palaeoecol.* 446, 125–143. <https://doi.org/10.1016/j.palaeo.2016.01.014>.
- McClung, W.S., Eriksson, K.A., Cuffey, C.A., 2013. Sequence stratigraphic hierarchy of the Upper Devonian Foreknobs Formation, central Appalachian Basin, USA: evidence for transitional greenhouse to icehouse conditions. *Palaeogeogr. Palaeoclimatol. Palaeoecol.* 387, 104–125. <https://doi.org/10.1016/j.palaeo.2013.07.020>.
- McGhee Jr., G.R., Clapham, P.M., Sheehan, P.M., Pottjer, D.J., Droser, M.L., 2013. A new ecological-severity ranking of major Phanerozoic biodiversity crises. *Palaeogeogr. Palaeoclimatol. Palaeoecol.* 370, 260–270. <https://doi.org/10.1016/j.palaeo.2012.12.019>.
- McGhee, G.R., Racki, G., 2021. Extinction: Late Devonian mass extinction. *Encyclopedia of Life Sciences (eLS)* 2. John Wiley & Sons, 1–12. <https://doi.org/10.1002/9780470015902.a0029301>.
- McKenzie, N.R., Horton, B.K., Loomis, S.H., Stockli, D.F., Planavsky, N.J., Lee, C.-T.A., 2016. Continental arc volcanism as the principal driver of icehouse-greenhouse variability. *Science* 352 (6284), 444–447. <https://doi.org/10.1126/science.aad5787>.
- McKenzie, N.R., Jiang, H., 2019. Earth's outgassing and climatic transitions: the slow burn towards environmental "catastrophes"? *Elements* 15, 325–330. <https://doi.org/10.2138/gselements.15.5.325>.
- McLaren, D.J., 1983. Boulders and biostratigraphy. *GAS Bull.* 94, 313–324. [https://doi.org/10.1130/0016-7606\(1983\)94<313:BAB>2.0.CO;2](https://doi.org/10.1130/0016-7606(1983)94<313:BAB>2.0.CO;2).
- McLaughlin, P.E., Emsbo, P., Brett, C.E., Bancroft, A.M., Desrochers, A., Vandenbroucke, T.R.A., 2019. The rise of pinnacle reefs: a step change in marine evolution triggered by perturbation of the global carbon cycle. *Earth Planet. Sci. Lett.* 515, 13–25. <https://doi.org/10.1016/j.epsl.2019.02.039>.
- Meijer Drees, N.G., 1993. The Devonian succession in the subsurface of the Great Slave and Great Bear Plains, Northwest Territories. In: Geological Survey of Canada, Bulletin, 393, p. 231 p. <https://doi.org/10.4095/183905>.
- Melchin, M.J., Mitchell, C.E., Holmden, C., Storch, P., 2013. Environmental changes in the late Ordovician-early Silurian: review and new insights from black shales and nitrogen isotopes. *GSA Bull.* 125, 1635–1670. <https://doi.org/10.1130/B30812.1>.
- Meyer, K.M., Kump, L.R., 2008. Oceanic euxinia in Earth history: causes and consequences. *Annu. Rev. Earth Planet. Sci.* 36, 251–288.
- Miller, K.G., Wright, J.D., Browning, J.V., 2005. Visions of ice sheets in a greenhouse world. *Mar. Geol.* 217, 215–231. <https://doi.org/10.1016/j.margeo.2005.02.007>.
- Mills, B.J.W., Krause, A.J., Scotese, C.R., Hill, D.J., Shields, G.A., Lenton, T.M., 2019. Modelling the long-term carbon cycle, atmospheric CO₂, and Earth surface temperature from late Neoproterozoic to present day. *Gondwana Res.* 67, 172–186. <https://doi.org/10.1016/j.gr.2018.12.001>.
- Mirchink, M.F., Mkrtchan, O.M., Khatyanov, F.I., Trokhova, A.A., Mitreikin, Y.B., Kuryaeva, V.V., 1974. Рифы Урало-Поволжья и их роль в размещении залежей нефти и газа и Методики поисков. Nedra, Moscow, 152 p. (in Russian).
- Montañez, I.P., 2021. Current synthesis of the penultimate icehouse and its imprint on the Upper Devonian through Permian stratigraphic record. In: Lucas, S.G., Schneider, J.W., Wang, X., Nikolaeva, S. (Eds.), *The Carboniferous Timescale*, 512. Geological Society, London, pp. 213–245. <https://doi.org/10.1144/SP512-2021-124>.
- Monty, C.L.V., 1995. The rise and nature of carbonate mud-mounds: an introductory actualistic approach. In: CLV, Monty, DWJ, Bosence, Bridges, P.H., Pratt, B.R. (Eds.), *Carbonate Mud-mounds—Their Origin and Evolution*, 23. Int. Assoc. Sediment. Spec. Publ., pp. 11–48.
- Morrow, D.W., 2018. Devonian of the northern Canadian mainland Sedimentary Basin: a review. *Bull. Can. Petrol. Geol.* 66, 623–694.
- Murphy, J.B., Keppie, J.D., 2005. The Acadian Orogeny in the Northern Appalachians. *Int. Geol. Rev.* 47 (2005), 663–687. <https://doi.org/10.2747/0020-6814.47.7.663>.
- Myrow, P.M., Ramezani, J., Hanson, A.E., Bowring, S.A., Racki, G., Rakociński, M., 2014. High-precision U-Pb age and duration of the latest Devonian (Famennian) Hangenberg event, and its implications. *Terra Nova* 26, 222–229. <https://doi.org/10.1111/ter.12090>.
- Narkiewicz, M., 2007. Development and inversion of Devonian and Carboniferous basins in the eastern part of the Variscan foreland (Poland). *Geol. Q.* 51, 231–256.
- Nikishin, A.M., Ziegler, P.A., Stephenson, R.A., Cloetingh, S.A.P.L., Furne, A.V., Fokin, P.A., Ershov, A.V., Bolotov, S.N., Korotaev, M.V., Alekseev, A.S., Gorbachev, V.I., Shipilov, E.V., Lankreijer, A., Bembinova, E.Yu., Shalimov, I.V., 1996. Late Precambrian to Triassic history of the east European Craton: dynamics of sedimentary basin evolution. *Tectonophysics* 268, 23–63. [https://doi.org/10.1016/S0040-1951\(96\)00228-4](https://doi.org/10.1016/S0040-1951(96)00228-4).
- Nikitin, Yu.I., Vilesov, A.P., Koryagin, N.N., 2018. Нефтеносные верхнефранские рифы – новое направление геолого-разведочных работ в Оренбургской области: Геология, геофизика и разработка нефтяных и газовых месторождений 5, 4–11. <https://doi.org/10.30713/2413-5011-2018-5-4-11>.
- North, F.K., 1988. The state of the system: An economic survey of the whole Devonian. In: MacMillan, N.J., Embry, A.F., Glass, D.J. (Eds.), *Devonian of the World*, vol. I. Canadian Society of Petroleum Geologists, Memoir 14, pp. 1–14.
- Over, D.J., 2007. Conodont biostratigraphy of the Chattanooga Shale, Middle and Upper Devonian, Southern Appalachian Basin, Eastern United States. *J. Paleontol.* 81, 1194–1217.
- Ovnatanova, N.S., Kononova, L.I., 2008. Frasnian conodonts from the Eastern Russian Platform. *Paleontol. J.* 42 (10), 997–1166. <https://doi.org/10.1134/S0013010108100018>.
- Owens, J.D., Reinhard, C.T., Rohrsen, M., Love, G.D., Lyons, T.W., 2016. Empirical links between trace metal cycling and marine microbial ecology during a large perturbation to Earth's carbon cycle. *Earth Planet. Sci. Lett.* 449, 407–417.
- Oschlies, A., 2021. A committed fourfold increase in ocean oxygen loss. *Nat. Commun.* 12, 2307. <https://doi.org/10.1038/s41467-021-22584-4>.
- Pană, D.I., Creaser, R.A., Toma, J., Playter, T.L., Corlett, H.J., Hauck, T.E., Peterson, J.T., Große, M., Poulton, T., 2018. Geochronology in support of the Alberta table of formations: rhenium-osmium isotope dating of selected Devonian and Jurassic core samples from central and northern Alberta. Alberta Energy Regulator, AER/AGS Open File Report 2018-06, 25 p.
- Pas, D., Da Silva, A.C., Poulain, G., Spassov, S., Boulvain, F., 2019. Magnetic Susceptibility Record in Paleozoic Succession (Rhenohercynian Massif, Northern Europe) – Disentangling Sea Level, local and Diagenetic Impact on the magnetic Records; *Frontiers. Earth Sci.* 19 <https://doi.org/10.3389/feart.2019.00341>.

- Pas, D., Da Silva, A.C., Over, D.J., Brett, C.E., Brandt, L., Over, J.-S., Hilgen, F.J., Dekkers, M.J., 2021. Cyclostratigraphic calibration of the Eifelian Stage (Middle Devonian, Appalachian Basin, Western New York, USA). *GSA Bull.* 133, 277–286. <https://doi.org/10.1130/B35589>.
- Paulmier, A., Ruiz-Pino, D., 2009. Oxygen minimum zones (OMZs) in the modern ocean. *Prog. Oceanogr.* 80, 113–128. <https://doi.org/10.1016/j.pcean.2008.08.001>.
- Pekar, S., Hucks, A., Fuller, M., Li, S., 2005. Glacioeustatic changes in the early and middle Eocene (51–42 Ma): shallow-water stratigraphy from ODP Leg 189 Site 1171 (South Tasman Rise) and deep-sea $\delta^{18}\text{O}$ records. *Geol. Soc. Am. Bull.* 117, 1081–1093. <https://doi.org/10.1130/B25486.1>.
- Penman, D.E., Caves Rugenstein, J.K., Ibarra, D.E., Winnicke, M.J., 2020. Silicate weathering as a feedback and forcing in Earth's climate and carbon cycle. *Earth-Sci. Rev.* 209 <https://doi.org/10.1016/j.earscirev.2020.103298>.
- Percival, L.M.E., Davies, J.H.F.L., Schaltegger, U., De Vleeschouwer, D., Da Silva, A.-C., Föllmi, K.B., 2018. Precisely dating the Frasnian-Famennian boundary: implications for the cause of the late Devonian mass extinction. *Sci. Rep.* 8, 9578.
- Percival, L.M.E., Selby, D., Bond, D.P.G., Rakociński, M., Racki, G., Marynowski, L., Adatte, T., Spangenberg, J.E., Föllmi, K.B., 2019. Pulses of enhanced continental weathering associated with multiple late Devonian climate perturbations: evidence from osmium-isotope compositions. *Palaeogeogr. Palaeoclimatol. Palaeoecol.* 524, 240–249. <https://doi.org/10.1016/j.palaeo.2019.03.036>.
- Percival, L.M.E., Bond, D.P.G., Rakociński, M., Marynowski, L., Hood, A.V.S., Adatte, T., Spandenberg, J.E., Föllmi, K.B., 2020. Phosphorus-cycle disturbances during the Late Devonian anoxic events. *Glob. Planet. Change* 184, 103070. <https://doi.org/10.1016/j.gloplacha.2019.103070>.
- Percival, L.M.E., Marynowski, L., Baudin, F., Goderis, S., De Vleeschouwer, D., Rakociński, M., Narkiewicz, K., Corradini, C., Da Silva, A.-C., Claeys, P., 2022. Combined nitrogen-isotope and cyclostratigraphy evidence for temporal and spatial variability in Frasnian-Famennian environmental change. *Geochem. Geophys. Geosyst.* 23, e2021GC010308 <https://doi.org/10.1029/2021GC010308>.
- Peucker-Ehrenbrink, B., Ravizza, G., 2000. The marine osmium isotope record. *Terra Nova* 12, 205–219. <https://doi.org/10.1046/j.1365-3121.2000.00295.x>.
- Philp, R.P., DeGarmo, C.D., 2020. Geochemical characterization of the Devonian-Mississippian Woodford Shale from the McAlester Cemetery Quarry, Criner Hills Uplift, Ardmore Basin, Oklahoma. *Marine Petrol. Geol.* 112, 104078.
- Pisarzowska, A., Racki, G., 2012. Isotopic geochemistry across the Early-Middle Frasnian transition (Late Devonian) on the south polish carbonate shelf: a reference for the global punctata event. *Chem. Geol.* 334, 199–220. <https://doi.org/10.1016/j.chemgeo.2012.10.034>.
- Pisarzowska, A., Racki, G., 2020. Comparative carbon isotope chemostratigraphy of major late Devonian biotic crises. *Stratigr. Timesc.* 5 <https://doi.org/10.1016/bs.sats.2020.08.001>.
- Pieuch, C.G., Ponte, R.M., 2014. Mechanisms of global-mean steric sea level change. *J. Clim.* 27, 824–834. <https://doi.org/10.1175/JCLI-D-13-00373.1>.
- Pisarzowska, A., Becker, R.T., Aboussalam, Z.S., Szczepa, M., Sobień, B., Kremer, B., Owoc, K., Racki, G., 2020a. Middlesex/punctata event in the Rhenish Basin (Padberg section, Sauerland, Germany) – Geochemical clues to the early-middle Frasnian perturbation of global carbon cycle. *Glob. Planet. Change* 191 <https://doi.org/10.1016/j.gloplacha.2020.103211>.
- Pisarzowska, A., Rakociński, M., Marynowski, L., Szczepa, M., Thoby, M., Paszkowski, M., Perri, M.C., Spalletta, C., Schönlaub, H.P., Kowalik, N., Gereke, M., 2020b. Large environmental disturbances caused by magmatic activity during the late Devonian Hangenberg Crisis. *Glob. Planet. Change* 188 (103155), 1–24.
- Playford, P.E., 1980. Devonian 'Great Barrier Reef' of Canning Basin, Western Australia. *AAPG Bull.* 64, 814–840.
- Playford, P.E., Hocking, R.M., Cockbain, A.E., 2009. In: *Devonian Reef Complexes of the Canning Basin, Western Australia*, Geological Survey of Western Australia, Bulletin, p. 145.
- Poludetkina, E.N., Smirnov, M.B., Fadeeva, N.P., et al., 2017. Proof of formation of organic matter in upper Devonian carbonate and carbonate-siliceous sediments of the South-Tatar uplift in constant photic layer anoxia. *Geochem. Int.* 55, 726–736. <https://doi.org/10.1134/S0016702917080079>.
- Polyansky, O.P., Prokopyev, A.V., Koroleva, O.V., Tomshin, M.D., Reverdatto, V.V., Selyatitsky, A.Yu., Travin, A.V., Vasiliev, D.A., 2017. Temporal correlation between dyke swarms and crustal extension in the middle Palaeozoic Vilyui rift basin, Siberian platform. *Lithos* 282–283, 45–64. <https://doi.org/10.1016/j.lithos.2017.02.020>.
- Pratt, B.R., 1995. The origin, biota and evolution of deep-water mud-mounds. In: Monty, C.L.V., Bosence, D.W.J., Bridges, P.H., Pratt, B.R. (Eds.), *Carbonate Mud-Mounds: Their Origin and Evolution*. International Association of Sedimentologists Special Publications, no. 23, pp. 49–123.
- Prestianni, C., Gerrienne, P., 2010. Early seed plant radiation: An ecological hypothesis. In: Vecoli, M., Clément, G., Meyer-Berthaud, B. (Eds.), *The Terrestrialization Process: Modelling Complex Interactions at the Biosphere-Geosphere Interface*, 339. Geological Society, London, pp. 71–80. <https://doi.org/10.1144/SP339.7>. Special Publications.
- Puchkov, V.N., 2009. The evolution of the Uralian orogeny. *Geol. Soc. Lond. Spec. Publ.* 327, 161–195. <https://doi.org/10.1144/SP327.9>.
- Pyle, L.J., Gal, L.P., Hadlari, T., 2015. Thermal maturity trends for Devonian Horn River Group units and equivalent strata in the Mackenzie Corridor, Northwest Territories and Yukon; Geological survey of Canada. Open File 7850. <https://doi.org/10.4095/296446>.
- Pyle, L.J., Gal, L.P., 2016. Reference Section for the Horn River Group and Definition of the Bell Creek Member, Hare Indian Formation in Central Northwest Territories. *Bull. Can. Petrol. Geol.* 64, 67–98.
- Qui, Z., Zou, C., Mills, B.J.W., Xiong, Y., Tao, H., Lu, B., Liu, H., Xiao, W., Poulton, S.W., 2022. A nutrient control on expanded anoxia and global cooling during the late Ordovician mass extinction. *Commun. Earth Environ.* 3, 82. <https://doi.org/10.1038/s43247-022-00412-x>.
- Racki, G., 2005. Toward understanding Late Devonian global events: few answers, many questions. In: Over, D.J., Morrow, J.R., Wignall, P.B. (Eds.), *Understanding Late Devonian and Permian-Triassic Biotic and Climatic Events: Towards an Integrated Approach*, 20. *Developments in Palaeontology & Stratigraphy*, pp. 5–36.
- Racki, G., 2020a. Volcanic scenario of the Frasnian-Famennian major biotic crisis and other late Devonian global changes: more answers than questions? *Glob. Planet. Change* 189 <https://doi.org/10.1016/j.gloplacha.2020.103174>.
- Racki, G., 2020. Volcanism as a prime cause of mass extinctions: Retrospectives and perspectives. In: Adatte, T., Bond, D.P.G., Keller, G. (Eds.), *Mass Extinctions, Volcanism, and Impacts: New Developments*. Geological Society of America Special Paper 544, pp. 1–34. [https://doi.org/10.1130/2019.2544\(01\)](https://doi.org/10.1130/2019.2544(01)).
- Racki, G., Rakociński, M., Marynowski, L., Wignall, P.B., 2018. Mercury enrichments and the Frasnian-Famennian biotic crisis: a volcanic trigger proved? *Geology* 46, 543–546. <https://doi.org/10.1130/G40233.1>.
- Rakociński, M., Marynowski, L., Pisarzowska, A., Beldowski, J., Siedlewicz, G., Zatoń, M., Perri, M.C., Spalletta, C., Schönlaub, H.P., 2020. Volcanic related methylmercury poisoning as the possible driver of the end-Devonian mass extinction. *Sci. Rep.* 10, 7344. <https://doi.org/10.1038/s41598-020-64104-2>.
- Rakociński, M., Pisarzowska, A., Corradini, C., Barkiewicz, K., Dubicka, S., Abdiev, N., 2021a. Mercury spikes as evidence of extended arc-volcanism around the Devonian-Carboniferous boundary in the South Tian Shan (southern Uzbekistan). *Sci. Rep.* 11, 5708. <https://doi.org/10.1038/s41598-021-85043-6>.
- Rakociński, M., Marynowski, L., Zatoń, M., Filipiak, P., 2021b. The mid-Tournaisian (Early Carboniferous) anoxic event in the Laurussian shelf basin (Poland): an integrative approach. *Palaeogeogr. Palaeoclimatol. Palaeoecol.* 566, 110236 <https://doi.org/10.1016/j.palaeo.2021.110236>.
- Ray, D.C., van Buchem, F.S.P., Baines, G., Davies, A., Gréselle, B., Simmons, M.D., Robson, C., 2019. The magnitude and cause of short-term eustatic Cretaceous sea-level change: A synthesis. *Earth Sci. Rev.* 197. <https://doi.org/10.1016/j.earscirev.2019.102901>.
- Reershemius, T., Planavsky, N.J., 2021. What controls the duration and intensity of ocean anoxic events in the Paleozoic and the Mesozoic? *Earth Sci. Rev.* <https://doi.org/10.1016/j.earscirev.2021.103787>.
- Requejo, A.G., Allan, J., Creaney, S., Gray, N.R., Cole, K.S., 1992. Aryl isoprenoids and diatom carotenoids in Paleozoic source rocks and oils from the Western Canada and Williston Basins. *Org. Geochem.* 19, 245–264.
- Retallack, G.J., Huang, C.M., 2011. Ecology and evolution of Devonian trees in New York, USA. *Palaeogeogr. Palaeoclimatol. Palaeoecol.* 299, 110–128. <https://doi.org/10.1016/j.palaeo.2010.10.040>.
- Riboulleau, A., Spina, A., Vecoli, M., Riquier, L., Quijada, M., Tribouillard, N., Averbuch, O., 2018. Organic matter deposition in the Ghadames Basin (Libya) during the late Devonian—A multidisciplinary approach. *Palaeogeogr. Palaeoclimatol. Palaeoecol.* 497, 37–51.
- Rixen, T., Cowie, G., Gaye, B., Goes, J., Rosário, Gomes H., Hood, R.R., Lachkar, Z., Schmidt, H., Segsneider, J., Singh, A., 2020. Reviews and syntheses: Present, past, and future of the oxygen minimum zone in the northern Indian Ocean. *Biogeosciences* 17 (6051–6080), 2020. <https://doi.org/10.5194/bg-17-6051-2020>.
- Roberts, A.P., Florindo, F., Chang, L., Heslop, D., Jovane, L., Larrasoana, J.C., 2013. Magnetic properties of pelagic marine carbonates. *Earth Sci. Rev.* 127, 111–139. <https://doi.org/10.1016/j.earscirev.2013.09.009>.
- Robinson, S.A., Heimhofer, U., Hesselbo, S.P., Petrizzo, M.R., 2017. Mesozoic climates and oceans – a tribute to Hugh Jenkens and Helmut Weissert. *Sedimentology* 64, 1–15. <https://doi.org/10.1111/sed.12349>.
- Rodríguez-Martínez, M., 2011. Mud mounds. In: Reitner, J., Thiel, V. (Eds.), *Encyclopedia of Geobiology*. Springer, pp. 667–675.
- Root, K.G., 2001. Devonian Antler fold and thrust belt and foreland basin development in the southern Canadian Cordillera: Implications for the Western Canada Sedimentary Basin. *Bull. Can. Petrol. Geol.* 49, 7–36. <https://doi.org/10.2113/49.1.7>.
- Ruvalcaba Baroni, I.R., Pohl, A., van Helmond, N.A.G.M., Papadomolaki, N.M., Coe, A. L., Cohen, A.S., van de Schootbrugge, B., Donnadiet, Y., Slomp, C.P., 2017. Ocean Circulation in the Toarcian (Early Jurassic): a Key Control on Deoxygenation and Carbon Burial on the European Shelf. *Paleoceanogr. Palaeoclimatol.* 33, 994–1012. <https://doi.org/10.1029/2018PA003394>.
- Ruvalcaba Baroni, I., Palastanga, V., Slomp, C.P., 2020. Enhanced organic carbon burial in sediments of oxygen minimum zones upon ocean deoxygenation. *Front. Mar. Sci.* 6, 839. <https://doi.org/10.3389/fmars.2019.00839>.
- Sahoo, S.K., Gilleaudeau, G.J., Wilson, K., Hart, B., Barnes, B.D., Faison, T., Bowman, A. R., Larsen, T.E., Kaufman, A.J., 2023. Basin-scale reconstruction of euxinia and late Devonian mass extinctions. *Nature*. <https://doi.org/10.1038/s41586-023-05716-2>.
- Sandberg, C.A., Morrow, J.R., Ziegler, W., 2002. Late Devonian Sea-level changes, catastrophic events, and mass extinctions. In: Koerber, C., MacLeod, K.G. (Eds.), *Catastrophic Events and Mass Extinctions: Impacts and beyond*, 356. Geological Society of America Special Paper, pp. 473–487. <https://doi.org/10.1130/0-8137-2356-6.473>.
- Sames, B., Wagreich, M., Wendler, J.E., Haq, B.U., Conrad, C.P., Melinte-Dobrinescu, M. C., Hug, X., Wendler, I., Wolfring, E., Yilmaz, I.O., Zorina, S.O., 2016. Review: short-term sea-level changes in a greenhouse world – a view from the cretaceous. *Palaeogeogr. Palaeoclimatol. Palaeoecol.* 441, 393–411. <https://doi.org/10.1016/j.palaeo.2015.10.045>.
- Sames, B., Wagreich, M., Conrad, C.P., Iqbal, S., 2020. Aquifer-eustasy as the main driver of short-term sea-level fluctuations during cretaceous hothouse climate phases. *Geol. Soc. Lond. Spec. Publ.* 498 <https://doi.org/10.1144/SP498-2019-105>.

- Sandberg, C.A., Ziegler, W., Dreesen, R., Butler, J.L., 1992. Conodont biochronology, biofacies, taxonomy, and event stratigraphy around middle Frasnian Lion Mudmound (F2n), Frasnien, Belgium. *Cour. Forschingsinst. Senckenberg* 150, 1–87.
- Savoy, L.E., Stevenson, R.K., Mountjoy, E., 2000. Provenance of Upper Devonian-lower Carboniferous miogeoclinal strata, southeastern Canadian Cordillera: link between tectonic and sedimentation. *J. Sediment. Res.* 70, 181–193.
- Schindler, E., 1990. Die Kellwasser-Krise (hohe Frasn-Stufe, Ober-Devon). *Göttinger Arbeiten Geol. Paläontol.* 46, 1–115.
- Schlager, W., 1989. Drowning unconformities on carbonate platforms. In: Crevello, P.D., Wilson, J.L., Sarg, J.F., Read, J.F. (Eds.), *Controls on Carbonate Platform and Basin Development*, 41. Society of Economic Paleontologists and Mineralogists Special Publication, pp. 15–25.
- Schlager, W., 2003. Benthic carbonate factories of the Phanerozoic. *Int. J. Earth Sci.* 92, 445–464. <https://doi.org/10.1007/s00531-003-0327-x>.
- Schlanger, S.O., Jenkyns, H.C., 1976. Cretaceous oceanic anoxic events: causes and consequences. *Geol. Mijnb.* 55, 179–184.
- Schoepfer, S.D., Algeo, T.J., Ward, P.D., Williford, K.H., Haggart, J.W., 2016. Testing the limits in a greenhouse ocean: did low nitrogen availability limit marine productivity during the end-Triassic mass extinction? *Earth Planet. Sci. Lett.* 451, 138–148. <https://doi.org/10.1016/j.epsl.2016.06.050>.
- Scholle, P.A., Arthur, M.A., 1980. Carbon Isotope Fluctuations in cretaceous Pelagic Limestones: potential Stratigraphic and Petroleum Exploration Tool. *AAPG Bull.* 64, 67–87. <https://doi.org/10.1306/2F91892D-16CE-11D7-8645000102C1865D>.
- Scotese, C.R., Song, H., Mills, B.J.W., van der Meer, D.G., 2021. Phanerozoic paleotemperatures: the Earth's changing climate during the last 540 million years. *Earth Sci. Rev.* 215 <https://doi.org/10.1016/j.earscirev.2021.103503>.
- Self, S., 2015. Chapter 16. Explosive super-eruptions and potential global impacts. In: Shroder, J.F., Papale, P. (Eds.), *Volcanic Hazards, Risks and Disasters*. Elsevier, pp. 399–418. <https://doi.org/10.1016/B978-0-12-396453-3.00016-2>.
- Sepkoski, J.J., 1996. Patterns of Phanerozoic extinction: a perspective from global data bases. In: Walliser, O.H. (Ed.), *Global Events and Event Stratigraphy*. Springer-Verlag, Berlin, pp. 35–51.
- Shatsillo, A.V., Pavlov, V.E., 2019. Systematics of Paleomagnetic Directions from Early–Middle Devonian Rocks of Minusa Troughs: New Data and Old Problems. *Izv. Phys. Solid Earth* 55, 471–487. <https://doi.org/10.1134/S1069351319030091>.
- Shaw, D.M., Cramer, J.J., Higgins, M.D., Truscott, M.G., 1986. Composition of the Canadian Precambrian shield and the continental crust of the earth. *Geol. Soc. Spec. Publ.* 24, 275–282. <https://doi.org/10.1144/GSL.SP.1986.024.01.24>.
- Shaw, D.J., Harris, N.B., 2022. Facies and systems tracts at high-resolution in an organic-rich mudstone: The Duvernay Formation, Kaybob area, Alberta, Canada. *Sediment. Geol.* 436, 106157 <https://doi.org/10.1016/j.sedgeo.2022.106157>.
- Shcherbakova, V.V., Biggin, A.J., Veselovskiy, R.V., Shatsillo, A.V., Hawkins, L.M.A., Shcherbakov, V.P., Zhidkov, G.V., 2017. Was the Devonian geomagnetic field dipolar or multipolar? Palaeointensity studies of Devonian igneous rocks from the Minusa Basin (Siberia) and the Kola Peninsula dykes. *Russ. Geophys. J. Int.* 209, 1265–1286. <https://doi.org/10.1093/gji/ggx085>.
- Siebert, C., Scholz, F., Kuhn, W., 2021. A new view on the evolution of seawater molybdenum inventories before and during the cretaceous Oceanic Anoxic Event 2. *Chem. Geol.* 582, 120399 <https://doi.org/10.1016/j.chemgeo.2021.120399>.
- Simmons, M.D., Miller, K.G., Ray, D.C., Davies, A., van Buchem, F.S.P., Gréselle, B., 2020. Chapter 13. Phanerozoic eustasy. In: Gradstein, F.M., Ogg, J.G., Schmidt, M. D., Ogg, G.M. (Eds.), *Geologic Time Scale 2020*, 1st edition. Elsevier, pp. 357–400. <https://doi.org/10.1016/B978-0-12-824360-2.00013-9>.
- Sinninghe Damsté, J.S., Kenig, F., Koopmans, M.P., Köster, J., Schouten, S., Hayes, J.M., de Leeuw, J.W., 1995. Evidence for gammacerane as an indicator of water column stratification. *Geochim. Cosmochim. Acta* 59, 1895–1900. [https://doi.org/10.1016/0016-7037\(95\)00073-9](https://doi.org/10.1016/0016-7037(95)00073-9).
- Śliwiński, M.G., Whalen, M.T., Newberry, R.J., Payne, J.H., Day, J.E., 2011. Stable isotope ($\delta^{13}\text{C}_{\text{carb}}$ and $\delta^{15}\text{N}_{\text{org}}$) and trace element anomalies during the late Devonian ‘punctuated event’ in the Western Canada Sedimentary Basin. *Palaeogeogr. Palaeoclimatol. Palaeoecol.* 307, 245–271. <https://doi.org/10.1016/j.palaeo.2011.05.024>.
- Smart, M.S., Filippelli, G.M., Gilhooly, W.P., Marshall, J.E.A., Whiteside, J.H., 2022. Enhanced terrestrial nutrient release during the Devonian emergence and expansion of forests: evidence from lacustrine phosphorus and geochemical records. *GSA Bull.* <https://doi.org/10.1130/B36384.1>.
- Smirnov, M.B., Fadeeva, N.P., Poludetkina, E.N., 2020. Distribution of anoxic conditions in the photic layer of sedimentation basin during formation of organic matter in the Domanik sediments of the northern and central areas of the Volga-urals Petroleum Basin. *Geochem. Int.* 58, 321–331. <https://doi.org/10.1134/S0016702920030106>.
- Smith, L.B., Schieber, J., Wilson, R.D., 2019. Shallow-water onlap model for the deposition of Devonian black shales in New York, USA. *Geology* 47, 279–283. <https://doi.org/10.1130/G45569.1>.
- Smolarek, J., Trela, W., Bond, D.P.G., Marynowski, L., 2016. Lower Wenlock black shales in the northern Holy Cross Mountains, Poland: sedimentary and geochemical controls on the Ireviken Event in a deep marine setting. *Geol. Mag.* 154, 247–264. <https://doi.org/10.1017/S0016756815001065>.
- Soreghan, G.S., Giles, K.A., 1999. Amplitudes of late Pennsylvanian glacioeustasy. *Geology* 27, 255–258.
- Souza, I.M.S., Zambrano, E.R.N., de Souza, E.S., Parra, C.J.O., Ribeiro, H.J.P.S., Cerqueira, J.R., Mortatti, J., de Oliveira, O.M.C., de Souza Queiroz, A.F., 2022. Biomarkers and PAH chemostratigraphy in the study of the Frasnian anoxic event in the Pimenteira Formation outcrop of the Parnaíba Basin, Brazil. *Palaeogeogr. Palaeoclimatol. Palaeoecol.* 598, 111033 <https://doi.org/10.1016/j.palaeo.2022.111033>.
- Spaak, G., Edwards, D.S., Allen, H.J., Grotheera, H., Summons, R.E., Coolen, M.J.L., Grice, K., 2018. Extent and persistence of photic zone euxinia in Middle-late Devonian seas – Insights from the Canning Basin and implications for petroleum source rock formation. *Mar. Pet. Geol.* 93, 33–56.
- Stanley, S.M., 2016. Estimates of the magnitudes of major marine mass extinctions in Earth history. *PNAS* 113, 6325–6334. <https://doi.org/10.1073/pnas.1613094113>.
- Stewart, E.M., Ague, J.J., 2018. Infiltration-driven metamorphism, New England, USA: Regional CO₂ fluxes and implications for Devonian climate and extinctions. *Earth Planet. Sci. Lett.* 489, 123–134. <https://doi.org/10.1016/j.epsl.2018.02.028>.
- Stigall, A.L., 2012. Speciation collapse and invasive species dynamics during the late Devonian “Mass Extinction”. *GSA Today* 22, 4–9. <https://doi.org/10.1130/G128A.1>.
- Stock, C.W., Sandberg, C.A., 2019. Latest Devonian (Famennian, expansa Zone) conodonts and sponge-microbe symbionts in Pinyon Peak Limestone, Star Range, southwestern Utah, lead to reevaluation of global Dasberg Event. *Palaeogeogr. Palaeoclimatol. Palaeoecol.* 534 <https://doi.org/10.1016/j.palaeo.2019.109271>.
- Stolfus, B.M., Cramer, B.D., Clark, R.J., Hogancamp, N.J., Day, J.E., Tassier-Surine, S.A., Witzke, B.J., 2020. An expanded stratigraphic record of the Devonian-Carboniferous boundary Hangenberg biogeochemical event from Southeast Iowa (U.S.A.). *Bull. Geosci.* 95 (4), 469–495.
- Stramma, L., Schmidtke, S., Levin, L.A., Johnson, G.C., 2010. Ocean oxygen minima expansions and their biological impacts. *Deep-Sea Research Part I* 57, 587–595. <https://doi.org/10.1016/j.dsr.2010.01.005>.
- Stupakova, A.V., Kalmykov, G.A., Korobova, N.I., Fadeeva, N.P., Gatovsky, Yu.A., Suslova, A.A., Sautkin, R.S., Pronina, N.V., Bolshakova, M.A., Zavyalova, A.P., Churapkina, V.V., Petrakova, N.N., Miftakhova, A.A., 2017. ДоМаниковск отложения Волго-Уральского бассейна – типы разреза, условия формирования и перспективы нефтегазоносности. *Георесурсы (Georesources). Spec. Issue* 1, 112–124. <https://doi.org/10.18599/grs.19.12>.
- Suan, G., van de Schootbrugge, B., Adatte, T., Fiebig, J., Oschmann, W., 2015. Calibrating the magnitude of the Toarcian carbon cycle perturbation. *Palaeogeography* 30, 495–509. <https://doi.org/10.1002/2014PA002758>.
- Summons, R.E., Powell, T.G., 1986. Chlorobiaceae in Paleozoic seas revealed by biological markers, isotopes and geology. *Nature* 319, 763–765.
- Summons, R.E., Powell, T.G., 1987. Identification of aryl isoprenoids in source rocks and crude oils: biological markers for the green Sulphur bacteria. *Geochim. Cosmochim. Acta* 51, 557–566.
- Suttner, T.J., Kido, E., Joachimski, M.M., Votržková, S., Pondelli, M., Corradini, C., Corrigan, M.G., Simonetto, L., Kubajko, M., 2021. Paleotemperature record of the Middle Devonian Kacák Episode. *Sci. Rep.* 11, 16559. <https://doi.org/10.1038/s41598-021-96013-3>.
- Takashima, R., Nishi, H., Yamanaka, T., Tomosugi, T., Fernando, A.G., Tanabe, K., Mori, K., Kawabe, F., Hayashi, K., 2011. Prevailing oxic environments in the Pacific Ocean during the mid-Cretaceous Oceanic Anoxic Event 2. *Nat. Commun.* 234 <https://doi.org/10.1038/ncomms1233>.
- Taylor, S.R., McLennan, S.M., 1985. *The Continental Crust: Its Composition and Evolution*. Blackwell, Oxford.
- Them II, T.R., Gill, B.C., Selby, D., Gröcke, D.R., Friedman, R.M., Owens, J.D., 2017. Evidence for rapid weathering response to climatic warming during the Toarcian Oceanic Anoxic Event. *Sci. Rep.* 7, 5003. <https://doi.org/10.1038/s41598-017-05307-y>.
- Them II, T.R., Jagoe, C.H., Caruthers, A.H., Gill, B.C., Grasby, S.E., Gröcke, D.R., Yin, R., Owens, J.D., 2019. Terrestrial sources as the primary delivery mechanism of mercury to the oceans across the Toarcian Oceanic Anoxic Event (Early Jurassic). *Earth Planet. Sci. Lett.* 507, 62–72. <https://doi.org/10.1016/j.epsl.2018.11.029>.
- Torsvik, T.H., Cocks, L.R.M., 2017. *Earth History and Palaeogeography*. Cambridge University Press, pp. 317–pp.
- Tribouillard, N., Algeo, T., Lyons, T.W., Riboulleau, A., 2006. Trace metals as paleoredox and paleoproductivity proxies: an update. *Chem. Geol.* 232, 12–32. <https://doi.org/10.1016/j.chemgeo.2006.02.012>.
- Tucker, M.E., Garland, J., 2010. High-frequency cycles and their sequence stratigraphic context: orbital forcing and tectonic controls on Devonian cyclicity, Belgium. *Geol. Belg.* 13, 213–240.
- Tulipani, S., Grice, K., Greenwood, P.F., Haines, P., Sauer, P.E., Schimmelmann, A., Summons, R.E., Foster, C., Böttcher, M.E., Playton, T., Schwark, L., 2015. Changes of palaeoenvironmental conditions recorded in late Devonian reef systems from the Canning Basin, Western Australia: a biomarker and stable isotope approach. *Gondwana Res.* 28, 1500–1515. <https://doi.org/10.1016/j.gr.2014.10.003>.
- Ulmishek, G.F., 1988. Upper Devonian-Tournaisian facies and oil resources of the Russian Craton's eastern margin. In: McMillan, N.J., Embry, A.F., Glass, D.J. (Eds.), *Devonian of the World, vol. I*. Canadian Society of Petroleum Geologists Memoir 14, pp. 527–549.
- Uyeno, T.T., Pedder, A.E.H., Uyeno, T.A., 2017. Conodont biostratigraphy and T-R cycles of the Middle Devonian Hume Formation at Hume River (type locality), northern Mackenzie Mountains, Northwest Territories, Canada. *Stratigraphy* 14, 391–404. <https://doi.org/10.29041/strat.14.1-4.391-404>.
- Uveges, B.T., Junium, C.K., Boyer, D.L., Cohen, P.A., Day, J.E., 2019. Biogeochemical controls on black shale deposition during the Frasnian-Famennian biotic crisis in the Illinois and Appalachian Basins, USA, inferred from stable isotopes of nitrogen and carbon. *Palaeogeogr. Palaeoclimatol. Palaeoecol.* 531, 108787 <https://doi.org/10.1016/j.palaeo.2018.05.031>.
- Vail, P.R., Mitchum, R.M., Thompson, S., 1977. Seismic stratigraphy and global changes of sea level, part 3: Relative changes of sea level from coastal onlap. In: Payton, C.E. (Ed.), *120 Seismic and Sequence Stratigraphy and Integrated Stratigraphy - New Insights and Contributions Seismic Stratigraphy: Applications to Hydrocarbon Exploration*, 26. AAPG Memoir, pp. 63–81.

- Van Bentum, E.C., Hetzel, A., Brumsack, H.-J., Forster, A., Reichart, G.-J., Sinninghe Damsté, J.S., 2009. Reconstruction of water column anoxia in the equatorial Atlantic during the Cenomanian–Turonian oceanic anoxic event using biomarker and trace metal proxies. *Palaeogeogr. Palaeoclimatol. Palaeoecol.* 280, 489–498. <https://doi.org/10.1016/j.palaeo.2009.07.003>.
- Van der Boon, A., Biggin, A.J., Thallner, D., Hounslow, M.W., Bono, R., Nawrocki, J., Wójcik, K., Paszkowski, M., Königshof, P., de Backer, T., Kabanov, P., Gouwy, S., VandenBerg, R., 2022. A persistent non-uniformitarian paleomagnetic field in the Devonian? *Earth Sci. Rev.* 231, 104073 <https://doi.org/10.1016/j.earscirev.2022.104073>.
- van Geldern, R., Joachimski, M.M., Day, J., Jansen, U., Alvarez, F., Yolkin, E.A., Ma, X.-P., 2006. Carbon, oxygen and strontium isotope records of Devonian brachiopod shell calcite. *Palaeogeogr. Palaeoclimatol. Palaeoecol.* 240, 47–67. <https://doi.org/10.1016/j.palaeo.2006.03.045>.
- van Hengstum, P.J., Gröke, D.R., 2008. Stable isotope record of the Eifelian–Givetian boundary Kačák–otomari event (Middle Devonian) from Hungry Hollow, Ontario, Canada. *Can. J. Earth Sci.* 45, 353–366. <https://doi.org/10.1139/E08-005>.
- Vilesov, A.P., Pyatunina, E.B., Chudinov, Y.V., 2009. In: Опыт комплексования современных геолого-геофизических методов исследования верхнедевонских рифов при поисково-бурении в северных районах Пермского края. In: Стратиграфия и региональная геология востока Русской платформы и Западного Урала. Пермь, pp. 72–82.
- Vilesov, A.P., Nikitin, Y.I., Akhtyamova, I.R., Shirokovskikh, O.A., 2019. Франские рифы Рыбчинской группы. Геология, геофизика и разработка нефтяных и газовых месторождений 7, 4–22. [https://doi.org/10.30713/2413-5011-2019-7\(331\)-4-22](https://doi.org/10.30713/2413-5011-2019-7(331)-4-22).
- Vellekoop, J., Esmeray-Senlet, S., Miller, K.G., Browning, J.V., Sluijs, A., van de Schootbrugge, B., Sinninghe Damsté, J.S., Brinkhuis, H., 2016. Evidence for Cretaceous–Paleogene boundary bolide “impact winter” conditions from New Jersey, USA. *Geology* 44, 619–622. <https://doi.org/10.1130/G37961.1>.
- Vierek, A., 2014. Small-scale cyclic deposition in the Frasnian (Upper Devonian) of the Holy Cross Mountains, Poland. *Geologos* 20, 239–258. <https://doi.org/10.2478/logo-s-2014-0019>.
- Vilesov, A.P., Ledenev, V.S., Solodov, D.V., Filichev, A.V., Bogomolova, N.V., Makarova, L.I., Grebenkina, N.Yu., Kazachkova, A.G., Sidubaev, A.S., 2021. Верхнепалеозойские рифовые системы Рубежского прогиба (южная часть Бузулукской впадины). ПРОНЕФТЬ. Профессионально о нефти 6, 30–42. <https://doi.org/10.51890/2587-7399-2021-6-3-30-42>.
- Vodrážková, S., Frýda, J., Suttner, T.J., Koptíková, L., Tonarová, P., 2013. Environmental changes close to the Lower-Middle Devonian boundary; the Basal Chotec Event in the Prague Basin (Czech Republic). *Facies* 59, 425–449. <https://doi.org/10.1007/s10347-012-0300-x>.
- Vorontsov, A., Yarmolyuk, V., Dril, S., Ernst, R., Perfilova, O., Grinev, O., Komaritsyna, T., 2021. Magmatism of the Devonian Altai–Sayan Rift System: Geological and geochemical evidence for diverse plume–lithosphere interactions. *Gondwana Res.* 89, 193–219. <https://doi.org/10.1016/j.gr.2020.09.007>.
- Wagreich, M., Lein, R., Sames, B., 2014. Eustasy, its controlling factors, and the limnoeustatic hypothesis – concepts inspired by Eduard Suess. *Austrian J. Earth Sci.* 107, 115–131.
- Walliser, O.H., 1984. Geologic processes and global events. *Terra Cognita* 4, 17–20.
- Walliser, O.H., 1985. Natural boundaries and Commission boundaries in the Devonian. *Cour.-Forsch.-Inst. Senckenberg* 75, 401–408.
- Walliser, O.H., 1996. Global Events in the Devonian and Carboniferous. In: Walliser, O.H. (Ed.), *Global Events and Event Stratigraphy in the Phanerozoic*. Springer-Verlag, Berlin, pp. 225–250.
- Wallmann, K., José, Y.S., Hopwood, M.J., Somes, C.J., Dale, A.W., Scholz, F., Achtenberg, E.P., Oschilles, A., 2022. Biogeochemical feedbacks may amplify ongoing and future ocean deoxygenation: a case study from the peruvian oxygen minimum zone. *Biogeochemistry* 159, 45–67. <https://doi.org/10.1007/s10533-022-00908-w>.
- Weeks, S.J., Currie, B., Bakun, A., Peard, K.R., 2004. Hydrogen sulphide eruptions in the Atlantic Ocean off southern Africa: implications of a new view based on SeaWiFS satellite imagery. *Deep-Sea Res. I Oceanogr. Res. Pap.* 51, 153–172. <https://doi.org/10.1016/j.dsr.2003.10.004>.
- Wendte, J.C., 1994. Cooking Lake platform evolution and its control on late Devonian Leduc reef inception and localization, Redwater, Alberta. *Bull. Can. Petrol. Geol.* 42, 499–528.
- Whalen, M.T., Eberli, G.P., van Buchem, F.S.P., Mountjoy, E.W., Homewood, P.W., 2000. Bypass margins, basin-restricted wedges and platform-to-basin correlation, Upper Devonian, Canadian Rocky Mountains: implications for sequence stratigraphy of carbonate platform systems. *J. Sediment. Research* 70, 913–936. <https://doi.org/10.1306/2DC40941-0E47-11D7-8643000102C1865D>.
- Wendte, J., Uyeno, T., 2005. Sequence stratigraphy and evolution of Middle to Upper Devonian Beaverhill Lake strata, south-central Alberta. *Bull. Can. Petrol. Geol.* 53, 250–354. <https://doi.org/10.2113/53.3.250>.
- Westermann, S., Vance, D., Cameron, V., Arcer, C., Robinson, S.A., 2014. Heterogeneous oxygenation states in the Atlantic and Tethys oceans during Oceanic Anoxic Event 2. *Earth Planet. Sci. Lett.* 404, 178–189. <https://doi.org/10.1016/j.epsl.2014.07.018>.
- Whalen, M.T., Day, J.E., 2010. Cross-basin variations in magnetic susceptibility influenced by changing sea level, paleogeography, and paleoclimate: upper Devonian, western Canada sedimentary basin. *J. Sediment. Res.* 80, 1109–1127. <https://doi.org/10.2110/jsr.2010.093>.
- White, D.A., Elrick, M., Romaniello, S., Zhang, F., 2018. Global seawater redox trends during the late Devonian mass extinction detected using U isotopes of marine limestones. *Earth Planet. Sci. Lett.* 503, 68–77.
- Wignall, P.B., 2001. Large igneous provinces and mass extinctions. *Earth-Sci. Rev.* 53, 1–33. [https://doi.org/10.1016/S0012-8252\(00\)00037-4](https://doi.org/10.1016/S0012-8252(00)00037-4).
- Wilson, M., Lyashkevich, Z.M., 1996. Magmatism and the geodynamics of rifting of the Pripyat–Dnieper–Donets rift, east European Platform. *Tectonophysics* 268, 65–81. [https://doi.org/10.1016/S0040-1951\(96\)00234-X](https://doi.org/10.1016/S0040-1951(96)00234-X).
- Witzke, B.J., Bunker, B.J., 1996. In: Witzke, B.J., Ludvigson, G.A., Day, J. (Eds.), *Paleozoic Sequence Stratigraphy: Views from the North American Craton*, 306. Geological Society of America Special Paper, pp. 307–330. <https://doi.org/10.1130/0-8137-2306-X.307>.
- Wong, P.K., Weissenberger, J.A.W., Gilhooly, M.G., 2017. Revised regional Frasnian sequence stratigraphic framework, Alberta outcrop and subsurface. In: Playton, T.E., Kerans, C., Weissenberger, J.A.W. (Eds.), *Advances in Devonian Carbonates: Outcrop Analogs, Reservoirs, and Chronostratigraphy*. SEPM Special Publication No. 107. <https://doi.org/10.2110/sepm.107.05>.
- Xu, B., Gu, Z., Wang, C., Hao, Q., Han, J., Liu, Q., Wang, L., Lu, Y., 2012. Carbon isotopic evidence for the associations of decreasing atmospheric CO₂ level with the Frasnian–Famennian mass extinction. *J. Geophys. Res.* v, 117. <https://doi.org/10.1029/2011JG001847>.
- Xun, Z., Allen, M.B., Whitham, A.G., Price, S.P., 1996. Rift-related Devonian sedimentation and basin development in South China. *J. SE Asian Earth Sci.* 14, 31–52. [https://doi.org/10.1016/S0743-9547\(96\)00020-7](https://doi.org/10.1016/S0743-9547(96)00020-7).
- Yans, J., Corfield, R.M., Racki, G., Preat, A., 2007. Evidence for perturbation of the carbon cycle in the Middle Frasnian punctata Zone (Late Devonian). *Geol. Mag.* 144, 263–270. <https://doi.org/10.1017/S0016756806003037>.
- Zambito, J.J., Joachimski, M.M., Brett, C.E., Baird, G.C., Aboussalam, Z.S., 2016. A carbonate carbon isotope record for the late Givetian (Middle Devonian) Global Taghanic Biocrisis in the type region (northern Appalachian Basin, Special Publications. In: Becker, R.T., Königshof, P., Brett, C.E. (Eds.), *Devonian Climate, Sea Level and Evolutionary Events*, 423. Geological Society, London, pp. 223–233. <https://doi.org/10.1144/SP423.7>. Special Publications.
- Zavyalova, A.P., Chupakhina, V.V., Stoupakova, A.V., Gatovsky, J.A., Kalmykov, G.A., Korobova, N.I., Suslova, A.A., Bolshakova, M.A., Sannikova, I.A., Kalmykov, A.G., 2019. Comparison of the Domanic outcrops in the Volga–Ural and Timan–Pechora basins. In: vol. 74. *Moscow University Geology Bulletin*, pp. 56–72.
- Zhang, J., Deng, C., Liu, W., Tang, Z., Wang, Y., Ye, T., Liang, W., Liu, L., 2021. Mercury anomalies link to extensive volcanism across the late Devonian Frasnian–Famennian boundary in South China. *Front. Earth Sci.* 9, 691827. <https://doi.org/10.3389/feart.2021.691827>.
- Zhang, R., Follows, M.J., Grotzinger, J.P., Marshall, J., 2001. Could the late Permian deep ocean have been anoxic? *Paleoceanography* 16, 317–329. <https://doi.org/10.1029/2000PA000522>.
- Zhou, K., Pratt, B.R., 2019. Composition and origin of stromatolite-bearing mud-mounds (Upper Devonian, Frasnian), southern Rocky Mountains, western Canada. *Sedimentology* 66, 2455–2489. <https://doi.org/10.1111/sed.12595>.
- Smart, M., Filippelli, G., Gilhooly, W., III, Ozaki, K., III, Reinhard, C., III, Marshall, J., III, Whiteside, J., III, in press. Volcanism-driven land plant expansion led to the Late Devonian mass extinction. *Commun. Earth Environ.*
- Corlett, H., Jones, B., 2011. The influence of paleogeography in epicontinental seas: A case study based on Middle Devonian strata from the MacKenzie Basin, Northwest Territories, Canada. *Sediment. Geol.* 239, 199–216. <https://doi.org/10.1016/j.sedg.2011.07.001>.
- Qie, W.K., Ma, X.P., Xu, H.H., Qiao, L., Liang, K., Guo, W., et al., 2018. Devonian integrative stratigraphy and timescale of China (online) *Science China. Earth Sci.* 62 (1), 112–134. <https://doi.org/10.1007/s11430-017-9259-9>.
- Nicoll, R.S., 1984. In: Clark, D.L. (Ed.), *Conodont Biofacies and Provincialism*, 196. Geological Society of America, Special Paper, pp. 127–141.
- Li, Y., Schieber, J., 2015. On the origin of a phosphate enriched interval in the Chattanooga Shale (Upper Devonian) of Tennessee—a combined sedimento-logic, petrographic, and geochemical study. *Sediment* 329, 40–61. <https://doi.org/10.1016/j.sedg.2015.09.005>.
- Becker, R.T., Gradstein, F.M., Hammer, O., 2012. The Devonian period. In: Gradstein, F.M., Ogg, J.G., Schmitz, M., Ogg, G. (Eds.), *The Geologic Time Scale*, 2. Elsevier, Amsterdam, pp. 559–601. <https://doi.org/10.1016/B978-0-444-59425-9.00022-6>.
- Pancost, R.D., Crawford, N., Magness, S., Turner, A., Jenkyns, H.C., Maxwell, J.R., 2004. Further evidence for the development of photic-zone euxinic conditions during Mesozoic oceanic anoxic events. *J. Geol. Soc. London* 161, 353–364. <https://doi.org/10.1144/0016764903-059>.
- Bennett, W.W., Canfield, D.E., 2020. Redox-sensitive trace metals as paleoredox proxies: A review and analysis of data from modern sediments. *Earth Sci. Rev.* 204, 103175. <https://doi.org/10.1016/j.earscirev.2020.103175>.
- Lowery, C.M., Self-Trail, J.M., Barrie, C.D., 2021. Enhanced terrestrial runoff during Oceanic Anoxic Event 2 on the North Carolina Coastal Plain, USA. *Climates of the Past* 17, 1227–1242. <https://doi.org/10.5194/cp-17-1227-2021>.
- Cobbett, R.N., Colpron, M., Crowley, J.L., Cordey, F., Blodgett, R.B., 2021. Late Devonian magmatism and clastic deposition in the upper Earn Group (central Yukon, Canada) mark the transition from passive to active margin along western Laurentia. *Can. J. Earth Sci.* 58, 471–494. <https://doi.org/10.1139/cjes-2020-0161>.